

N O T I C E

THIS DOCUMENT HAS BEEN REPRODUCED FROM
MICROFICHE. ALTHOUGH IT IS RECOGNIZED THAT
CERTAIN PORTIONS ARE ILLEGIBLE, IT IS BEING RELEASED
IN THE INTEREST OF MAKING AVAILABLE AS MUCH
INFORMATION AS POSSIBLE

NASA TECHNICAL MEMORANDUM

NASA TM-76536

ANISOTROPY OF MACHINE BUILDING MATERIALS

Ye.K. Ashkenazi

(NASA-TM-76536) ANISOTROPY OF MACHINE
BUILDING MATERIALS (National Aeronautics and
Space Administration) 102 p HC A06/MF A01

N81-19487

CSCL 20K

Unclass

G3/39 41715

Translation of "Anizotropiya mashinostroitel'nykh
materialov," Mashinostroyeniye Press, Leningrad,
1969, pp. 1-111.



NATIONAL AERONAUTICS AND SPACE ADMINISTRATION
WASHINGTON, D.C. 20546 MARCH 1981

STANDARD TITLE PAGE

1. Report No. NASA TM-76536	2. Government Accession No.	3. Recipient's Catalog No.	
4. Title and Subtitle. ANISOTROPY OF MACHINE BUILDING MATERIALS		5. Report Date March 1981	
7. Author(s) Ye.K. Ashkenazi		6. Performing Organization Code	
9. Performing Organization Name and Address Leo Kanner Associates Redwood City, California 94063		8. Performing Organization Report No.	
12. Sponsoring Agency Name and Address National Aeronautics and Space Administration, Washington, D.C. 20546		10. Work Unit No.	
15. Supplementary Notes Translation of "Anizotropiya mashinostroitel'nykh materialov," Mashinostroyeniye Press, Leningrad, 1969, pp. 1-111.		11. Contract or Grant No. NASW-3199	
		13. Type of Report and Period Covered Translation	
		14. Sponsoring Agency Code	
16. Abstract The results of experimental studies of the anisotropy of elastic and strength characteristics of various structural materials, including pressure worked metals and alloys, laminated fiberglass plastics and laminated wood plastics, are correlated and classified. Strength criteria under simple and complex stresses are considered as applied to anisotropic materials. Practical application to determining strength of machine parts and structural materials is discussed.			
17. Key Words (Selected by Author(s))		18. Distribution Statement Unlimited-Unclassified	
19. Security Classif. (of this report) Unclassified	20. Security Classif. (of this page) Unclassified	21. No. of Pages	22. Price

ANNOTATION

Many materials used in machine building display anisotropy, i.e., dependence of mechanical properties on the orientation of forces with respect to the structural pattern. Pressure worked metals and alloys, plastics reinforced with fibers, filaments or cloth (fiberglass plastics, textolites) and laminated wood plastics are such materials.

The results of experimental studies of the anisotropy of the elastic properties and strength of various structural materials are collected and classified in the book. One of the most important questions of the strength of materials, strength criteria under complex stresses, is considered as applied to anisotropic materials.

The book is intended for design engineers, technologists and investigators working in the field of machine building, as well as in other fields which require increased knowledge of the strength and mechanical properties of structural materials.

FOREWORD

As a result of the development of modern technology, the parameters of machines have increased and, therefore, the mechanical properties and especially the strength of structural material requirements have been increased. Obtaining high strength materials is connected with the order of their micro- and macrostructures. Such materials include oriented films of crystalline polymers, polymers reinforced with fiber-glass, cloth, paper or wood veneer, and crystal fiber reinforced metals [1, 2].

The mechanical properties of these materials differ in different structural directions, i.e., the materials are anisotropic.

This monograph is an attempt to correlate data from study of the anisotropy of materials of various physical natures, based on a unified phenomenological approach. This leads to some practical conclusions, which are important in the design of machine parts and in development of their production technology.

In mechanics, the hypothesis of a uniform, continuous medium, which is the basis of the classical theory of elasticity and the theories of plasticity and creep, is widely applied in mechanics. In this work, this hypothesis is used in discussion of both plastic properties and strength of anisotropic materials. In this case, the physical aspects of the failure of anisotropic substances are not considered. This (phenomenological) approach to questions of the strength of anisotropic solids¹ (including solids of nonhomogeneous structure) is similar to the standard consideration of polycrystalline steel as a uniform, continuous, isotropic medium.

The results of study of the principles of change in strength of anisotropic materials of varied physical nature as a function of the orientation of the main stresses to the axes of structural symmetry of the material are presented in this work. Here, data of the corresponding experiments to determine the mechanical property characteristics, tests of variously oriented samples of anisotropic materials as a whole, are used, whether they are rolled metal alloys or such composite heterogeneous materials as fiberglass.

In principle, another approach is possible. It is the study of mechanical properties of a material as a function of the properties of its component structural elements (for example, in fiberglass the binder and glass fibers separately). The experiment then has to be set up differently.

Both approaches have their problems and their fields of use. The second approach is not considered in this work, since the physical nature of the failure of anisotropic substances is not considered.

¹See also [52].

It is important to designers and technologists working in the field of machine building to know how to estimate the strength of a finished part from the results of mechanical tests of samples of the structural material, precisely what types of tests are necessary for anisotropic materials, and how to test the effect of the anisotropy of a material on the strength of the part.

To estimate the strength of an isotropic material, it is sufficient to determine one strength characteristic, by which the permissible stress is selected but, for anisotropic materials, an entire set of mechanical strength characteristics is necessary. These characteristics are determined experimentally, with varied orientation of the external forces to the structural patterns in the material (for example, to the direction of rolling of a metal sheet or to the direction of preferred placement of the fibers in fiberglass). Determination of the required number of characteristics and of those properties by which the anisotropy system of the material differs is one of the basic tasks of this book.

In the first chapter, the selection of an anisotropy calculation scheme is substantiated for the materials most used in machine building, and data are presented on the elastic properties of bodies of varied elastic symmetry. As one of the most important applications of this theory, the features of strain gauge determination of stresses in parts made of anisotropic materials are discussed in Section 12.

Theories of strength or criteria of equally dangerous stresses are among the most controversial and, at the same time, important problems of the strength of materials, and it is further complicated for anisotropic bodies. The second chapter deals with this problem. In it, two phenomenological criteria of equally dangerous stresses are proposed. The first criterion is a correlation of plasticity conditions, formulated for crystals by R. Mises in 1928. The second criterion differs from the first in higher fourth order terms but, in cases of practical importance, it results in simpler and more convenient formulas, which have been experimentally confirmed for a broader class of materials.

In the third chapter, experimental data on the anisotropy characteristics of the strength of metals and nonmetallic materials, in single static (machine) loading and under dynamic loads, are correlated. These data were processed in accordance with the theoretical assumptions of Chapter 2 and the requirements of engineering calculations of the strength of anisotropic materials.

One of the most important conclusions for the practice is the inadmissibility of estimating the anisotropy of a sheet material, based only on study of its properties in two mutually perpendicular directions, longitudinal and transverse. In many cases, the diagonal direction is most characteristic. In order to be sure of the lack of anisotropy, the properties of sheet material must be investigated in these three directions.

Anisotropy can develop in machine parts as a result of a certain production technology. Anisotropy of metal parts cut after pressure working can turn out to be especially hazardous. The design of critical

parts without taking into account the development of anisotropy in them for some reason can lead to serious errors. More than that, testing of variously oriented samples cut from a finished part to estimate its degree of anisotropy is difficult practically. Nondestructive methods, the so called pulse method in particular, can be used to monitor the degree of anisotropy of the material of a finished part. The features of this application are explained briefly in Section 12.

The methods of application of nondestructive methods to a more detailed estimation of the elastic properties and strength of anisotropic materials are not considered in this book.

The book is intended for persons with mathematical training in a higher technical school. It has no detailed presentation of mathematical conclusions, and the principal attention is given to explanation of the method of use of all the formulas presented. Derivation of the formulas can be found in books listed in the references.

The author thanks honored scientist and engineer Prof. V.A. Gastev and Prof. Ya.B. Fridman, for valuable advice on the basic conclusions of the book.

TABLE OF CONTENTS

Foreword	iii
Chapter 1. Symmetry of Elastic Properties	1
Section 1. Anisotropy Calculation Schemes	1
Section 2. Elastic Constants	9
Section 3. Some Experimental Data on Elastic Property Anisotropy	18
Chapter 2. Strength Criteria	23
Section 4. Strength of Anisotropic Materials	23
Section 5. Quadratic Criterion of Equally Hazardous Stresses	26
Section 6. Equation of Equally Hazardous Stresses in the Form of a Polynomial of the Fourth Degree	33
Section 7. Strength Surfaces	43
Chapter 3. Anisotropy of Strength Characteristics from Experimental Data	53
Section 8. Strength and Plasticity of Metals	53
Section 9. Strength of Nonmetals	62
Section 10. Scatter of Strength Characteristics	68
Section 11. Fatigue	72
Chapter 4. Anisotropy in Machine Parts and Structures	78
Section 12. Strain Measurement Characteristics	78
Section 13. Effect of Anisotropy on Machine Part Strength	80
Section 14. Use of Strength Criteria for Calculation of Pipe Wall Thickness	84
References	90

ANISOTROPY OF MACHINE BUILDING MATERIALS

Ye.K. Ashkenazi

CHAPTER 1. SYMMETRY OF ELASTIC PROPERTIES

1. Anisotropy Calculation Schemes

Anisotropy arises in materials, in connection with the primary orientations of their structural elements. In ferrous and nonferrous metal products, such orientation usually is a result of pressure working but, in structural plastics, it is due to the oriented arrangement of the reinforcing fibers.

Crystals, which have diverse forms of symmetry, are distinguished by considerable anisotropy of all properties. Therefore, great progress in study of the symmetry of physical properties and structure of anisotropic bodies has been made in crystal physics. The science of symmetry, extensively used in crystal physics, can be applied in the mechanics of anisotropic materials, finding new possibilities for study of the mechanical properties of anisotropic bodies and for correlation of test results.

The symmetry of crystals is due to their regular internal structure. Therefore, both the shape and properties of crystals are symmetrical. Symmetry of the mechanical properties usually is attributed to a continuous medium, in which different structural directions are not equivalent, and the structure can be considered uniform.

A change in the characteristics of any property as a function of direction and its symmetry can be studied, by analysis of the symmetry of a geometric figure which represents this change.

From an arbitrary coordinate origin, we plot radius vectors which represent the magnitude of some mechanical characteristic of the material in the corresponding direction. The resulting geometric figure represents the change of the characteristic under consideration as a function of the direction of the force in the material. As an example, the figure of the change in modulus of elasticity of resonant spruce timber, plotted from the data of [3], is shown in Fig. 1. The x, y and z axes are coincident with the three axes of structural symmetry of the timber: z with the fiber direction, x with the radial and y with the tangential directions.

A figure which can be coincident with itself as it rotates around the axis of symmetry or when it is reflected in the plane of symmetry, i.e., by the so called symmetrical transformations, customarily is

*Numbers in the margin indicate pagination in the foreign text.

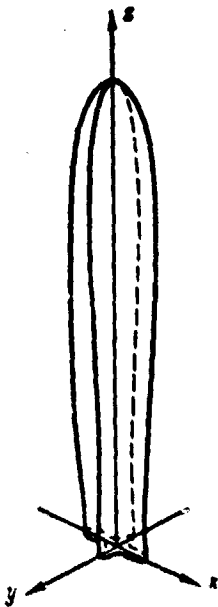


Fig. 1. Three dimensional figure of anisotropy of modulus of elasticity E of resonant spruce wood.

called symmetrical. If rotation of the figure itself is replaced by rotation of the coordinate axes system, the symmetrical transformation can be represented mathematically as the change in the characteristic under consideration upon rotation of the coordinate axes.

The properties of anisotropic solids which have symmetry in the sense indicated above can be characterized quantitatively by mathematical quantities, the transformation of which upon rotation of the coordinate axes will occur according to specific linear relationships. In this case, quantities which are transformed by different relationships but have common characteristic features can correspond to different properties of the same medium.

Let a symmetrical figure which represents a characteristic of the properties of a material be placed in a rectangular x , y , z coordinate system, the origin of which coincides with the center of this figure. We replace the old x , y , z coordinate system with a new one (also rectangular), x' , y' , z' , with the coordinate origin left in place. In this case, the coordinate axes rotate, but the figure itself remains stationary.

We consider the mutual location of the figure and the coordinate system. Rotation of the axes gives the same results as rotation of the figure itself with the coordinate system stationary.

Transformation of the coordinates of points of the figure is determined by the angles between the old and new axes. Not the angles themselves, but their cosines usually are given. They are designated by the letter C with two subscripts, the first of which corresponds to the number of the new axis and the second, to the number of the old axis.¹ For example:

$$C_{13} = \cos(x', z).$$

The angles between the positive directions of the axes can change from 0 to 180° , i.e., each value of the cosine unambiguously defines an angle. The complete system (matrix) of the cosine in rotation of the axes is given in Table 1.

The known relationships between the cosines in Table 1 flow from the conditions of mutual perpendicularity of the axes in the rectangular coordinate system:

¹ Subscripts i and k successively take the values 1, 2 and 3, in which the first is considered here to be the x axis, the second the y and the third the z .

1. The sum of the squares of the cosines in one line or in one column is one; for example:

$$(first \text{ column}); \quad C_{11}^2 + C_{21}^2 + C_{31}^2 = 1$$

$$C_{12}^2 + C_{22}^2 + C_{32}^2 = 1$$

(second line);

2. The sum of the products of cosines of the same group in two different lines or in two different columns is zero; for example:

$$C_{11}C_{12} + C_{21}C_{22} + C_{31}C_{32} = 0$$

(first two columns);

$$C_{11}C_{31} + C_{12}C_{32} + C_{13}C_{33} = 0$$

(lines one and three).

TABLE 1. DIRECTING COSINES

	x	y	z
x'	C_{11}	C_{12}	C_{13}
y'	C_{21}	C_{22}	C_{23}
z'	C_{31}	C_{32}	C_{33}

The formulas for linear transformation of the coordinates of points of a figure can contain the products of two, three or a larger number of cosines, depending on the nature of the figure representing given properties of the material, the nature of these properties or, in other words, the order of the tensor² which corresponds to the property of the anisotropic material under consideration.

The symmetries of such quantities as stress and elastic deformation at a point in any continuum correspond to transformation of components of a second order tensor in rotation of a rectangular coordinate system. This transformation is reduced to summation of products which contain multiples of two cosines of the angles of rotation of the coordinate axes. The elastic constants of anisotropic media are components of a fourth order tensor in three dimensional space, and their transformation upon rotation of the coordinate axes requires summation of the products

²Tensors are mathematical quantities which transform according to specific linear relationships upon rotation of the coordinate axes, and which have a series of properties common to all these quantities. For more detail, see I.Ye. Taranov and A.I. Borisenko, Vektor analiz i nachalo tenzornogo ischisleniya [Vector Analysis and the Basis of Tensor Calculus], Vysshaya Shkola Press, Moscow, 1963, or A.J. MacConnel, Vvedeniye v tenzornyj analiz [Introduction to Tensor Analysis], Fizmatgiz Press, Moscow, 1963.

which contain multiples of four cosines of the angles of rotation of the axes.

Tensors which describe properties of an anisotropic body (for example, the elastic constant tensor) and tensors, the symmetry of which is independent of the properties of the body (for example, the stress tensor) should be differentiated.

Stress can be isotropic, for example, in the case of hydrostatic pressure. If a body is isotropic, elastic deformations under this stress will be the same in all directions (elastic decrease in volume with constant shape). In an anisotropic body subjected to all round compression, the decrease in dimensions in different directions will not be the same. Therefore, the shape of the body changes. /10

In anisotropic materials in general, normal stresses in an arbitrary direction cause both linear and angular deformations and, in turn, tangential stresses can be the cause of both angular and linear deformations. It follows from this that the lack of change in angle between two mutually perpendicular surfaces does not mean the absence of tangential stresses on these surfaces, i.e., the direction of the main deformations in anisotropic materials does not coincide with the direction of the main stresses. This was shown by M.F. Okatov as long ago as 1865. He noted that the axis of an ellipsoid of deformation coincides with the axes of the stress ellipsoid in an anisotropic material, only in the event the main stresses act along the axes of elastic symmetry of the material. With any other orientation, these ellipsoids are not coaxial.

Before studying the mechanical properties of a material, the calculation scheme of its anisotropy must be established.

The basic assumption introduced in consideration of all mechanical properties of an anisotropic material is that, instead of an actual, usually highly nonuniform material, some idealized, continuous, uniform medium is considered, which has symmetry of structure and symmetry of properties. The characteristics of the properties are determined experimentally on samples of the actual material, but the number of required characteristics is determined, according to the assumed symmetry of the medium (anisotropy calculation scheme).

Materials most often are found in industry to which, with a sufficient degree of accuracy, the presence of three mutually perpendicular planes of symmetry of mechanical properties can be assigned in each unit volume. Such materials are called orthotropic or orthogonally anisotropic, and the axes of mutual intersection of the planes of symmetry are called the principal axes of symmetry of the properties of the material.

In crystal physics, the connection between the symmetry of the crystal and the symmetry of physical properties is considered, on the basis that the symmetry of a physical property should be higher than the symmetry of the crystal (Neyman principle).

In 1944, V.L. German proved the following theorem, which generalizes the Neyman principle to the case of continuous anisotropic media: "If a medium has an axis of structural symmetry of order n , it is axially isotropic relative to this axis for all physical properties, the characteristics of which are determined by tensors of order r , if r is less than n ($r < n$). Thus, for example, for elastic properties ($r=4$), with a fifth order axis of symmetry³ ($n=5$), the plane perpendicular to this axis will be the plane of isotropy." /11

This theorem has an important practical application in analysis of the symmetry of properties of multilayer materials composed of orthotropic layers, for example, wood veneer or laminated fiberglass. All directions in the plane of a sheet of such a material will be equivalent to each other with respect to elastic properties, if the angle between the direction of the fibers in adjacent layers is less than 2° . Thus, for example, in a laminated material in which the angle between the fibers in adjacent layers is 60 or 45° , all directions in the plane of the sheet should be equivalent to each other. In this case, the plane of the sheet is the plane of isotropy, and the axis perpendicular to it is an axis of symmetry of infinite order. Such a material customarily is called transversely (axially) isotropic or transtropic.

Such laminated transversely isotropic materials include, for example, sheets made of wood veneer or laminated fiberglass, in which the direction of the fibers in adjacent layers are rotated with respect to each other by some uniform angle. In this case, the laminated material as a whole has a star structure. The fibers in fiberglass plastic sheets are oriented in three directions at angle $\alpha=60^\circ$ to each other. F-60 aviation plywood is such a material [4]. DSP-G laminated wood plastic, in which the fiber directions in adjacent layers of the veneer are at angle $\alpha=30^\circ$, is widely used for the production of gears, bushings, friction pulleys and other parts [5].

Laminated wood chip board with oriented fibers in the layers, sometimes also have a star structure with $\alpha=60^\circ$. Keylwerth [6] found that the modulus of shear and strength of such sheets under pure shear proves to be higher than that of sheets with the same fiber orientation throughout.

The anisotropy calculation scheme of laminated sheet material which consists of an odd number of layers is determined by the fiber structure of the separate layers and their mutual layout.

Sheet material is transversely isotropic, if all the directions in the plane of the sheet are equivalent and, therefore, the plane of the sheet is the plane of isotropy.

The plane of a sheet of laminated material can be the plane of iso- /12

³A fifth order axis of symmetry is that axis, around which it is sufficient to turn a figure by one fifth of the circumference, i.e., by angle $\alpha_0 = 2\pi/5 = 72^\circ$, to obtain complete coincidence of all points of the figure with their initial positions.

tropy is two cases:

1. if the layers are isotropic; then, the anisotropy of the material is determined only by the difference between its properties in the plane of the sheet and its properties in the direction perpendicular to the plane of the sheet; the direction perpendicular to the layers usually is weaker (under tension), because of the effect of the binder (the adhesive layers between the layers);

2. if the layers are anisotropic, but are rotated relative to each other, so that the whole sheet has an axis of symmetry of at least fifth order.

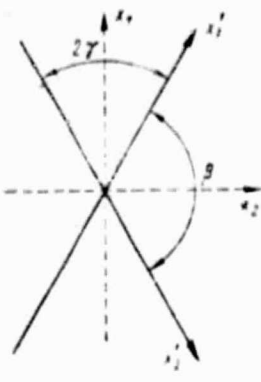


Fig. 2. Fiber directions x'_1 and x'_2 with non-orthogonal placement.

In laminated fiberglass production, cases of nonorthogonal stacking of the layers are known, in which the axis perpendicular to the plane of the sheet cannot be considered an axis of symmetry of infinite order. This results when the fibers are placed in two directions (x'_1 and x'_2 , Fig. 2) in the plane of the sheet, so that the angles between these directions are not equal ($2\gamma \neq \beta$). If the fibers are placed parallel to the x'_1 and x'_2 axes, the axes of symmetry are the x_1 and x_2 axes, in which the x_2 axis is a bisector of angle β and the x_1 axis is a bisector of angle 2γ . Such a material can be considered orthogonally anisotropic (orthotropic), if the layers with the fibers placed in the x'_1 and x'_2 directions are correctly alternated. In this case, the planes of symmetry are the mid-plane of the sheet and the two planes perpendicular to the first, containing the x_1 and x_2 axes.

Considerable anisotropy of mechanical properties occurs in crystal polymers oriented by prestretching. The development of "necks" in stretching crystal polymer samples is a phase transformation of unfavorably oriented crystal microformations to favorable orientations to the force field [7]. New samples cut from stretched necks display strong anisotropy. Upon stretching in the direction coincident with the direction of the initial stretching, deformation of the sample proves to be small, and the strength is increased. Samples cut transverse (to the initial stretching) display great deformability and low strength.

The ordering of polymer structures during their orientation leads to anisotropy of mechanical properties of both a quantitative and a qualitative nature. In stretching along the direction of orientation, the strength is determined by the strengths of the chemical bonds in the chain molecules, which are more or less parallel and uniform in this case. During stretching in the transverse direction, the strength of an oriented polymer is determined only by the strengths of the intermolecular reactions, and these strengths are considerably less than the other [7]. In this case, the orthogonal anisotropy calculation

scheme evidently can be used in films.

In wood structure components, the anisotropy calculation scheme is determined by the shape, dimensions and position of the cross sections with respect to the wood structure components. With sufficiently large cross sections and without their correct orientation to the annual rings (planks, beams, strips), the direction of the wood fibers can be considered the axis of symmetry of its structure, and the plane perpendicular to this axis to be the plane of isotropy of all its properties [3].

In application of the hypothesis of orthogonal anisotropy to unit volumes of wood, it is better to conform to its structure. This hypothesis corresponds to the results of testing "small, clean" samples (GOST [All-Union State Standard] 11483-65 to 11499-65), and it is based on the assumption of the existence of three planes of symmetry in the unit volume of wood.

Strong anisotropy is characteristic of all kinds of wood. Its moduli of elasticity along and across the fibers differ by nearly 20 times and the strengths, by 40 times. Wood derivative materials are anisotropic: plywood, laminated wood plastics (DSP-B, ГБ-В).

In the works of V.A. Kargin [8] and J. Bernal [1], the thought is developed of the necessity of studying the art of reinforcing structural materials in nature. Wood and bone are two reinforced anisotropic materials which, during natural selection, turned out to be adapted by nature for the best resistance to mechanical loads. In this sense, study of the strength of wood acquires new importance, and it becomes a kind of problem of bionics in the development of high strength, reinforced structural materials.

High strength fiberglass reinforced plastics are being used more and more extensively in industry. In the case of reinforcing with unidirectional fiberglass (or spun fiberglass), their anisotropy proves to be extremely great (SVAM, STER, AG-4S, etc.), especially in producing items by winding. Fiberglass reinforced laminates can be classified as anisotropic substances, if their mechanical characteristics are determined by testing samples of the reinforced material.

Another approach to reinforcing with plastics is possible [9]. The concept of fiberglass laminates as an essentially heterogeneous composite material leads to the necessity for separate mechanical testing of specimens of the binder and reinforcing fibers. In this case, some cases of their combined performance in a material, depending on the fiberglass plastic production technology, remain outside the field of view of the investigator. Thus, for example, it is known that the strength of laminated plastics depends on the order of alternation of the layers, and not only on their number and orientation. It is easy to discover such a dependence, by determining the characteristics from testing samples of the laminated material. It is not possible to calculate the mechanical characteristics on the basis of analysis of the combined performance of the fiber and binder, as it is not possible to study the effect of other technological factors on the strength of laminated fiberglass and wood materials.

/14

The anisotropy of the mechanical properties of steel frequently is a consequence of the primary orientation of the crystals after plastic deformation (drawing, rolling or other pressure working). In this case, the assumption of anisotropy of the mechanical properties of steel corresponds better to reality than the conventional assumption, which considers steel as a quasiisotropic material. Many nonferrous metals and alloys also have mechanical property anisotropy. As a rule, metals are considerably less anisotropic than fiberglass laminates or wood. Besides, cases of failure of metal parts are known, the cause of which is the anisotropy of the metal, which was not taken into account by the designer [10].

Analysis of metal flow during pressure working (rolling, extrusion, drawing) permits the proposal that symmetry of the mechanical properties of semifinished metal products of simple geometric shape is close to the symmetry of orthotropic substances, which have three mutually perpendicular planes of symmetry of the properties at each point. In this sense, the anisotropy of pressure worked metals can be considered by the same methods as the anisotropy of wood in small volumes.

As early as the work of V.P. Yermakov (1871), it was shown that "iron wire drawn through a wire drawing die" can be classified as a transverse isotropic substance. The concept of transverse isotropic substances and the name itself in the Russian language evidently was first introduced by Yermakov.

In pressure working intermediate products of cylindrical shape with a circular cross section, the plane perpendicular to the direction of the cylinder generatrix can be considered the plane of isotropy. In this case, the metal is classified as a transverse isotropic substance.

In rolling sheet metal, its properties in two directions perpendicular to the rolling direction differ quite highly.

The statistical data presented in [12, 88], on factory monitoring of massive shapes made of pressure worked light alloys, have shown a 32 and 44% decrease in strength in the directions of the thickness and the width of the product, respectively, compared with the longitudinal direction. In this case, the orthogonal anisotropy scheme is suitable for description of the symmetries of the properties of the material of pressure worked products. /15

In parts of more complicated configurations, after pressure working, an unusual texture develops, in which the orthogonal anisotropy scheme can only be applied to unit volumes of the material, and the entire part has curvilinear anisotropy. A graphic example of curvilinear (cylindrical) anisotropy is the wood in a straight grain trunk.

Study of turbine wheels [11] made by forging or stamping has shown that their material is anisotropic after heat treatment. The cylindrical anisotropy calculation scheme apparently corresponds most closely to reality in this case.

Cases in which, besides anisotropy, considerable nonuniformity of the mechanical properties develops should be specially considered.

Thus, for example, forged metal products with a nonuniform degree of deformation can be distinguished by considerable heterogeneity. In this case, uniformly oriented specimens cut from various places in the item differ more strongly in their properties than differently oriented samples cut from one place.

In this work, the anisotropy of materials is considered only in those cases when their nonuniformity is negligible.

2. Elastic Constants

Test data permit all structural materials to be considered elastic and subject to Hooke's law, within certain limits. Hooke's law, i.e., the law of linear elasticity, can be considered a consequence of the simplest hypothesis that the elastic potential is a quadratic function of the stress components.

The first experimental study of the elastic properties of anisotropic substances (crystals) was that of V. Foykht [14], whose tests confirmed the law of linear elasticity for crystals.

For an anisotropic substance, Hooke's law can be written in the following abbreviated form:

$$\epsilon_{ik} = c_{iklm} \sigma_{lm} \quad (1)$$

where subscripts i , k , ℓ and m have the values 1, 2 and 3 in succession; 16

ϵ_{ik} is the relative deformation, linear with $i=k$ and angular with $i \neq k$;

$\sigma_{\ell m}$ is the stress, normal with $i=k$ and tangential with $i \neq k$ (for example, with $\ell=1$, $m=1$, σ_{11} designates normal stress in the direction of the first axis of symmetry of the material, i.e., the x axis and, with $\ell=2$ and $m=2$, σ_{22} designates the same along the y axis);

c_{iklm} are the elastic constants which characterize the materials and are determined experimentally.

It is assumed that, in Eq. (1), summation over the subscript found twice on the right side of the equation, i.e., over subscripts ℓ and m , is carried out. In the abbreviated form, the summation symbol is omitted. If Eq. (1) is written with the summation symbols, it takes this form:

$$\epsilon_{ik} = \sum_{l=1}^{l=3} \sum_{m=1}^{m=3} c_{iklm} \sigma_{lm}.$$

For a detailed expression for calculations from Eq. (1), for example, the relative elongation along the x axis, $i=k=1$ must be assumed. The following results in the general case of an anisotropic material:

$$\epsilon_{ii} = c_{1111}\sigma_{11} + c_{1112}\sigma_{12} + c_{1113}\sigma_{13} + c_{1121}\sigma_{21} + c_{1122}\sigma_{22} + c_{1123}\sigma_{23} + c_{1131}\sigma_{31} + c_{1132}\sigma_{32} + c_{1133}\sigma_{33}. \quad (2)$$

In the general case of an anisotropic material, the values of 81 elastic constants c_{iklm} , which form a so called fourth order tensor, are used in calculation of all deformations. A fourth order tensor is a set of values (component) which, in rotation of the coordinate axes, change by the following linear relationship, which contains the product of four cosines of the angles between the new and old directions of the axes as multipliers:

$$c_{i'k'l'm'} = c_{iklm} C_{i'i} C_{k'k} C_{l'l} C_{m'm}. \quad (3)$$

Eq. (3) permits calculation of the constants for randomly oriented directions in the material (new coordinate axes), if their values are known for some specific directions (old coordinate axes). Eq. (3) is written in abbreviated form, which assumes summation over all the subscripts found twice on the right side. All the subscripts have the values 1, 2 and 3 in turn. The letters C designate the cosines of the angles between the old and new rectangular Cartesian coordinate system, in accordance with Table 1.

We consider an orthotropic material, in which there are three mutually perpendicular planes of symmetry of the elastic properties.

In indication of the elastic constant tensor components in the planes of symmetry, their values should not change since, for two directions uniformly inclined to the planes of symmetry, the elastic properties of an orthotropic material should be the same. Mathematically, this indication is equivalent to transformation of the coordinates by one of the three directing cosine matrices presented in Table 2 (the general designation is presented in Table 1). It is assumed that the plane of symmetry (in matrix I) is the xz plane,⁴ the xy plane in matrix II and the yz plane in matrix III.

The existence of three planes of symmetry (orthogonal anisotropy of the material) requires that the values of the components not change, in order to substitute cosines C from matrices I, II and III in Eq. (3). This condition can be satisfied, only by transformation of those initial components c_{iklm} , in which either all four subscripts are equal to each other or they are equal in pairs. Actually, if, for example,

⁴This matrix corresponds to reversing the direction of the y axis alone:
 $c_{22} = \cos(y'; y) = -1$.

TABLE 2. DIRECTING COSINES

Марканс I			Марканс II			Марканс III					
	x	y	x	y	z	x	y	z			
x'	1	0	0	x'	1	0	0	x'	-1	0	0
y'	0	-1	0	y'	0	1	0	y'	0	1	0
z'	0	0	1	z'	0	0	-1	z'	0	0	1

Key: a. matrix

component c_{1123} is included on the right side of Eq. (3), with $i'=k'=1$, $\ell'=2$ and $m'=3$, the corresponding term will have the following product of the cosines as the multiplier: $C_{11}^2 C_{22} C_{33}$. This, when indicated in the xy plane of symmetry, i.e., $C_{11}=1$, $C_{22}=1$ and $C_{33}=-1$, leads to a change in sign of this term and to a change in the values of all components but, according to the condition of symmetry of the components, they should not change in such a transformation. Consequently, in the x, y and z axes of symmetry (principal axis), component c_{1123} should equal zero. In transformation of those components in which the subscripts are equal by pairs, negative one is included in the square, the sign of the term does not change, and the condition of symmetry is satisfied. Therefore, only those components the subscripts of which are at least equal by pairs, i.e., a total of 21 components, can be on nonzero initial (principal) axes.

Since this equality follows from the equilibrium condition:

$$\sigma_{12} = \sigma_{21}; \sigma_{13} = \sigma_{31} \text{ and } \sigma_{23} = \sigma_{32},$$

it happens that elastic constant tensor c_{iklm} does not change upon transposition of the subscripts, i.e., that

$$\begin{aligned} c_{iikk} &= c_{kkii}; \\ c_{ikik} &= c_{kiki} = c_{ikki} = c_{kikk}. \end{aligned} \quad | \quad (4)$$

As a result, the elastic constant tensor in the principal x, y and z axes of symmetry of an orthotropic substance has nine independent elastic constants, and it can be written in a form (Table 3), in which the following conventional symbols of the technical elastic constants are introduced:

/18

$$\left. \begin{aligned} c_{1111} &= \frac{1}{E_x}; \\ c_{2222} &= \frac{1}{E_y}; \\ c_{3333} &= \frac{1}{E_z}; \end{aligned} \right\} \quad (5)$$

$$4c_{1212} = \frac{1}{G_{xy}};$$

$$4c_{2323} = \frac{1}{G_{yz}};$$

$$4c_{3131} = \frac{1}{G_{zx}};$$

$$c_{1122} = -\frac{\mu_{xy}}{E_x} = -\frac{\mu_{yx}}{E_y};$$

$$c_{2233} = -\frac{\mu_{yz}}{E_y} = -\frac{\mu_{zy}}{E_z};$$

$$c_{3311} = -\frac{\mu_{zx}}{E_z} = -\frac{\mu_{xz}}{E_x},$$

(6)

where E is the tensile or compressive modulus of elasticity in the direction of the axis specified in the subscript;
 G is the modulus of shear as a result of tangential stresses on areas parallel to one and perpendicular to another of the axes specified in the subscript;
 μ is the coefficient of transverse deformation in the direction of the first of the axes specified in the subscript, as a result of normal stresses in the direction of the second axis.

TABLE 3. TECHNICAL ELASTIC CONSTANTS IN XYZ AXES OF SYMMETRY OF ORTHOTROPIC MATERIAL

	11	22	33	12	23	31
11	$\frac{1}{E_x}$	$\frac{\mu_{xy}}{E_x}$	$\frac{\mu_{yz}}{E_y}$	0	0	0
22	$\frac{\mu_{xy}}{E_y}$	$\frac{1}{E_y}$	$\frac{\mu_{zx}}{E_z}$	0	0	0
33	$\frac{\mu_{yz}}{E_z}$	$\frac{\mu_{zx}}{E_z}$	$\frac{1}{E_x}$	0	0	0
12	0	0	0	$\frac{1}{G_{xy}}$	0	0
23	0	0	0	0	$\frac{1}{G_{yz}}$	0
31	0	0	0	0	0	$\frac{1}{G_{zx}}$

Thus, if the x, y and z axes are the axes of symmetry of an orthotropic material, the following should be placed in Eq. (2)

$$c_{1113} = c_{1121} = c_{1123} = c_{1131} = c_{1132} = 0$$

Then, Eq. (2) takes the following form

$$\epsilon_{11} = c_{1111}\sigma_{11} + c_{1122}\sigma_{22} + c_{1133}\sigma_{33};$$

With Eq. (5) and (6) taken into account, together with Eq. (1), we obtain

$$\begin{aligned}\epsilon_x &= \frac{\sigma_x}{E_x} - \frac{\mu_{yx}}{E_y} \sigma_y - \frac{\mu_{zx}}{E_z} \sigma_z; \\ \epsilon_y &= -\frac{\mu_{xy}}{E_x} \sigma_x + \frac{\sigma_y}{E_y} - \frac{\mu_{yz}}{E_z} \sigma_z; \\ \epsilon_z &= -\frac{\mu_{xz}}{E_x} \sigma_x - \frac{\mu_{yz}}{E_y} \sigma_y + \frac{\sigma_z}{E_z}; \\ \gamma_{xy} &= \frac{\tau_{xy}}{G_{xy}}; \\ \gamma_{yz} &= \frac{\tau_{yz}}{G_{yz}}; \\ \gamma_{zx} &= \frac{\tau_{zx}}{G_{zx}}.\end{aligned}\tag{7}$$

To determine the relative linear deformation in the direction of an axis randomly oriented in an orthotropic material, Eq. (2) should be used, in which the elastic constants are calculated by Eq. (3), based on the experimentally determined values of the elastic constants in the axes of symmetry of the material (see Table 3). The values of the elastic constants in the directions of the axes of symmetry of an orthotropic material in Table 3 are expressed by the technical elastic constants according to Eqs. (5) and (6). Numerical data on the values of these characteristics of some structural materials are presented in Section 3.

To determine the entire set of nine elastic constants of wood, it is sufficient to test the uniaxial compression or (better) tension of six types of samples (Fig. 3) [15, 16]. Longitudinal resistance sensors for measurement of the deformations in these samples are positioned differently with respect to the axes of symmetry of the wood (Fig. 3). The force is applied to all samples along the axis parallel to the longer side of the parallelepiped. The samples shown in Fig. 3a, b and c are used to determine the values of E and μ in the principal directions of symmetry, and the samples shown in Fig. 3d, e and f, to determine them in the diagonal directions. For example, from the results of testing the sample shown in Fig. 3f, the modulus of shear is determined

$$G_{xy} = \frac{E_{xy}^{(45)}}{2(1 + \mu_{xy}^{(45)})}.$$

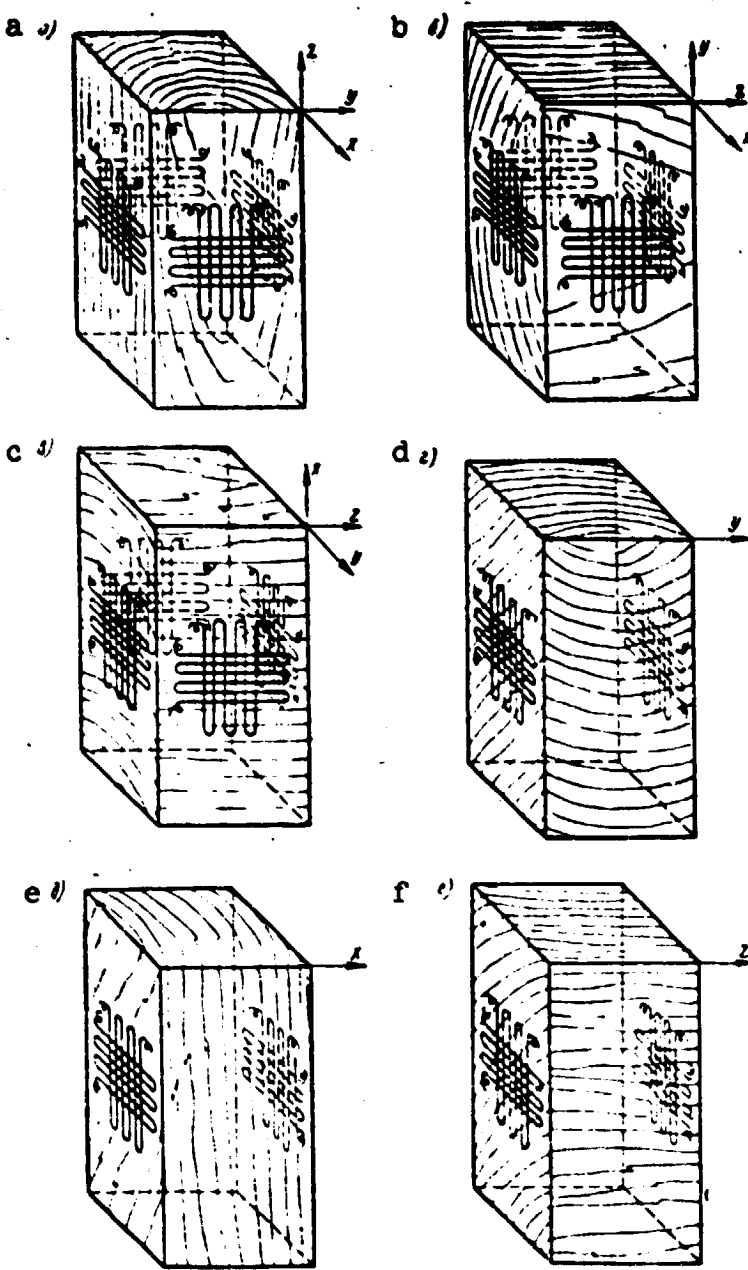


Fig. 3. Samples for determination of set of elastic constants of wood by means of strain gauges.

The method of determination of the elastic constants of any orthotropic material can be the same as for wood.

Unfortunately, the complete set of elastic constants has been determined experimentally for few anisotropic structural materials, although the method of determination has been quite well developed. These data are required in order to estimate the effect of anisotropy of the elastic properties of a material on the pattern of stress distribution in a part, by using the formulas of the theory of elasticity

of an anisotropic material [17]. The effect of anisotropy can sometimes be very noticeable. For example, in stretching a sheet along the axis of greatest rigidity, the coefficient of stress concentration around a circular opening increases with increase in the degree of anisotropy of the material, but it decreases when stretched in the transverse direction. The results of study of the change in the coefficient of concentration for this case are presented in [9], as a function of the coefficient of reinforcing and the degree of anisotropy of fiber-glass laminates. /21

The modulus of elasticity E_x' , and modulus of shear $G_{x'y'}$, for randomly oriented directions in an orthotropic material are determined by the following formulas, which arise from Eq. (3):

$$\frac{1}{E_x'} = \frac{n_1^4}{E_x} + \frac{l_1^4}{E_y} + \frac{m_1^4}{E_z} + \left(\frac{4}{E_{xz}^{(45)}} - \frac{1}{E_x} - \frac{1}{E_y} \right) n_1^2 l_1^2 + \left(\frac{4}{E_{yz}^{(45)}} - \frac{1}{E_y} - \frac{1}{E_z} \right) l_1^2 m_1^2 + \left(\frac{4}{E_{zx}^{(45)}} - \frac{1}{E_z} - \frac{1}{E_x} \right) m_1^2 n_1^2; \quad (8)$$

$$\frac{1}{G_{x'y'}} = \frac{(n_1 l_2 + l_1 n_2)^2}{G_{xy}} + \frac{(l_1 m_2 + m_1 l_2)^2}{G_{yz}} + \frac{(m_1 n_2 + n_1 m_2)^2}{G_{zx}} - \frac{4 n_1 l_1 n_2 l_2}{G_{xy}^{(45)}} - \frac{4 l_1 m_1 l_2 m_2}{G_{yz}^{(45)}} - \frac{4 m_1 n_1 m_2 n_2}{G_{zx}^{(45)}}. \quad (9)$$

For simplification, instead of the cosine notation (Table 1), the notation presented in Table 4 is used in these formulas.

TABLE 4. SIMPLIFIED DIRECTING COSINE NOTATION

	x	y	z
x'	n_1	l_1	m_1
y'	n_2	l_2	m_2
z'	n_3	l_3	m_3

For the two dimensional problem, the elastic properties of an orthotropic sheet are determined with four constants. If the experimentally determined values $E_0 = E_x$, $E_{90} = E_y$ and $E_{45} = E_{45}$ are adopted as the initial values, the formulas for the elastic constants at angle α to the axes of symmetry can be written [18]:

$$E_\alpha = \frac{E_0}{\cos^4 \alpha + b \sin^2 2\alpha - c \sin^4 \alpha}, \quad (10)$$

where $b = \frac{E_0}{E_{45}} - \frac{1+c}{4}$; $c = \frac{E_0}{E_{90}}$;

$$G_a = \frac{G_0}{\cos^2 2\alpha + \frac{G_0 \sin^2 2\alpha}{G_{45}}}; \quad (11)$$

$$G_0 = \frac{E_{45}}{2(1+\mu_{45})}; \quad (12)$$

$$G_{45} = \frac{E_0 E_{45}}{E_0 (1+\mu_{45}) + E_{45} (1+\mu_0)}. \quad (13)$$

Here, all the elastic constants are determined for uniaxial stresses and pure shear in the planes of symmetry of an orthotropic material.

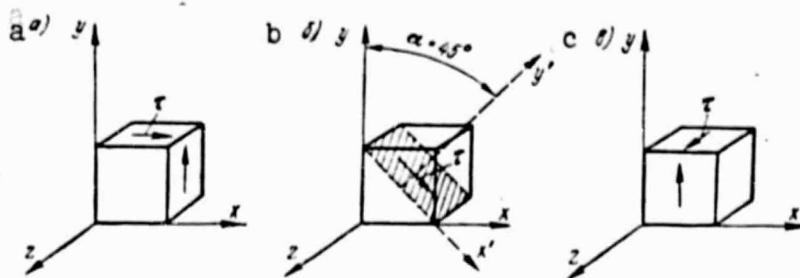


Fig. 4. Orientation of tangential stresses in determination of modulus of shear: a. G_0 in xy plane; b. G_{45} in xy plane; c. G_0 in yz plane.

Tangential stress τ orientation diagrams in pure shear, which correspond to different moduli of shear determined by Eqs. (12) and (13), are shown in Fig. 4. In shear along the planes of symmetry parallel to the x and y axes (Fig. 4a), modulus G_0 in the xy plane is determined by Eq. (12). In shear along planes at a 45° angle to the x and y axes of symmetry (Fig. 4b), modulus G_{45} in the xy plane is determined by Eq. (13). Here, for example, the rolling direction of a steel sheet or the direction of the fibers of a laminated fiberglass lining can be selected as the x axis. /22

If angle $\alpha \neq 45^\circ$, the tangential stress orientation scheme (Fig. 4b) corresponds to the quantity G_α , determined by Eq. (11). If the pure shearing stress turns around the y axis, so that one area of action of tangential stresses always remains parallel to the y axis, after rotating the scheme shown in Fig. 4a by 90° , another scheme (Fig. 4c) results, which corresponds to modulus G_{yz} . When rotating the scheme (Fig. 4a) around the y axis to any angle β , the modulus of shear is determined by the formula

$$G_\beta = \frac{1}{\frac{\cos^2 \alpha}{G_{xy}} + \frac{\sin^2 \alpha}{G_{yz}}}. \quad (14)$$

Graphs of change of modulus of elasticity E_x , of some pressure worked nonferrous and ferrous metals, plotted from experimental data, are shown in [12, 13]. These graphs confirm the suitability of Eq. (8) and, consequently, of the calculation scheme of the orthogonal anisotropy of elastic properties to these materials.

Experimental data confirm the practical suitability of the assumption that both metals and such materials of nonuniform structure as wood and wood materials [3, 5, 18], textolites and fiberglass laminates [19, 20] are orthotropic, uniform, continuous media with respect to elastic properties. /23

Only a material, the moduli of elasticity of which are the same (in the case of sheet material) in three directions (the directions of greatest rigidity, that perpendicular to it and the diagonal; see Eqs. (8) and (10)) can be considered isotropic with respect to elastic properties.

Monitoring the isotropy of a sheet from measurements of the deformations in two mutually perpendicular directions alone can lead to mistakes, since it often turns out that the diagonal is most indicative in estimation of the anisotropy expressly in those cases when it is not very strongly expressed.

The elastic properties of a transversely isotropic material are determined by five independent characteristics in the axes of symmetry. The corresponding formulas are easy to obtain if, for example, all subscripts y are replaced by x in the formulas for an orthotropic material, with consideration that the properties in the xy plane are the same in all directions. In other words, for a transversely isotropic material, the following must be used in Table 3 (if z is an axis of symmetry of infinite order):

$$\left. \begin{aligned} \frac{1}{E_x} &= \frac{1}{E_y}; \quad \frac{1}{G_{yz}} = \frac{1}{G_{zx}}; \\ -\frac{\mu_{xz}}{E_z} &= -\frac{\mu_{yz}}{E_y} = -\frac{\mu_{xz}}{E_x} = -\frac{\mu_{zy}}{E_z}; \end{aligned} \right\} \quad (15)$$

$$G_{xy} = \frac{E_x}{2(1 + \mu_{xy})}. \quad (16)$$

For cubic system crystals, which include monocrystals of the pure metals aluminum, nickel, copper, iron (see Table 6), three elastic property characteristics are independent. For such a case of symmetry, the following must be used in Table 3

$$\left. \begin{aligned} c_{1111} &= c_{2222} = c_{3333}; \\ c_{1122} &= c_{2233} = c_{3311}; \\ c_{1212} &= c_{2323} = c_{3131}. \end{aligned} \right\} \quad (17)$$

or else

$$\left. \begin{aligned} \frac{1}{E_x} &= \frac{1}{E_y} = \frac{1}{E_z}; \\ -\frac{\mu_{xy}}{E_x} &= -\frac{\mu_{yz}}{E_y} = -\frac{\mu_{zx}}{E_z}; \\ \frac{1}{G_{xy}} &= \frac{1}{G_{yz}} = \frac{1}{G_{zx}}. \end{aligned} \right\} \quad (18)$$

In distinction from isotropic and transversely isotropic materials, /2/ there is no symmetry relationship (16) in this case.

With this relationship, a total of two elastic constants become independent, and the material is isotropic. Thus, the three relationships (18) and obligatory relationship (16) are used as isotropy criteria.

For an isotropic material, the figures⁵ which represent the change in moduli of elasticity E and G should revert to spherical surfaces. Consequently, a material, the moduli of elasticity E and G of which are the same, not only in the x, y and z directions, but in diagonal directions, is isotropic. For isotropic materials and for cubic system crystals, $E_{xy}^{(45)} = E_{yx}^{(45)} = E_{zx}^{(45)}$ but, for the former, $E^{(45)} = E^{(0)}$ and for the latter, no.

3. Some Experimental Data on Elastic Property Anisotropy

Curves of change of the modulus of elasticity in the planes of sheets of different materials, to which orthogonal symmetry of the elastic properties is attributed, are shown in polar diagrams (Fig. 5, 6). The curves presented in Fig. 5 were plotted from the data of [21], and the curves shown in Fig. 6, from the data of [22]. For comparison, a diagram of the change of modulus of elasticity E of resonant spruce wood, a material with the strongest anisotropy [3], is presented in Fig. 7.

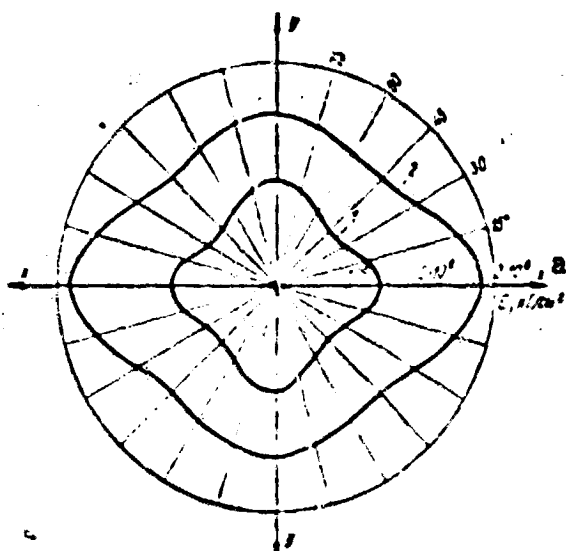


Fig. 5. Polar diagram of modulus of elasticity E of rolled metals:
1. copper; 2. iron.

Key: a. E, kg/cm²

In all these materials, in the plane for which the diagrams were plotted, there are two axes of symmetry of the figures which represent the change in modulus of elasticity. The diagrams confirm that the degree of anisotropy cannot be decided only by comparison of the value of E in the x and y axes of symmetry.

The curves of change of moduli E and G vs. direction are approximated well by Eq. (8) and (9). As a rule, modulus of shear G has the highest value for the three orientations which correspond to the lowest values of modulus E. This regularity is characteristic of metallic monocrystals and strongly anisotropic nonmetallic materials.

The surfaces of change of modulus E (Fig. 8) and modulus of

⁵For an anisotropic material, such figures are shown in Fig. 8 and 9.

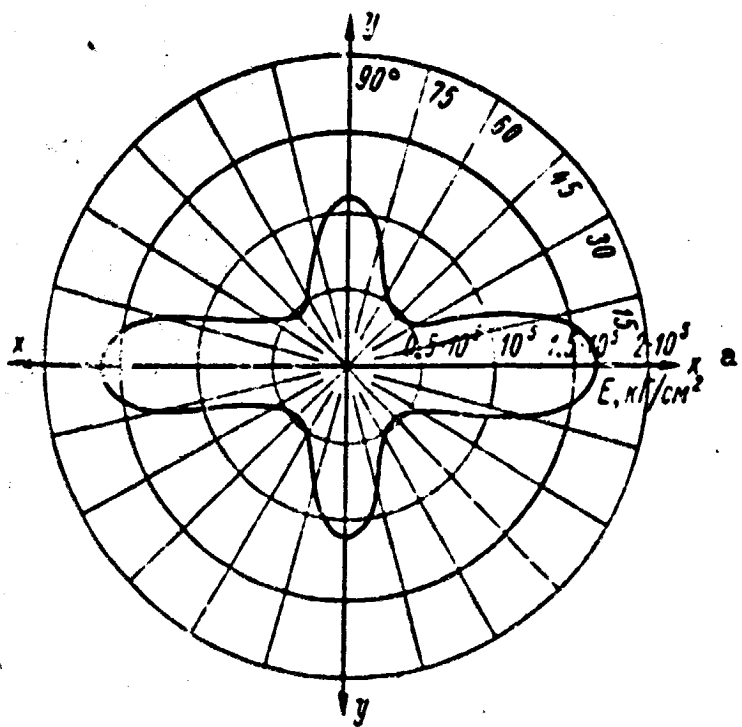


Fig. 6. Polar diagram of modulus of elasticity E of 10 mm thick 9-ply aviation plywood (x. direction of lining fibers).

Key: a. E , kg/cm^2

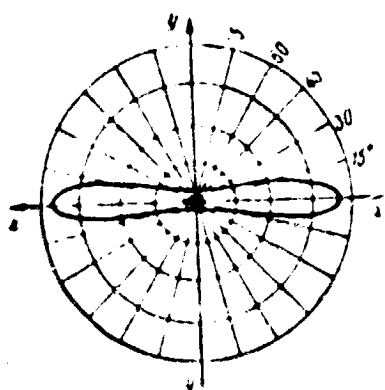


Fig. 7. Polar diagram of modulus of elasticity E of resonant spruce wood (x. fiber direction).

shear G (Fig. 9) plotted by Goens and Shmid [26] illustrate this regularity for an iron monocrystal, the symmetry of which is that of the cubic system (see Section 2). These surfaces confirm that, with equal moduli in the directions of the three axes of symmetry, the material cannot be isotropic, if its moduli have other values in the diagonal directions than on the axes of symmetry. Moduli G for an iron mono-
crystal has a higher value in those directions in which moduli E are smaller. /27

This principle remains valid for pressure worked metal alloys. To decide on the isotropy of rolled sheet, not only the longitudinal and transverse but, without fail, the diagonal direction must be investigated. The latter frequently proves to be the most characteristic.

Modulus of elasticity E of rolled metal alloys displays comparatively small anisotropy. The diagonal direction, which makes a 45° angle with the rolling direction in the plane of the sheet, is the most characteristic of it. It was noted in [12, 13, 23] that, for rolled metals, modulus E_{45} in the diagonal direction proves to be the smallest but, after annealing and recrystallization of the metals, E_{45} exceeds moduli E_0 and E_{90} , sometimes by 1.5-2 times (Fig. 10-12). Anisotropy of the elastic properties, determined from the $E_0:E_{90}$ ratio is almost absent in these cases, and the diagonal direction displays a different type of anisotropy of the same metal in different states.

To some extent, anisotropy develops in all metals after pressure working and, as a rule, it is not eliminated by annealing.

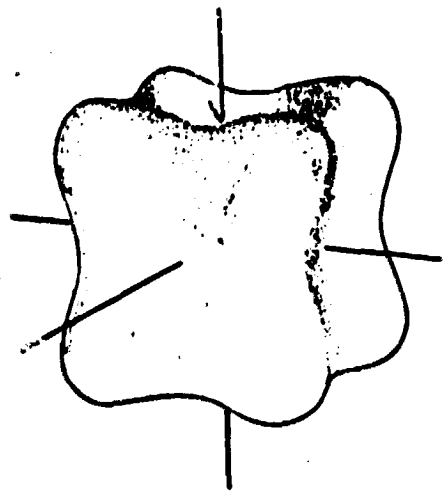


Fig. 8. Three dimensional figure of anisotropy of modulus of elasticity E of α -iron monocrystal (axes of symmetry of crystal shown by straight lines).

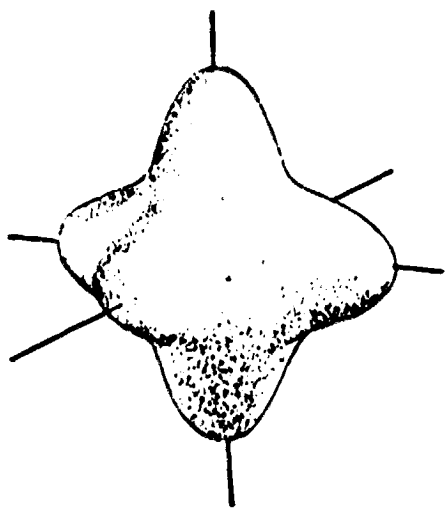


Fig. 9. Three dimensional figure of anisotropy of modulus of shear G of α -iron monocrystal (axes of symmetry of crystal shown by straight lines).

Metals, the crystal lattices of which has hexagonal symmetry, develop greater anisotropy after cold rolling than metals with a cubic lattice. The anisotropy of metals depends on the method of rolling, the degree of cold working and the method and temperature of the interoperation and final annealing [56].

Table 5 presents experimental data on the technical elastic constants of orthotropic nonmetallic materials, of which considerable anisotropy of the elastic properties is characteristic. The elastic constants of metallic monocrystals presented in Table 6 were calculated from the data of [26]. Information is assembled in these tables on the complete set of elastic constants in the axes of symmetry which, unfortunately, is available for only a limited number of materials.

/28

A large amount of experimental data on the elastic constants of various crystals is presented in [27], where surfaces and curves of change vs. orientation toward the axes of elastic symmetry were plotted for them.

The elastic properties of wood materials, fiberglass laminates and laminated materials in general are distinguished by a lower modulus of shear G_{zx} than modulus of elasticity E_x . Thus, for satin weave fiberglass cloth plastics, in the plane of the layers with mutually perpendicular placement of the cloth layers, this ratio $G_{zx}/E_x = \frac{1}{17} / \frac{1}{13}$ but, with

the longitudinal-diagonal reinforcing system used in shipbuilding, $G_{zx}/E_x =$

$\frac{1}{14} / \frac{1}{15}$ [29]. Therefore, calculation of

/29

the elastic deformations and natural oscillations in bending of fiberglass plastics should be carried out, with verification of the effect of shear on the magnitude of the deflection required.

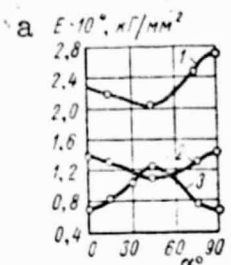


Fig. 10. Anisotropy of modulus of elasticity E (angle between rolling direction and sample axis plotted on abscissa):
1, 2. sheets of iron and copper in rolled state;
3. copper sheets after recrystallization.

Key: a. $E \cdot 10^4$, kg/mm²

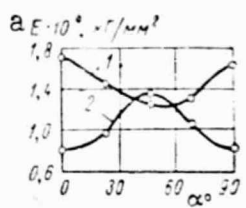


Fig. 11. Anisotropy of modulus of elasticity E of Fe-Ni alloy in rolled state (curve 1) and after recrystallization (curve 2).

Key: a. $E \cdot 10^4$, kg/mm²

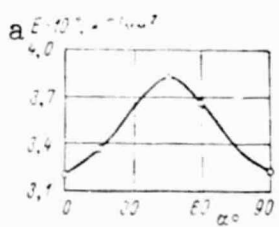


Fig. 12. Anisotropy of modulus of elasticity E of molybdenum sheet rolled in two alternate directions and annealed.

Key: a. $E \cdot 10^4$, kg/mm²

It is characteristic of reinforced materials that, with mutually perpendicular placement of the reinforcing fibers, modulus of elasticity E in the xy plane turns out to be the least under diagonal tension, for which the modulus of shear usually is the greatest (Fig. 13). Diagonal placement of part of the reinforcing increases the modulus of shear G of the reinforced material. If the same number of reinforcing fibers are placed in the longitudinal, transverse and two diagonal directions, the sheet material can be considered isotropic in the plane of the sheet (transversely isotropic). In this case, modulus of shear $G_0 = G_{45}$ turns out higher [6] than with mutually perpendicular placement of the reinforcing fibers.

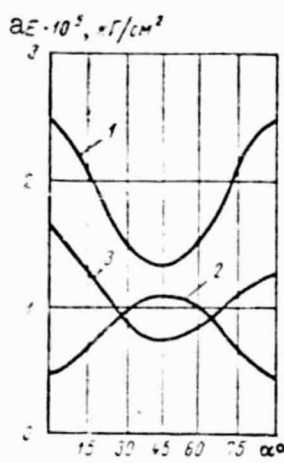


Fig. 13. Anisotropy of elastic properties of fiberglass plastics: 1. modulus of elasticity E of SVAM with 1:1 fiber ratio; 2. modulus of shear G of SVAM with 1:1 fiber ratio; 3. modulus of elasticity E of PN-1 binder fiberglass cloth plastic.

Key: a. $E \cdot 10^5$, kg/cm²

TABLE 5. ELASTIC CONSTANTS OF ORTHOTROPIC NONMETALS

a Материал	b Модули упругости, кГ/см ² ·10 ⁴						c Коэффициент попечной деформации μ		
	E_x	E_y	E_z	G_{xy}	G_{yz}	G_{zx}	μ_{xy}	μ_{yz}	μ_{zx}
d Древесина резонансной ели [3]	10,3	0,77	0,395	0,524	0,354	0,421	0,031	0,248	0,441
e ДСП-Б [5, 24]	32,7	7,1	4,6	1,21	1,98	2,52	0,07	0,30	0,36
f СВАМ, 1:15 (по данным С. М. Перекальского)	46	16	11,2	5,65	3,30	4,35	0,093	0,36	0,30
g СВАМ, 1:1 (по данным С. М. Перекальского)	26	26	7,8	4,51	3,0	3,0	0,13	0,24	0,24
h Стеклотекстолит сантинового переплетения на смоле ПН-3 (по данным М. В. Гершберга)	17,5	13,1	5,30	2,82	2,38	2,34	0,10	0,17	0,229

Notes: 1. Subscripts x and z designate axes of symmetry of greatest and least rigidity.
 2. First subscript of factor μ designates the direction of deformation and the second, the direction of active stress.

Key: a. Material
 b. Modulus of elasticity, kg/cm²·10⁴
 c. Transverse deformation factor μ
 d. Resonant spruce wood
 e. DSF-B
 f. SVAM, 1:15 (from data of S.M. Perekal'skiy)
 g. SVAM, 1:1 (from data of S.M. Perekal'skiy)
 h. Satin weave PN-3 resin fiber-glass laminate (from data of M.V. Gershberg)

TABLE 6. ELASTIC CONSTANTS OF MONOCRYSTALS OF PURE CUBIC SYSTEM METALS

a Материал	b $E_x \cdot 10^6$, кГ/см ²	c $G_{xy} \cdot 10^6$, кГ/см ²
Алюминий d	0,64	0,365
Никель e	1,27	0,391
Медь f	0,68	0,416
Чугун g	1,35	0,372

Key: a. Material
 b. $E_x \cdot 10^6$, kg/cm²
 c. $G_{xy} \cdot 10^6$, kg/cm²
 d. Aluminum
 e. Nickel
 f. Copper
 g. α -iron

CHAPTER 2. STRENGTH CRITERIA

4. Strength of Anisotropic Materials

The majority of machine parts operate under complex biaxial and triaxial stresses, for which strength testing of an anisotropic material has peculiarities, which consist primarily of the need for experimental determination of an entire set of mechanical characteristics.

/30

For isotropic materials, the strength usually is expressed by an equation which connects the three principal stresses with a single strength characteristic of the material. For anisotropic materials, such an equation does not solve the problem, since a hazardous state depends on both the principal stresses and their orientation towards the axes of symmetry of the material. Therefore, the equation of equally hazardous stresses of orthotropic materials should not contain three, but six quantities, for example, the three principal stresses and three directing cosines, which record their orientation towards the three axes of symmetry of the material.

The equation of equally hazardous conditions for orthotropic materials has a simpler and more symmetrical form, if it does not include the principal stresses, but the stresses on areas perpendicular to the x, y and z axes of symmetry of the material. In this case, the strength characteristics are determined in the axes of symmetry of the material. The entire set of strength characteristics which is included in the equation of equally hazardous states can be determined experimentally.

If the three principal stresses are randomly oriented towards the three x, y and z axes of symmetry of an orthotropic material, the stresses on areas perpendicular to the axes of symmetry can be calculated easily from the known strength of materials formulas, just as in the case of random orientation of these areas. Designation of these stresses with letter and number subscripts is presented in Table 7. Designations with numerical subscripts are more convenient for shortening the writing down of the formulas. Here, as before, the number 1 means the x axis, the number 2, the y axis and the number 3, the z axis. For example, stresses designated by the symbol σ_x or σ_{11} are normal stresses on an area perpendicular to the first axis of symmetry of the material x. In abbreviated notation, stress is designated by the symbol σ_{ik} , in which subscripts i and k have the values 1, 2 and 3 in succession.

/31

The stresses, the designations of which are presented in Table 7, combine into the following sums, the values of which do not change upon rotation of the coordinate axes and, therefore, are called invariants:

$$I_1 = \sigma_{ik}\delta_{ik} = \quad (19)$$

$$= \sigma_1^2 + \sigma_2^2 + \sigma_3^2$$

$$I_2 = \sigma_{ik}\sigma_{ik} = \sigma_1^2 + \sigma_2^2 + \sigma_3^2 + \\ + 2\tau_{1y}^2 + 2\tau_{2x}^2 + 2\tau_{3z}^2.$$

(20)

TABLE 7. NOTATION FOR STRESSES ALONG AREAS OF SYMMETRY OF ORTHOTROPIC MATERIAL

Обозначения с букв. индексами			Обозначения с цифровыми индексами		
σ_x	τ_{xy}	τ_{xz}	σ_{11}	σ_{12}	σ_{13}
τ_{xy}	σ_y	τ_{yz}	σ_{21}	σ_{22}	σ_{23}
τ_{xz}	σ_z	σ_z	σ_{31}	σ_{32}	σ_{33}

Key: a. Letter subscript notation
 b. Numerical subscript notation

In these formulas, the abbreviated notation of invariant sums I_1 and I_2 is given first and, then, the detailed notation. In the abbreviated notation, subscripts i and k should be given the values 1, 2 and 3 in succession, and summation over these subscripts should be carried out. The value of δ_{ik} should be one if $i=k$ and zero, if $i \neq k$.

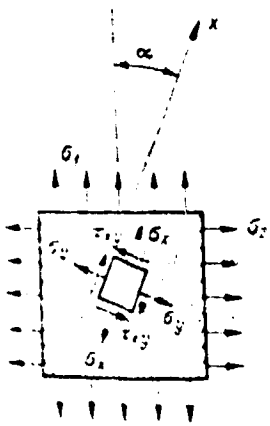


Fig. 14. Stresses σ_x , σ_y and τ_{xy} in two dimensional stress in xy planes of symmetry of material (in Table 7).

How stresses σ_x , σ_y and τ_{xy} act with planar stress in the xy plane of symmetry of the material, with fixed principal stresses σ_1 and σ_2 (the x axis is coincident with the direction of the fibers), is shown in Fig. 14.

The equally hazardous stress functions should be invariant, in the sense of Eq. (19) and (20). Upon rotation of the coordinate axes, the values of the stress components and of the material constants change, but the values of the functions should not change. Two types of these functions will be considered in Section 5 and Section 6. Eq. (19) and (20) are used in designation of the criteria in Section 6.

Stresses in which transition of the material from one mechanical state to another occurs are considered to be equally hazardous (maximum) stresses. This can be a transition from the elastic state either to the plastic state or directly to failure.

The criteria of limiting states of isotropic materials are assumed to differ in the case of development of plastic deformations (then, this criterion is called the plasticity condition) and in the case of brittle failure (strength condition). If the plasticity condition and brittle failure criterion are formulated differently for an anisotropic material, the orientation in which a given stress should apply one condition and that in which it should apply the other condition must be known beforehand.

It is known that the behavior of an anisotropic material can be brittle or plastic, all other conditions being equal, only because of different orientation of a given stress. Thus, for example, wood deforms plastically (it is squeezed together) under radial compression, but it undergoes brittle shearing, if the direction of the compressive force makes an angle of 45° to the fiber direction and lies in the radial plane. It is similar in crystals: the form of disruption of strength depends on the orientation of the force to the so called cleavage plane.

The demarcations between the brittle and plastic forms of hazardous states is not very distinct, even for isotropic materials [32].

A generalized understanding of a hazardous state of anisotropic materials is possible. Either brittle failure (if plastic deformation did not precede it), or the appearance of noticeable inelastic deformation (if it is a hazard to performance of the part) can be considered hazardous.

It is customarily considered that hydrostatic pressure does not affect the strength of isotropic materials and does not change the shape of the material. The equally hazardous stress functions (strength criterion or plasticity condition) for isotropic substances usually are written in a form, in which the addition of equal all around compression or tension does not change the value of these functions.

It follows from this that, in itself, hydrostatic pressure or equal all around tension cannot change an isotropic material to a hazardous condition. This situation is not evident, and it is questioned by many authors. Thus, in the works of N.K. Snitko [25], it was pointed out that, if the atomic structure of the material is considered, unlimited resistance to uniform all around tension of any magnitude should be recognized as improbable. It is clear that some limiting resistance to all around tension should exist, in which the bonds between separate particles should be disrupted.

A similar conclusion can be reached for the deformation of anisotropic materials under equal all around compression. Further, the tests of A. Fepple showed that, for example, for such an anisotropic material as wood, the effect of hydrostatic pressure cannot be disregarded. Fepple subjected wooden cubes to equal all around compression, and they squeezed together and acquired an irregular shape [25]. The shape of any strongly anisotropic material changes as a result of hydrostatic pressure, since the decrease in dimensions does not occur uniformly in different directions. If these changes remain after removal of the load, it is evident that the hydrostatic pressure can result in plastic deformation, i.e., a hazardous state, of the anisotropic material. The effect of hydrostatic pressure can be especially significant in the case of strong anisotropy. For polymers, it is found even in the absence of anisotropy [30].

There are very few data in the literature on the effect of hydrostatic pressure on the behavior of anisotropic materials.

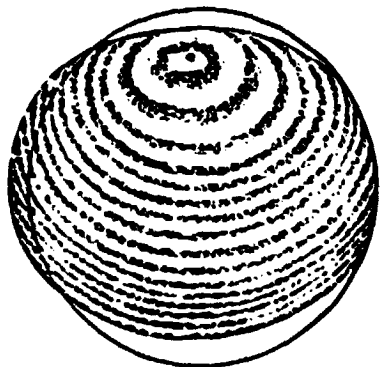


Fig. 15. Shape of pine ball after exposure to hydrostatic pressure.

The shape of a pine ball, which was photographed by A.L. Rabinovich [18] after exposure to hydrostatic pressure $p=60 \text{ kg/mm}^2$, is shown in Fig. 15. It is clearly evident in the figure that uniform pressure on all sides changed the shape of the ball. It suffered residual deformation across the fibers and was changed into an ellipsoid. Thus, hydrostatic pressure may be the cause of a hazardous condition of the wood. Bridgman [31] reached similar conclusions, in study of the effect of hydrostatic pressure on the yield stress of quartz.

The equally hazardous stress functions for anisotropic bodies should conform to this characteristic of it and take hydrostatic pressure into account.

5. Quadratic Criterion of Equally Hazardous Stresses

In 1928, in his classic work on the plasticity of crystals [33], Mises proposed the plasticity condition in the form of an equation, which connects six components of stress (Table 7) with the yield stress under uniaxial stress and under pure shear in different crystallographic directions.

The plasticity condition can be considered a special case of the equation of equally hazardous states. We investigate the plasticity function proposed by Mises, for its suitability as a general equation of equally hazardous stresses (strength criterion).

The plasticity function was proposed by Mises in the form of a uniform polynomial of the second degree. Initially, he wrote this quadratic function without introduction of the assumption of independence of the yield stress of crystals from hydrostatic pressure. For a material with a general type of anisotropy, the Mises plasticity condition ([33], p. 163) has the following form in our notation:

$$\begin{aligned}
 & A_{1111}\sigma_x^2 + A_{2222}\sigma_y^2 + A_{3333}\sigma_z^2 + 4A_{3232}\tau_{xy}^2 + 4A_{1313}\tau_{xz}^2 + 4A_{2121}\tau_{yz}^2 + \\
 & + 2A_{1112}\sigma_x\sigma_y + 2A_{2233}\sigma_y\sigma_z + 2A_{3311}\sigma_z\sigma_x + 2A_{1133}\sigma_x\tau_{xy} + \\
 & - 2A_{1113}\sigma_x\tau_{xz} + 2A_{1112}\sigma_y\tau_{xy} + 2A_{2233}\sigma_y\tau_{yz} + 2A_{2213}\sigma_y\tau_{xz} + \\
 & + 2A_{1112}\sigma_x\tau_{yz} + 2A_{3322}\sigma_z\tau_{xy} + 2A_{3313}\sigma_z\tau_{xz} + 2A_{3312}\sigma_z\tau_{xy} + \\
 & - 4A_{3213}\tau_{xz}\tau_{yz} - 4A_{3112}\tau_{xz}\tau_{xy} - 4A_{1233}\tau_{xy}\tau_{yz} = 1.
 \end{aligned} \tag{21}$$

In this equation, coefficients A_{iklm} are constants of the material, the number of which is 21 in the general case of anisotropy.

If the x, y and z axes coincide with the axes of symmetry of an orthotropic material, on symmetry considerations, all terms which

contain tangential stresses in the first degree and the products of different tangential stresses should be discarded, since these terms can change sign upon reflection in the planes of symmetry of the material (see Section 1).

Eq. (21), in the axes of symmetry of an orthotropic material, will contain nine constants A_{iklm} , and it takes the following form

$$A_{1111}\sigma_x^2 + A_{2222}\sigma_y^2 + A_{3333}\sigma_z^2 + 2A_{1122}\sigma_x\sigma_y + 2A_{2233}\sigma_y\sigma_z + 2A_{3311}\sigma_z\sigma_x + 4A_{1113}\tau_{xz}^2 + 4A_{3232}\tau_{yz}^2 + 4A_{2121}\tau_{xy}^2 = 1. \quad (22)$$

In this expression, the relationships between coefficients A_{iklm} can be selected so that the addition of hydrostatic pressure, i.e., of invariant I_1 (see Section 4) does not change the value of Eq. (22). Then, function (22) will comply with the special assumption of Mises, of the insensitivity of the plasticity condition to hydrostatic pressure.

By using the stress designations (Table 7), we write quadratic function (22) in abbreviated form [37, 11]

$$A_{iklm}\sigma_{ik}\sigma_{lm} = 1. \quad (23)$$

We write the relationships between the material constants A_{iklm} , in which the addition of I_1 does not change the value of Eq. (23), thus

$$A_{iklm}\delta_{ik} = 0. \quad (24)$$

For an orthotropic material, relationship (24) can be derived from the condition of invariability of Eq. (22), by substitution in it of /35

$$\left. \begin{array}{l} \sigma_x = \sigma'_x - p; \\ \sigma_y = \sigma'_y - p; \\ \sigma_z = \sigma'_z - p; \\ \tau_{xy} = \tau_{yz} = \tau_{zx} = 0. \end{array} \right\} \quad (25)$$

By making the coefficients in terms which contain the hydrostatic pressure intensity p in the first degree equal to zero, from Eq. (22), we obtain

$$\left. \begin{array}{l} A_{1111} + A_{1122} + A_{1133} = 0; \\ A_{2222} + A_{2211} + A_{2233} = 0; \\ A_{3333} + A_{3311} + A_{3322} = 0. \end{array} \right\} \quad (26)$$

By making the coefficient with p^2 equal to zero, we obtain a condition which is a consequence of Eq. (26)

$$A_{1111} + A_{2222} + A_{3333} + 2A_{1122} + 2A_{2233} + 2A_{3311} = 0 \quad (27)$$

We write condition (27) in abbreviated form

$$A_{iklm}\delta_{ik}\delta_{lm} = 0 \quad (28)$$

We investigate quadratic function (22), which is sensitive to hydrostatic pressure, as an equation of equally hazardous stresses of anisotropic materials, without taking relationships (24)-(28) into account.

In plane stress which is randomly oriented in the xy plane of symmetry of the material, from formula (22), we obtain

$$A_{1111}\sigma_x^2 + A_{2222}\sigma_y^2 + 2A_{1122}\sigma_x\sigma_y + 4A_{1112}\tau_{xy}^2 = 1. \quad (29)$$

To determine coefficients A_{iklm} , we consider particular cases of limiting stresses:

1. we set $\sigma_y = \tau_{xy} = 0$ and $\sigma_x = \sigma_0$ (σ_0 is the ultimate strength under uniaxial tension along the x axis of symmetry); then, from formula (29), we obtain

$$A_{1111}\sigma_0^2 = 1 \text{ or } A_{1111} = \frac{1}{\sigma_0^2}; \quad (30)$$

2. with $\sigma_x = \tau_{xy} = 0$ and $\sigma_y = \sigma_{90}$ (σ_{90} is the tensile strength along the y axis)

$$A_{2222} = \frac{1}{\sigma_{90}^2}; \quad (31)$$

3. with $\sigma_x = \sigma_y = 0$ and $\tau_{xy} = \tau_0$ (τ_0 is the ultimate strength under pure shear along the areas of symmetry of the material), 36

$$4A_{1112} = \frac{1}{\tau_0^2}; \quad (32)$$

4. with $\sigma_x = \sigma_y = \tau_{xy} = \frac{\sigma_{45}}{2}$ (σ_{45} is the "diagonal" tensile strength at an angle of 45° with the x and y axes of symmetry in the xy plane),

$$2A_{1122} = \frac{4}{\sigma_{45}^2} - \frac{1}{\sigma_0^2} - \frac{1}{\sigma_{90}^2} - \frac{1}{\tau_0^2}; \quad (33)$$

5. with the use of another stress, pure shear along the same diagonal areas, in which $\sigma_x = +\tau_{45}$, $\sigma_y = -\tau_{45}$, $\tau_{xy} = 0$ (τ_{45} is the ultimate strength under pure shear along the diagonal areas), we obtain

$$2A_{1122} = \frac{1}{\sigma_0^2} + \frac{1}{\sigma_{90}^2} - \frac{1}{\tau_{45}^2}. \quad (34)$$

For the two dimensional problem, expression (29) takes the following form

$$\frac{\sigma_x^2}{\sigma_0^2} + \frac{\sigma_y^2}{\sigma_{90}^2} + \frac{\tau_{xy}^2}{\tau_0^2} + \sigma_x \sigma_y \left(\frac{4}{\sigma_{45}^2} - \frac{1}{\sigma_0^2} - \frac{1}{\sigma_{90}^2} - \frac{1}{\tau_0^2} \right) = 1 \quad (35)$$

or

$$\frac{\sigma_x^2}{\sigma_0^2} + \frac{\sigma_y^2}{\sigma_{90}^2} + \frac{\tau_{xy}^2}{\tau_0^2} + \sigma_x \sigma_y \left(\frac{1}{\sigma_0^2} + \frac{1}{\sigma_{90}^2} - \frac{1}{\tau_{45}^2} \right) = 1. \quad (36)$$

Both of these alternate versions of the strength criterion (formulas (35) and (36)) contain four constants of the material for the two dimensional problem. They are determined from uniaxial stress and pure shear tests.

We assume that safety factor k is the same in different directions in the material, in the first approximation. Then, for practical verification of the strength, the strength condition is obtained from the quadratic criterion (formula (35)), in this form

$$\sqrt{\sigma_x^2 + c^2 \sigma_y^2 + d^2 \tau_{xy}^2 + s \sigma_x \sigma_y} \leq [\sigma_0],$$

where $[\sigma_0] = \sigma_0/k$ is the permissible longitudinal stress (usually, this is the direction of greatest strength);

$$c = \frac{\sigma_0}{\sigma_{90}}; \quad d = \frac{\sigma_0}{\tau_0}; \quad s = 4a^2 - c^2 - d^2 - 1; \quad a = \frac{\sigma_0}{\sigma_{45}};$$

σ_x and σ_y are the normal stresses in the part along the areas of symmetry of the material (σ_x along the x axis and σ_y along the y axis, in which the x axis coincides with the direction of greatest strength of the material); τ_{xy} is the tangential stresses on the part (in the same place as stresses σ_x and σ_y), along areas perpendicular to the x and y axes.

In work already mentioned [33], a characteristic of anisotropic materials was noted for the first time, which permits testing the suitability of the plasticity criterion (and, consequently, strength) by

the results of uniaxial tensile testing of variously oriented samples.

From expression (29), we obtain a formula for calculation of the tensile strength σ_B in random direction of x' , as a function of orientation of the x' axis, determined according to Table 8.

TABLE 8. DIRECTING COSINES

	x	y	z
x'	$\cos \alpha$	$\sin \alpha$	0
y'	$-\sin \alpha$	$\cos \alpha$	0
z'	0	0	1

For this, we substitute the following stress values in formula (35):

$$\left. \begin{aligned} \tau_{xy} &= \sigma_s \cos \alpha \sin \alpha; \\ \sigma_x &= \sigma_s \cos^2 \alpha; \\ \sigma_y &= \sigma_s \sin^2 \alpha \end{aligned} \right\} \quad (37)$$

and we obtain

$$\frac{1}{\sigma_s^2} = \frac{\cos^4 \alpha}{\sigma_0^2} + \frac{\sin^4 \alpha}{\sigma_{45}^2} + \sin^2 \alpha \cos^2 \alpha \left(\frac{4}{\sigma_{45}^2} - \frac{1}{\sigma_0^2} - \frac{1}{\sigma_{45}^2} \right). \quad (38)$$

We now derive a formula from expression (36), which determines the pure shearing strength τ_b , in which tangential stresses act along an area normal to x' parallel to the y' axis. For this, we substitute the following stress values in formula (36):

$$\left. \begin{aligned} \tau_{xy} &= \tau_s \cos 2\alpha; \\ \sigma_x &= \tau_s \sin 2\alpha; \\ \sigma_y &= -\tau_s \sin 2\alpha \end{aligned} \right\} \quad (39)$$

and we obtain

$$\frac{1}{\tau_s^2} = \frac{\cos^2 2\alpha}{\tau_0^2} + \frac{\sin^2 2\alpha}{\tau_{45}^2}. \quad (40)$$

Formulas (38) and (40) can be written in this more convenient form /38 for practical use and comparison with experimental results:

$$\sigma_s = \frac{\sigma_0}{\sqrt{\cos^4 \alpha + B \sin^2 2\alpha + c^2 \sin^4 \alpha}} \quad (41)$$

$$(\text{where } c = \frac{\sigma_0}{\sigma_{45}}; B = a^2 - \frac{1+c^2}{4}; a = \frac{\sigma_0}{\sigma_{45}});$$

$$\tau_s = \frac{\tau_0}{\cos^2 2\alpha + \left(\frac{\tau_0}{\tau_{45}} \right)^2 \sin^2 2\alpha}. \quad (42)$$

It is easy to see that, in the general case of bulk stress, the following formulas for strength σ_B and τ_B , randomly oriented toward the three x, y and z axes of symmetry of the material, follow from formula (22) (for comparison, see formulas (8) and (9)):

$$\frac{1}{\sigma_s^2} = \frac{n_1^4}{(\sigma_x^{(0)})^2} + \frac{l_1^4}{(\sigma_y^{(0)})^2} + \frac{m_1^4}{(\sigma_z^{(0)})^2} + \\ + n_1^2 l_1^2 \left[\frac{4}{(\sigma_{xy}^{(45)})^2} - \frac{1}{(\sigma_x^{(0)})^2} - \frac{1}{(\sigma_y^{(0)})^2} \right] + \\ + l_1^2 m_1^2 \left[\frac{4}{(\sigma_{yz}^{(45)})^2} - \frac{1}{(\sigma_y^{(0)})^2} - \frac{1}{(\sigma_z^{(0)})^2} \right] + \\ + m_1^2 n_1^2 \left[\frac{4}{(\sigma_{zx}^{(45)})^2} - \frac{1}{(\sigma_z^{(0)})^2} - \frac{1}{(\sigma_x^{(0)})^2} \right]; \quad (43)$$

$$\frac{1}{\tau_s^2} = \frac{(n_1 l_2 + l_1 n_2)^2}{(\tau_{xy}^{(0)})^2} + \frac{(l_1 m_2 + m_1 l_2)^2}{(\tau_{yz}^{(0)})^2} + \frac{(m_1 n_2 + n_1 m_2)^2}{(\tau_{zx}^{(0)})^2} - \\ - \frac{4 n_1 l_1 n_2 l_2}{(\tau_{xy}^{(45)})^2} - \frac{4 l_1 m_1 l_2 m_2}{(\tau_{yz}^{(45)})^2} - \frac{4 m_1 n_1 m_2 n_2}{(\tau_{zx}^{(45)})^2}, \quad (44)$$

where x, y, z are the principal axes of symmetry of the orthotropic material; σ_B is the strength in uniaxial tensile or compressive stress along the x' axis, randomly oriented in the material; τ_B is the pure shearing strength, when tangential stresses act along the y' axis in an area normal to x'.

The direction of the provisional x', y' and z' axes to the principal x, y and z axes of symmetry of the material is determined by Table 9.

TABLE 9. DIRECTING COSINES

	x	y	z
x'	n_1	l_1	m_1
y'	n_2	l_2	m_2
y'	n_3	l_3	m_3

The tensile (compressive) strengths in the axes of symmetry in Eq. (43), (44), $\sigma_x^{(0)}$, $\sigma_y^{(0)}$, $\sigma_z^{(0)}$ and, in the directions in the planes of symmetry at an angle of 45° to the axes of symmetry, $\sigma_{xy}^{(45)}$, $\sigma_{yz}^{(45)}$, $\sigma_{zx}^{(45)}$.

The pure shearing strengths along areas parallel to the planes of symmetry of the material are designated $\tau_{xy}^{(0)}$, $\tau_{yz}^{(0)}$, $\tau_{zx}^{(0)}$ and, along areas at a 45° angle with two axes of symmetry and perpendicular to the third, $\tau_{xy}^{(45)}$, $\tau_{yz}^{(45)}$, $\tau_{zx}^{(45)}$. The lower subscripts show the

axes of the areas of action of the stress which form a 45° angle.

Surfaces are presented in Fig. 16 and 17, which show the change in compressive strength σ_B of pine wood samples [34] and fiberglass plastic cloth (from E.V. Ganov data [35]). Both surfaces were plotted from experimental data.

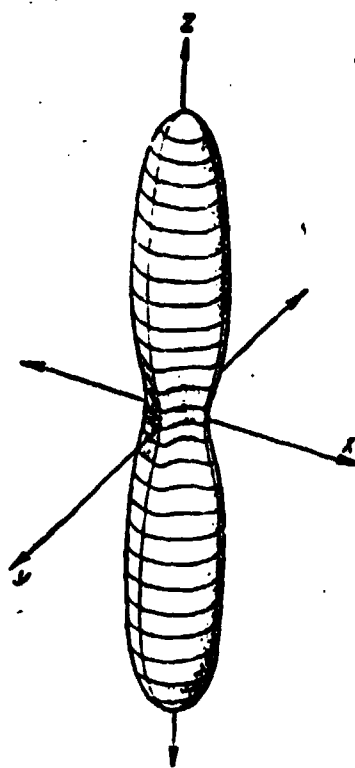


Fig. 16. Surface of change in compressive strength σ_B wood vs. orientation toward fiber z, radial y and tangential x directions.

It was shown experimentally in [36, 37, 41] that expressions (43) and (44), which determine the strength σ_B and τ_B of anisotropic materials vs. sample orientation to the axes of structural symmetry, approximate well the results of testing slightly anisotropic metals and some fiberglass laminates, but contradict tests of such strongly anisotropic materials as wood. The difference in shapes of the σ_B surfaces of these materials are shown in Fig. 16 and 17.

In equal biaxial compression, the strength σ_D can be calculated, if the values $\sigma_x = \sigma_y = \sigma_D$ and $\tau_{xy} = 0$ are substituted in formula (35):

$$\sigma_D = \frac{\sigma_0 \tau_0}{\sqrt{4\tau_0^2 - \sigma_0^2}}. \quad (45)$$

For plywood and fiberglass plastics, this formula gives values which are close to experimental values [36].

For materials with low shearing strength (wood), relationship $\tau_0 < \sigma_{45}/2$ [39] is possible, in which formula (45) gives imaginary values of σ_D .

With hydrostatic pressure p , it follows from formula (22) that

$$p_0 = \frac{1}{A_{11m} A_{22m} A_{33m}}. \quad (46)$$

A pine ball (Fig. 15) was photographed at $p=60 \text{ kg/cm}^2$ [18]. Pressure p_0 at which irreversible changes in shape of the pine ball began were not indicated in [18]. It obviously was less than 60 kg/cm^2 .

Calculations by formula (46) gave $p_0 = 15 \text{ kg/cm}^2$ for pine wood. Thus, it does not contradict test data, as applied to plastic deformation of pine wood under hydrostatic pressure.

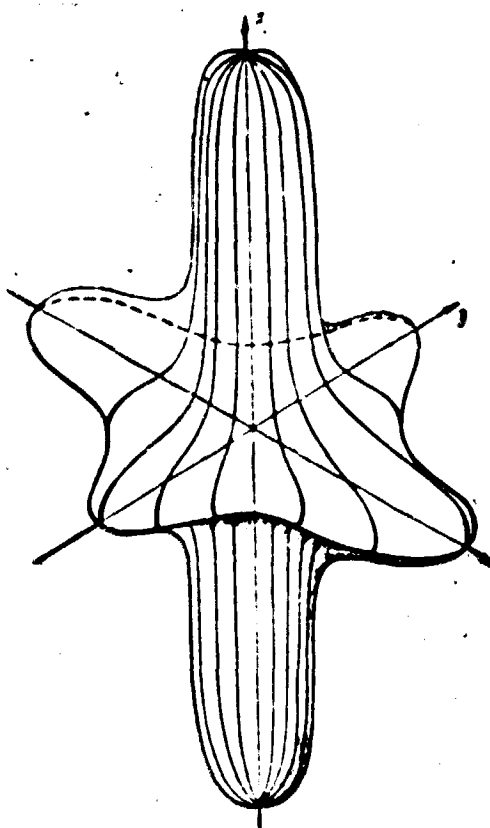


Fig. 17. Surface of change in compressive strength σ_B of fiberglass cloth plastic vs. orientation toward direction perpendicular to layers x , warp fibers z and woof fibers y of cloth.

It should be noted that Mises assumed the tensile and compressive strength to be the same (symmetry inversion of the material characteristics). For many materials used in practice, the anisotropy of which is substantial (wood, fiberglass plastics), the difference between the tensile and compressive strengths in the same direction turns out to be appreciable. For plane stress, the Mises equation can be used for such /41 materials with the use of the "piecewise approximation" method. For all stresses in which only tensile stresses σ_x and σ_y act along the areas of symmetry or one of them is compressive, but less than the second, tensile, in absolute value, it should be considered that coefficients A_{iklm} are determined by tension and shear. For those plane stresses in which either both stresses σ_x and σ_y are compressive or the compressive stress is greater than the tensile, A_{iklm} should be determined by compression and shear. In [36, 37], this formulation of the question is called the piecewise approximation, and it becomes clear in a graphical representation of the maximum planar stress surfaces in the σ_x , σ_y and τ_{xy} coordinate axes (see Section 7).

6. Equation of Equally Hazardous Stresses in the Form of a Polynomial of the Fourth Degree

It was shown in [22, 36-41] that experimental data on strength, with variously oriented uniaxial and pure shearing stresses, are approximated well by formulas for conversion of fourth order tensor components, constructed by analogy with the formulas of change in the elastic constants upon rotation of the coordinate axes. These formulas, called tensorial in [22, 36-41], differ from formulas (43) and (44), which follow from the quadratic strength criterion, they are simpler, and they correspond to the experimental data for a broader class of materials.

With the use of the notation used in formulas (43) and (44), we obtain tensorial formulas in this form (for comparison, see formulas (8) and (9)):

$$\frac{1}{\sigma_{\alpha}} = \frac{n_1^2}{\sigma_{xx}^{(0)}} + \frac{l_1^2}{\sigma_y^{(0)}} + \frac{m_1^2}{\sigma_z^{(0)}} + n_1^2 l_1^2 \left(\frac{4}{\sigma_{xy}^{(45)}} - \frac{1}{\sigma_x^{(0)}} - \frac{1}{\sigma_y^{(0)}} \right) + \\ + l_1^2 m_1^2 \left(\frac{4}{\sigma_{yz}^{(45)}} - \frac{1}{\sigma_y^{(0)}} - \frac{1}{\sigma_z^{(0)}} \right) + \\ + m_1^2 n_1^2 \left(\frac{4}{\sigma_{zx}^{(45)}} - \frac{1}{\sigma_z^{(0)}} - \frac{1}{\sigma_x^{(0)}} \right) \quad (47)$$

$$\frac{1}{\tau_{\alpha}} = \frac{(n_1 l_1 + l_1 m_1)^2}{\tau_{xy}^{(0)}} + \frac{(l_1 m_1 + m_1 n_1)^2}{\tau_{yz}^{(0)}} + \frac{(m_1 n_1 + n_1 l_1)^2}{\tau_{zx}^{(0)}} - \\ - \frac{4 n_1 l_1 m_1}{\tau_{xy}^{(45)}} - \frac{4 l_1 m_1 n_1}{\tau_{yz}^{(45)}} - \frac{4 m_1 n_1 l_1}{\tau_{zx}^{(45)}}. \quad (48)$$

For slightly anisotropic materials (metals, fiberglass plastics), /42
Eq. (47) and (48) give results which practically coincide with the
results of calculation by Eq. (43) and (44). For strongly anisotropic
wood, where Eq. (43) contradicts test results, the tensorial formulas
do not lead to such contradictions. For slightly anisotropic materials,
Eq. (47) and (48) also conform well to tests, like Eq. (43) and (44)
but, for strongly anisotropic materials, they conform considerably better.
The surfaces presented in Fig. 16 and 17 are approximated well by Eq.
(47).

In the special case of uniaxial stress, for which the quadratic
criterion leads to Eq. (41), a simpler expression follows from Eq. (47),
which permits calculation of the strength at angles α to the axes of
symmetry of the material (see Table 8):

$$\sigma_{\alpha} = \frac{\sigma_0}{\cos^4 \alpha + b \sin^2 2\alpha / \sqrt{c \sin^4 \alpha}} \quad (49)$$

where $c = \frac{\sigma_0}{\sigma_{xx}}$; $a = \frac{\sigma_0}{\sigma_{yy}}$; $b = a - \frac{1 - c}{4}$.

For pure shear, the following is obtained from Eq. (48):

$$\tau_{\alpha} = \frac{\tau_0}{\cos^2 2\alpha + \frac{1}{\tau_{yy}^{(0)}} \sin^2 2\alpha} \quad (50)$$

Because of their relative simplicity, Eq. (49) and (50) have found
practical application both in wood science and in machine building.
Estimation of the degree of anisotropy which develops in metal parts
after pressure working were carried out by these formulas in the work
of I.G. Miklayev and Ya.B. Fridman [12, 13, 18]. For fiberglass plastics,
these formulas proved to be useful in resolving questions of the effect
of cross grain, which arises for technological reasons, on the strength
characteristics in production of a ship hull [35, 42]. Eq. (49) was

corroborated in estimation of the anisotropy of the fatigue strength of wood [43], fiberglass plastics [44] and metals [66]. In [45], Eq. (49) was applied to study of a problem of wood science. Based on deformation assumptions, in 1946, A.L. Rabinovich [18, 90] obtained and experimentally confirmed special Eq. (49). A formula for shearing similar to Eq. (49) was presented without derivation in Kollman [46], where she also confirmed it experimentally (see Section 9). All the experiments mentioned were performed on flat specimens.

It should be noted that the tests of Ya.S. Sidorin [29, 47], performed on flat specimens and on fiberglass plastic tubes, showed that Eq. (49) and (50) conform to the results of such tests, although the absolute values of characteristics σ_{45} and τ_{45} , obtained on tubular specimens, were considerably higher than on the flat ones.

We furnish a problem: to find the invariant function of six stress components (Table 7), which would lead to experimentally confirmed tensorial Eq. (47) and (48) for randomly oriented uniaxial and pure shearing stresses. We study this function as an equation of equally hazardous stresses or (by using the geometric representation [48, 87]) a strength surface equation. /43

We consider two dimensional stress in the xy plane.

From Eq. (47), we obtain (see Tables 8 and 9)

$$\frac{1}{\sigma_s} = \frac{\cos^4 \alpha}{\sigma_0} + \frac{\sin^4 \alpha}{\sigma_{90}} + \sin^2 \alpha \cos^2 \alpha \left(\frac{4}{\sigma_{45}} - \frac{1}{\sigma_0} - \frac{1}{\sigma_{90}} \right). \quad (51)$$

In the xy plane, Eq. (48) gives

$$\frac{1}{\tau_d} = \frac{\cos^2 2\alpha}{\tau_0} + \frac{\sin^2 2\alpha}{\tau_{45}}, \quad (52)$$

where, as before (see Section 5), for the xy planes of symmetry of the material, $\sigma_x^{(0)} = \sigma_0$, $\sigma_y^{(0)} = \sigma_{90}$ and $\sigma_{xy}^{(45)} = \sigma_{45}$.

In Section 5, analogous Eq. (38) and (40) corresponded to the two dimensional problem. A distinctive feature of them was that all the strength characteristics there were squared and not to the first power, as in Eq. (51) and (52).

From Eq. (51) and (52), we obtain equations for curves through which the strength surface should pass (see Section 7, Fig. 19-21). For this, we change to the σ_x , σ_y and τ_{xy} coordinate system, in which the strength criteria can be represented geometrically in the form of some limit surface.

After jointly solving Eq. (51) and (37), we obtain equations for the P or C curve, which reflects the results of uniaxial tensile or compressive testing of variously oriented samples in σ_x , σ_y and τ_{xy} coordinates:

$$\left. \begin{aligned} \sigma_s &= \frac{\sigma_x^2}{\sigma_0} + \frac{\sigma_y^2}{\sigma_{00}} + \tau_{xy}^2 \left(\frac{4}{\sigma_{45}} - \frac{1}{\sigma_0} - \frac{1}{\sigma_{00}} \right); \\ \tau_{xy}^2 - \sigma_x \sigma_y &= 0; \\ \sigma_s &= \sigma_x + \sigma_y. \end{aligned} \right\} \quad (53)$$

From Eq. (52) and (39), we obtain equations for the T curve, which reflects the results of pure shear testing of variously oriented samples in σ_x , σ_y and τ_{xy} coordinates:

$$\left. \begin{aligned} \tau_s &= \frac{\tau_{xy}^2}{\tau_0} + \frac{\sigma_x^2}{\tau_{45}}; \\ \sigma_x + \sigma_y &= 0; \\ \tau_s &= \sqrt{\sigma_x \sigma_y - \tau_{xy}^2} \end{aligned} \right\} \quad (54)$$

or, more briefly, for the P and C curves:

$$\left. \begin{aligned} \frac{\sigma_x^2}{\sigma_0} + \frac{\sigma_y^2}{\sigma_{00}} + \tau_{xy}^2 \left(\frac{4}{\sigma_{45}} - \frac{1}{\sigma_0} - \frac{1}{\sigma_{00}} \right) &= \sigma_x + \sigma_y; \\ \tau_{xy}^2 - \sigma_x \sigma_y &= 0, \end{aligned} \right\} \quad (55)$$

for the T curve:

$$\left. \begin{aligned} \frac{\tau_{xy}^2}{\tau_0} + \frac{\sigma_x^2}{\tau_{45}} &= \sqrt{\tau_{xy}^2 - \sigma_x \sigma_y}; \\ \sigma_x + \sigma_y &= 0. \end{aligned} \right\} \quad (56)$$

The P, C and T curves are presented in Fig. 19 b and 20 b.

We compile a strength surface equation in the form of a polynomial, which would contain Eq. (55) and (56), which follow from the tensorial formulas and are consistent with test data for a broad class of orthotropic materials.

To decide from the first of Eq. (56), this polynomial should have fourth and second power terms for the stresses.

Thus, experimentally verified Eq. (47) and (48) lead to equally hazardous stress functions, in the form of a fourth power polynomial [86, 87].

We write the desired polynomial in abbreviated form

$$a_{iklm} a_{nopr} \sigma_{ik} \sigma_{lm} \sigma_{no} \sigma_{pr} + e_{iklm} \sigma_{ik} \sigma_{lm} = 0 \quad (57)$$

or in expanded form with two dimensional stress (see stress notation in Table 7)

$$\begin{aligned}
 & a_{1111}\sigma_1^4 + a_{2222}\sigma_2^4 + 16a_{1122}\sigma_1^4 + 2a_{1111}a_{2222}\sigma_1^2\sigma_2^2 + 4a_{1122}^2\sigma_1^2\sigma_2^2 + \\
 & + 4a_{1111}a_{1122}\sigma_1^3\sigma_2 + 4a_{1111}a_{2222}\sigma_1\sigma_2^3 + 8a_{1111}a_{1122}\sigma_1^2\sigma_2^2 + \\
 & + 8a_{2222}a_{1122}\sigma_1^2\sigma_2^2 + 16a_{1122}a_{2222}\sigma_1\sigma_2 + e_{1111}\sigma_1^4 + e_{2222}\sigma_2^4 + \\
 & + e_{1122}\sigma_1^2\sigma_2^2 + e_{1122}\sigma_1\sigma_2^3 = 0. \tag{58}
 \end{aligned}$$

Here, symmetry of the coefficients which corresponds to orthogonal symmetry of the material and was presented in detail in [87], is assumed.

To find the coefficients of polynomial (58), we substitute the relationship $\sigma_{12}^2 = \sigma_{11}\sigma_{22}$, which follows from the second equation of system (55), and we raise the first equation of system (55) to the second power, and we compare the coefficients with the same powers of similar stresses. Then, we substitute $\sigma_{22} = -\sigma_{11}$, from the second equation of system (56), in Eq. (58), and we compare the result with the squared first equation of system (56). As a result, we obtain

$$\left. \begin{aligned}
 a_{1111} &= \frac{1}{\sigma_0}; \\
 a_{2222} &= \frac{1}{\sigma_{00}}; \\
 a_{1122} &= \frac{1}{4\tau_0}; \\
 2a_{1122} &= \frac{4}{\sigma_{45}} - \frac{1}{\sigma_0} - \frac{1}{\sigma_{00}} - \frac{1}{\tau_0} = \frac{1}{\sigma_0} + \frac{1}{\sigma_{00}} - \frac{1}{\tau_{45}}
 \end{aligned} \right\} \tag{59}$$

and

$$e_{1111} = e_{2222} = e_{1122} = e_{1122} = -1. \tag{60}$$

Then, Eq. (58) takes the following form:

$$\begin{aligned}
 & \frac{\sigma_1^4}{\sigma_0} + \frac{\sigma_y^4}{\sigma_{00}} + \frac{\tau_{xy}^4}{\tau_0^2} + \sigma_x^2\sigma_y^2 \left[\frac{2}{\sigma_0\sigma_{00}} + \left(\frac{4}{\sigma_{45}} - \frac{1}{\sigma_0} - \frac{1}{\sigma_{00}} - \frac{1}{\tau_0} \right)^2 \right] + \\
 & + 2\sigma_x\sigma_y \left(\frac{\sigma_x^2}{\sigma_0} + \frac{\sigma_y^2}{\sigma_{00}} \right) \left(\frac{4}{\sigma_{45}} - \frac{1}{\sigma_0} - \frac{1}{\sigma_{00}} - \frac{1}{\tau_0} \right) + \frac{2\sigma_x^2\tau_{xy}^2}{\sigma_0\tau_0} + \\
 & + \frac{2\sigma_y^2\tau_{xy}^2}{\sigma_{00}\tau_0} + \frac{2\sigma_x\sigma_y\tau_{xy}^2}{\tau_0} \left(\frac{4}{\sigma_{45}} - \frac{1}{\sigma_0} - \frac{1}{\sigma_{00}} - \frac{1}{\tau_0} \right) - \\
 & - \sigma_x^2 - \sigma_y^2 - \sigma_{xy}^2 - \tau_{xy}^2 = 0
 \end{aligned} \tag{61}$$

or

$$\begin{aligned}
 & \left[\frac{\sigma_x^2}{\sigma_0} + \frac{\sigma_y^2}{\sigma_{00}} + \frac{\tau_{xy}^2}{\tau_0} + \sigma_x\sigma_y \left(\frac{4}{\sigma_{45}} - \frac{1}{\sigma_0} - \frac{1}{\sigma_{00}} - \frac{1}{\tau_0} \right) \right]^2 - \\
 & - \sigma_x^2 - \sigma_y^2 - \sigma_x\sigma_y - \tau_{xy}^2 = 0.
 \end{aligned} \tag{62}$$

With Eq. (60) kept in mind, in place of Eq. (57), we write the following expression:

$$a_{iklm}a_{nopr}\sigma_{ik}\sigma_{lm}\sigma_{no}\sigma_{pr} - \frac{(\sigma_{ik}\delta_{ik})^2 + \sigma_{ik}\sigma_{ik}}{2} = 0. \quad (63)$$

Eq. (63) is an invariant expression of the equally hazardous stress functions written in abbreviated (tensor) form in the form of a fourth power polynomial. In particular cases of uniaxial and pure shearing stresses, randomly oriented to the x, y and z axes of symmetry of an orthotropic material, from this strength criterion, tensorial Eq. (47), (48), (49) and (50) follow, which approximate test results well.

Eq. (63) can be written thus: /46

$$a_{iklm}\sigma_{ik}\sigma_{lm} = \sqrt{\frac{(\sigma_{ik}\delta_{ik})^2 + \sigma_{ik}\sigma_{ik}}{2}}. \quad (64)$$

In this form, it is more convenient to compare the proposed criterion with the quadratic criterion (Section 5).

In Eq. (64), to determine coefficients a_{iklm} , the same two dimensional stresses as were used for determination of the coefficients in Eq. (23) can be used:

$$\begin{aligned} 1) \quad & \sigma_x = \tau_{xy} = 0; \quad \sigma_y = \sigma_0; \quad a_{1111} = \frac{1}{\sigma_0}; \\ 2) \quad & \sigma_x = \tau_{xy} = 0; \quad \sigma_y = \sigma_0; \quad a_{2222} = \frac{1}{\sigma_0}; \\ 3) \quad & \sigma_x = \sigma_y = 0; \quad \tau_{xy} = \tau_0; \quad 4a_{1212} = \frac{1}{\tau_0}; \\ 4) \quad & \sigma_x = \sigma_y = \tau_{xy} = \frac{\sigma_0}{2}; \quad 2a_{1122} = \frac{4}{\sigma_0} - \frac{1}{\sigma_0} - \frac{1}{\sigma_0} - \frac{1}{\tau_0}; \\ 5) \quad & \sigma_x = -\sigma_y = \tau_{xy}; \quad \tau_{xy} = 0; \quad 2a_{1122} = \frac{1}{\sigma_0} + \frac{1}{\sigma_0} - \frac{1}{\tau_0}. \end{aligned} \quad | \quad (65)$$

The numbering of these equations (1-5) corresponds to the special cases of limiting stresses (see pp. 27-28).

From Eq. (64), for the two dimensional problem, we obtain

$$\begin{aligned} & \frac{\sigma_1 + \sigma_0 \tau_0 + \tau_0 + \sigma_0}{\tau_0} = \\ & = \left(\frac{\sigma_1}{1} - \frac{\sigma_0}{1} + \frac{\sigma_0}{1} \right) \tau_0 \sigma_0 + \frac{\sigma_1}{\tau_0} + \frac{\sigma_0}{\tau_0} + \frac{\sigma_0}{\tau_0} \end{aligned} \quad (66)$$

or

$$\begin{aligned} & \frac{\sigma_1 + \sigma_0 \tau_0 + \tau_0 + \sigma_0}{\sigma_0} = \\ & = \left(\frac{\sigma_1}{1} - \frac{\sigma_0}{1} - \frac{\sigma_0}{1} - \frac{\sigma_0}{1} \right) \tau_0 \sigma_0 + \frac{\sigma_1}{\tau_0} + \frac{\sigma_0}{\tau_0} + \frac{\sigma_0}{\tau_0} \end{aligned} \quad (67)$$

If it is assumed again that the safety factors (see Section 5) are approximately the same for different directions in the material, for practical application, the following strength condition is obtained from the fourth power criterion in two dimensional stress:

$$\frac{\sigma_x^2 + \sigma_y^2 + c\sigma_x\sigma_y + d\tau_{xy}^2}{\sigma_x^2 + \sigma_y^2 + \tau_{xy}^2 + \sigma_x\sigma_y} \leq [\sigma_{el.}] \quad (68)$$

where $[\sigma_0] = \sigma_0/k$ is the permissible longitudinal stress coincident with the x axis of symmetry of the material (the axis of greatest strength); $\sigma_x, \sigma_y, \tau_{xy}$ are the normal and tangential stresses at the same place (at one point) of the part, in areas perpendicular to the x and y axes of symmetry of the material; /47

$$c = \frac{\sigma_0}{\sigma_{43}}; \quad e = 4a - c - d - 1; \quad a = \frac{\sigma_0}{\sigma_{43}}; \quad d = \frac{\sigma_0}{\tau_0}.$$

Examples of the application of strength condition (68) are presented in Section 14.

Eq. (66) is obtained from Eq. (4.17) of [36], if the following is assumed in the latter:

$$\lambda = \frac{2}{\sigma_0\tau_0}; \quad \mu = \frac{2}{\sigma_0\tau_0}; \quad \rho = 0,$$

i.e., third power stress terms are excluded [87].

Fourth power strength criteria which do not contain third power terms, the advisability of study of which was shown (on other considerations) in [48], contain four strength characteristics of an orthotropic material in the case of the two dimensional problem but, in the general case of six dimensional stress space (Eq. (64)), nine such characteristics.

The criteria can be generalized to materials of differing tensile and compressive strengths, if the piecewise approximation method presented in detail in Section 7 is used. Without the use of the piecewise approximation, Eq. (64) only fits material with complete inversion symmetries of the strength characteristics, just as in Eq. (23). In the piecewise approximation method, the equation is written twice: separately for that part of the strength surface (see Section 7) which is on one side of the diagonal plane passing vertically through curve T and separately for the other part of the surface.

Eq. (66) or (67) describes the surface in the $\sigma_x, \sigma_y, \tau_{xy}$ coordinate system. In this equation, the strength surface has an isolated singular point, the coordinate origin. The isolation of this point can be shown analytically, if the surface intersection curve is analyzed (see Eq. (66)), from a coordinate plane for which $\sigma_y = 0$. The equation of this curve has the following form:

$$j = \frac{\sigma_x^4}{\sigma_0} + \frac{\tau_{xy}^4}{\tau_0} + \frac{2\sigma_x^2\tau_{xy}^2}{\sigma_0\tau_0} - \sigma_x^2 - \sigma_y^2 = 0. \quad (69)$$

It is easy to see that both partial derivatives of this function with variable σ_x and τ_{xy} revert to zero at $\sigma_x = \tau_{xy} = 0$. For proof of the isolation, it is sufficient to show that the expression for A has a negative value at the singular point:

$$A = \left[\frac{\partial^2 f}{\partial \sigma_x \partial \tau_{xy}} \right]^2 - \frac{\partial f}{\partial \sigma_x} \cdot \frac{\partial f}{\partial \tau_{xy}}.$$

Simple calculations show that $A = -4$ at $\sigma_x = \tau_{xy} = 0$, i.e., the coordinate origin is an isolated singular point of the curve plotted from Eq. (69) and, consequently, the surface plotted from Eq. (66).

There are no experimental data for strongly anisotropic materials which permit exhaustive testing of the strength criterion. Experimental data on uniaxial and some biaxial stresses permit Eq. (64) to be considered a strength criterion which does not contradict test data for many anisotropic materials under two dimensional stress (see Sections 7 and 14).

Fourth power strength criteria (Eq. (64)) fit a broader class of materials than the quadratic criterion (Eq. (23)) and, in simple cases of practical importance, it results in more convenient formulas.

For such slightly anisotropic materials as pressure worked metals and many fiberglass plastics, calculations by criteria (64) and (23) give results very close to each other, although Eq. (64) does not lead to Eq. (23).

For equal biaxial compression with $\sigma_x = \sigma_y = \sigma_d$, $\sigma_z = 0$ and $\tau_{xy} = 0$, there follows from the fourth power criterion (Eq. (66))

$$\sigma_d = \frac{\tau_0 \sigma_{45} \sqrt{3}}{4\tau_0 - \sigma_{45}}, \quad (70)$$

which leads to unlikely values, only when the values of σ_{45} are close to $4\tau_0$, i.e., in the event $\tau_0 \ll \sigma_{45}/4$. This relationship of the strength characteristics does not occur, even for a material with such a low shearing strength as wood.

Thus, in biaxial compression, the fourth power criterion better fits materials with low shearing strength than the quadratic criterion.

In determination of σ_d by Eq. (45), based on the quadratic criterion, it had unlikely values, even with $\tau_0 \ll \sigma_{45}/2$.

As a result of hydrostatic pressure p, from Eq. (64), we obtain

$$p_0 = \frac{\sqrt{6}}{\sigma_{45} \delta_{45} \delta_{45}}. \quad (71)$$

With the same data as in Section 5, calculation by Eq. (71) gives $p_0 = 18 \text{ kg/cm}^2$ for pine wood, i.e., a value consistent with the data of [18] and close to the results of the use of the quadratic criterion.

The condition of sensitivity of the strength criterion to equal all around compression requires that there be some hydrostatic pressure, which is capable of putting the material in hazardous condition, even in the case of an isotropic material.

We investigate both strength criteria (quadratic and fourth power), under conditions of limiting transition to an isotropic material. In the event the material is isotropic, quadratic strength criterion Eq. (23) changes to the formula

$$\left(\frac{I_1}{\sigma_0}\right)^2 + \frac{I_2 - I_1^2}{2\tau_0^2} = 1, \quad (72)$$

where I_1 and I_2 are the invariants of the stress tensor calculated by Eq. (19) and (20); σ_0 and τ_0 are the hazardous stresses for an isotropic material under uniaxial and pure shearing stresses. In developed form, Eq. (72) has the following form

$$(\sigma_x - \sigma_y - \sigma_z)^2 + \left(\frac{\sigma_0}{\tau_0}\right)^2 (\tau_{xx}^2 + \tau_{yy}^2 + \tau_{zz}^2 - \sigma_x \sigma_y - \sigma_y \sigma_z - \sigma_z \sigma_x) = \sigma_0^2 - \quad (73)$$

Thus, in the case of an isotropic material, the quadratic criterion requires experimental determination of two constants of the material, σ_0 and τ_0 . A decrease of the number of constants to one can be produced, only as a consequence of assuming that the strength criterion is insensitive to the addition of hydrostatic pressure. This assumption (Eq. (24)) leads to the known relationship between the strength characteristics of an isotropic material

$$\tau_0 = \frac{\sigma_0}{\sqrt{3}},$$

which is experimentally confirmed for few isotropic materials. Thus, for example, it is known that, for many rocks [49] and some homogeneous plastics [50], there is the following relationship

$$\tau_0 < \frac{\sigma_0^{\text{com}}}{2}.$$

With $\sigma_0^2 = 3\tau_0^2$, i.e., on the assumption of insensitivity of the material to the addition of hydrostatic pressure, Eq. (72) changes to the equation known by the name of the Mises plasticity condition

$$\frac{3I_2 - I_1^2}{2} = \sigma_0^2, \quad (74)$$

or, in developed form in the principal stresses:

$$(\sigma_1 - \sigma_0)^2 + (\sigma_2 - \sigma_0)^2 + (\sigma_3 - \sigma_0)^2 = 2\sigma_0^2. \quad (75)$$

The fourth power strength criterion (Eq. (64)), upon transition to an isotropic material, has this form:

$$\frac{I_1^2}{\sigma_0} + \frac{I_3^2 - I_1^2}{3\tau_0} = \sqrt{\frac{2I_1^2 + I_3^2}{3}}, \quad (76)$$

where

$$I_1 = \sqrt{\frac{3I_2^2 - I_3^2}{2}}.$$

In this nomenclature, i.e., I_1 and I_3 , the quadratic criterion (Eq. (72)) is written

$$\frac{I_1^2}{\sigma_0^2} + \frac{I_3^2 - I_1^2}{\tau_0^2} = 1. \quad (77)$$

In the special case of two dimensional stress, when $\sigma_y = \sigma_z = \tau_{zy} = \tau_{zx} = 0$, from the quadratic criterion sensitive to hydrostatic pressure (Eq. (73)), we obtain the following expression:

$$\sqrt{\sigma_x^2 + \left(\frac{\sigma_0}{\tau_0}\right)^2 \tau_{xy}^2} = \sigma_0. \quad (78)$$

Two strength characteristics of the material, σ_0 and τ_0 , are included in this formula, only because the effect of all around tension (compression) was taken into account.

The criteria for testing fatigue strength of steel bars, which have been confirmed experimentally and in practice, usually are written in this form.¹

Thus, in calculation of the fatigue strength of isotropic materials, strength criteria sensitive to hydrostatic pressure evidently should be used.

The fourth power criterion (Eq. (76)) for this case gives

$$\frac{\sigma_x^2 + \left(\frac{\sigma_0}{\tau_0}\right)^2 \tau_{xy}^2}{\sqrt{\sigma_x^2 + \tau_{xy}^2}} = \sigma_0.$$

¹Data are presented in the book of Veybull [78], which experimentally confirm the effect of hydrostatic pressure on fatigue strength.

For a graphical representation of the criterion, we plot I_1 on the abscissa and I_3 on the ordinate. Then, from Eq. (76) and (77), we obtain the curves presented in Fig. 18. The dependence on the maximum octahedral tangential stress on hydrostatic pressure can be decided from this figure. Accordingly, strength criteria sensitive to hydrostatic pressure (quadratic and fourth power) can be interpreted as a certain generalization of the strength theory of Mohr ([92], p. 117). /51

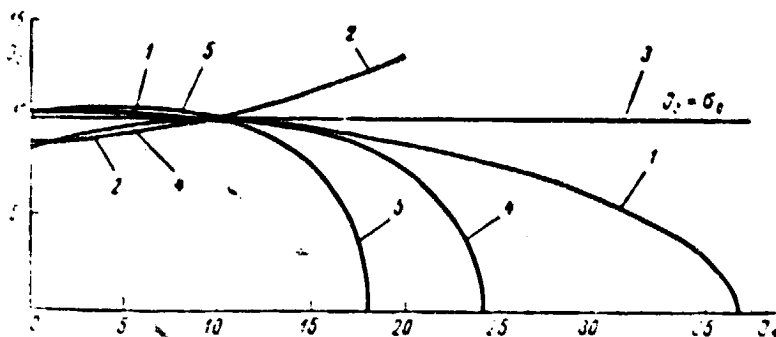


Fig. 18. Limit curves $I_3 = f(I_1)$ for isotropic material with various ratios of strength σ_0 and τ_0 (curves 1, 2 and 3 plotted from Eq. (77), based on quadratic criterion; curves 4 and 5, from Eq. (76), based on fourth power criterion): 1 and 5. $\sigma_0:\tau_0=5:3$; 2 and 4. $\sigma_0:\tau_0=[illegible]:2$; 3. $\sigma_0:\tau_0=\sqrt{3}$.

Eq. (76) and (77) can be compared with the results of the compression tests of S.B. Aynbinder, on polymer samples exposed to hydrostatic pressure [30, 50]. In this case, the values of σ_0/τ_0 calculated by Eq. (76) will be higher than the same value calculated by Eq. (77), and they will correspond quite well with experiments.

7. Strength Surfaces

For two dimensional stress, the stress tensor can represent a point in an orthogonal coordinate system, if those components of the tensor which act on the areas of symmetry of the material are laid out on the axes. If the two dimensional stress is randomly oriented in the xy plane of symmetry of the material, the stresses designated σ_x , σ_y and τ_{xy} must be laid out on the three coordinate axes. In simple (proportional) loading, the change in stresses σ_x , σ_y and τ_{xy} from the unloaded state to a hazardous or limiting state is represented by a ray, i.e., a straight line, through the coordinate origin. We call the locus of the points on such rays, which correspond to limiting or equally hazardous two dimensional stresses, a strength surface. The strength surface should have such a form that any ray drawn from the coordinate origin can intersect it only once. /52

We consider strength surfaces for orthotropic materials under simple static load, at constant temperature and with a low rate of brief tests.

It was noted in [48] that, at the present state of science, the appearance of the strength surface can only be explained empirically. A strength surface has to be plotted empirically, based on some amount of test data, and this surface then has to be described by mathematical relationships. The cause of development and nature of the hazardous state is not considered in such an approach. The same strength surface equation can correspond to hazardous states of varied physical character. The well known strength theory of Mohr for isotropic materials and all of its generalizations are based on approximately the same concepts.

Strength surfaces in two dimensional stress have been plotted from experimental data for several orthotropic materials [36, 37]. The results of experiments with variously oriented uniaxial and pure shearing and equal biaxial compressive stresses in the xy plane of symmetry of the material were used as the sources. Two such surfaces are presented in Fig. 19 c and 20 c, where the letters P and C designate curves which represent the results of tensile and compressive tests of variously oriented samples in σ_x , σ_y and τ_{xy} coordinates, and the letter T designates a curve which represents the results of pure shearing tests of variously oriented samples.²

The strength surface should contain P, C and T curves, which correspond to particular cases of limiting two dimensional stresses.

All the points in Fig. 19 a and 20 a were plotted from average results of testing variously oriented samples. We illustrate the plotting with an example. Let the average tensile strength of the material σ_B at an angle of 15° to the fibers (to the x axis) be σ_{15} . To plot a point which corresponds to the value of σ_{15} , the σ_x , σ_y and τ_{xy} coordinates of this point must be calculated by Eq. (37), with $\sigma_B = \sigma_{15}$ and $\alpha = 15^\circ$ (see Fig. 14). The results of compressive and shearing tests of variously oriented samples can be treated analogously. The coordinates of all points calculated from experimental data in this way are shown in Fig. 19 a and 20 a. /54

Besides, in the negative abscissa region (Fig. 19 a and 20 a), a point which corresponds to the averaged results of equal biaxial compressive testing, variously oriented in the xy plane, are plotted in planes for which $\tau_{xy} = 0$ [36]. The surfaces presented in Fig. 19 c and 20 c are plotted approximately, by graphical extrapolation of experimental data. Pine wood, the surface for which is shown in Fig. 20, can be considered a model of a strongly anisotropic material with low shearing strength.

Points which fit the strength surface located in the first positive

²An analysis of the experimental errors in producing this stress is given in [36].

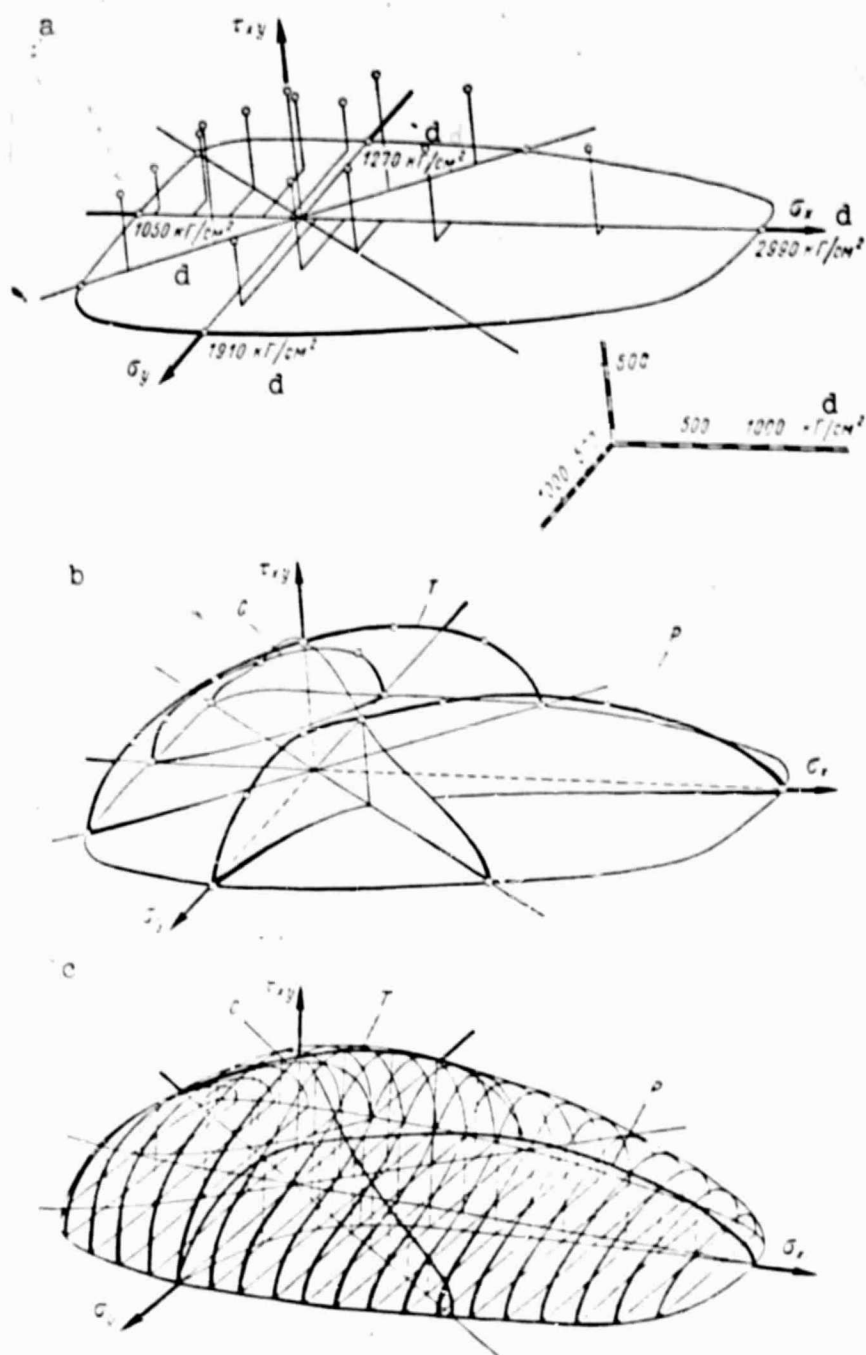
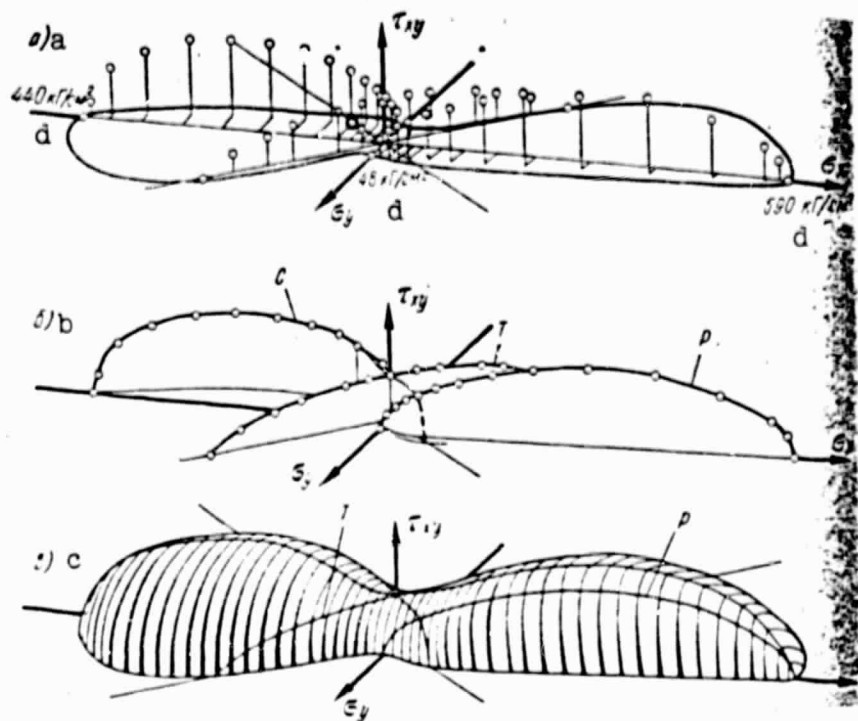


Fig. 19. Equally hazardous stress surface for cold cured fiberglass cloth plastic made of linen weave cloth on PN-1 polyester resins.

Key: $d. \text{ kg}/\text{cm}^2$

quadrant of the coordinate system were calculated for pine wood by fourth power Eq. (62). The calculations were performed in a Minsk-1⁴ digital computer. The initial data were the same as in plotting the surfaces (Fig. 20) [36], i.e., $\sigma_0 = 590 \text{ kg}/\text{cm}^2$, $\sigma_{90} = 48 \text{ kg}/\text{cm}^2$, $\sigma_{45} = 100 \text{ kg}/\text{cm}^2$ and $\tau_0 = 64 \text{ kg}/\text{cm}^2$. The surface, plotted from 1200 points, the /55

coordinates of which were calculated by Eq. (62), showed that the strength criterion in the form of a fourth power polynomial approximates the experimental data well, for such a strongly anisotropic material as wood [89].



ORIGINAL PAGE IS
OF POOR QUALITY

Fig. 20. Equally hazardous stress surface for pine wood.

Key: kg/cm^2

Part of a strength surface in the positive quadrant was given in [51], in which normal stresses σ_x and τ_y retain the same signs (positive). The surface was plotted from an equation (criterion) proposed by I.I. Gol'denblatt and V.N. Kopnov [52]. This criterion can be considered a generalization of the quadratic equally hazardous state function to a special type of material, in which there is no inversion symmetry of the strength characteristics. Test results presented in [51] showed better correspondence of the criterion with experiment.

The experimental data of [51] were used by the authors of [89], to plot a strength surface from the fourth power equation (see Section 6), and for testing the convergence of this equation with test data. The following initial data were used in the calculation [51]: $\sigma_0 = 4300 \text{ kg}/\text{cm}^2$; $\sigma_{90} = 2800 \text{ kg}/\text{cm}^2$; $\tau_0 = 1000 \text{ kg}/\text{cm}^2$; $\tau_{45} = 2120 \text{ kg}/\text{cm}^2$.

The coordinates of the points of the strength surface from these data and from the fourth power equation (Eq. (67)) were calculated in the Minsk-14 digital computer at the Military Academy of Logistics and Transport. The following notation was introduced for compilation of

the calculation program: $\sigma_x = X$; $\sigma_y = Y$; $\tau_{xy} = Z$. Then, the value of Z from Eq. (67) was expressed by X and Y in the following form:

$$Z = \pm \sqrt{\tau_0 \left[\left(\frac{\tau_0}{2} - XY \left(\frac{1}{\sigma_0} + \frac{1}{\sigma_{90}} + \frac{1}{\tau_{45}} \right) - \left(\frac{X^2}{\sigma_0} + \frac{Y^2}{\sigma_{90}} \right) \right] \pm \sqrt{\frac{\tau_0^2}{4} - X^2 \left(\frac{\tau_0}{\sigma_0} - 1 \right) - Y^2 \left(\frac{\tau_0}{\sigma_{90}} - 1 \right) - XY \left[\tau_0 \left(\frac{1}{\sigma_0} + \frac{1}{\sigma_{90}} - \frac{1}{\tau_{45}} \right) - 1 \right]} \right\}}. \quad (79)$$

The machine solution of Eq. (79) consisted of determination of the values of the ordinate Z_1 of each point of the strength surface, based on the assigned abscissas of this point X_1 and Y_1 . Values of X_1 and Y_1 were fed in at specific uniform intervals (steps), which were $0.02\sigma_0$ on the X axis and $0.02\sigma_{90}$ on the Y axis.

With $\sigma_0 > \sigma_{90}$, the region of change in values of X_1 which satisfied Eq. (79) is within $0 \leq X_1 \leq \sigma_0$, but the values of Y_1 can somewhat exceed σ_{90} .

Eq. (79) satisfies four values of Z_1 , i.e., four roots, of which two roots can be real numbers of equal absolute value, but opposite sign, and two can be complex numbers, or all four roots can be complex numbers. The latter case concerns those values of the X_1 and Y_1 abscissas, for which there are no points on the strength surface described by Eq. (79). Therefore, the following order was adopted in solution of this equation. For each value of the X_1 abscissa, in turn over equal intervals, the Y_1 abscissa was changed, and all ordinates of points Z_1 were calculated, until four complex roots were obtained. All positive real roots of Eq. (79) are Z_1 ordinates of points on the strength surface. Each pair of real values of Z_1 (positive and negative) on the machine printout corresponds to a pair of numbers which designates the characteristic and mantissa of the desired value. The number of complex roots of the equation also is indicated on the tape. /56

The surface presented in Fig. 21 was plotted in the positive quadrant from points, the coordinates of which were calculated by the method indicated above, by the fourth power strength criterion, i.e., by Eq. (79). The coordinates of 1200 points were calculated for plotting the surface. The portion of the points with the same abscissas $X_1 = \sigma_x$ was connected by curved lines. In order to compare the surface plotted by the fourth power criterion (Eq. (67)) with experimental data, V.D. Protasov and V.N. Kopnov had to plot points corresponding to these data on the surface (Fig. 21). For this, individual values of X_1 and Y_1 were fed in directly from the keyboard, and the ordinates of points Z_1

required for comparison of the calculated values with the experimental data of [51] were determined by Eq. (79). Everywhere, these points lay quite close to the surface plotted by the fourth power criterion.

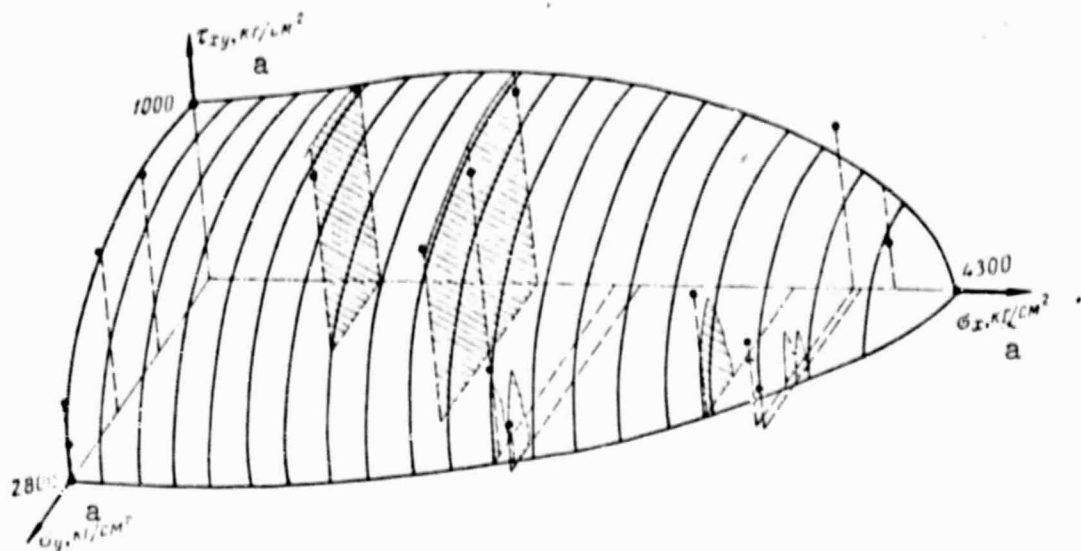


Fig. 21. Equally hazardous two dimensional stress surface for fiberglass laminate, plotted from fourth power criterion: •. [51] experimental data.

Key: a. kg/cm^2

The strength criterion in the form of a fourth power polynomial was thus confirmed for fiberglass laminates by the experiments of [51].

The strength surfaces shown in Fig. 19 and 20 were plotted from the results of testing variously oriented flat samples, and the surface presented in Fig. 21 was plotted from the results of testing tubing. In determination of the strength characteristics of anisotropic materials in directions not coincident with the axes of symmetry, both test methods are used. [28, 47, 84, 85] dealt with comparison of the results of testing flat and tubular samples.

In comparing Fig. 19 and 21, it can be concluded that the fourth power polynomial describes the strength surface sufficiently well in both methods of obtaining experimental data.

There is interest in examination of the shape of the strength surface in the limiting transition to an isotropic material. /58

The strength surface of an isotropic material should cut out identical segments on the coordinate axes on which normal stresses σ_x and σ_y are plotted (Fig. 22). The line of intersection of this surface with the vertical coordinate plane (for example, curve 1 with $\sigma_y = 0$) represents the Mohr envelop, and the line of intersection of the surface with the coordinate plane for which $\tau_{xy} = 0$ (curve 2) is an elliptical curve (the Mises ellipse), in coordinates equal to the principal stresses. Some

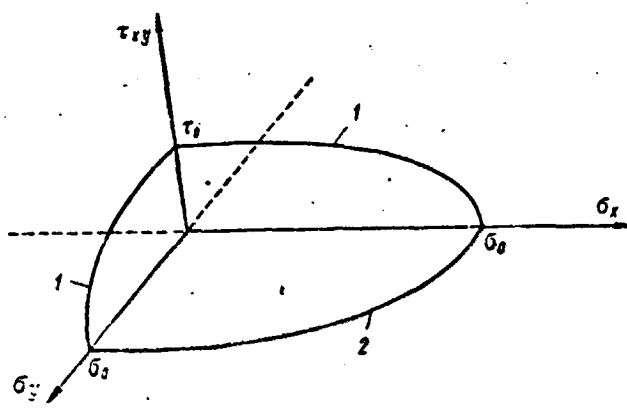


Fig. 22. Equally hazardous two dimensional stress surface for isotropic material (limiting transition).

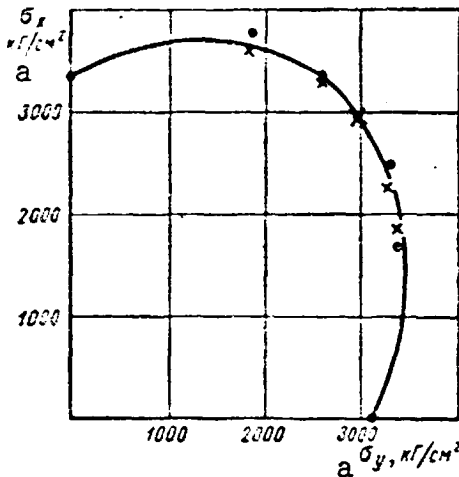


Fig. 23. Comparison of results of calculation by strength criteria and experimental data of [53]: ●. experimental data; x. quadratic criterion calculation (Eq. (81)); curve plotted by fourth power criterion (Eq. (85)).

Key: a. kg/cm²

idea of the actual shape of curve 2 can be obtained, by examining the results of biaxial tensile testing of rolled steel samples. Such a curve is plotted in Fig. 23 from the experimental data of [53] and the fourth power strength criterion.

Tubular samples of rolled 45 steel were tested by V.N. Bastun and N.I. Chernyak [53], by combined internal pressure and axial loading. The yield stress as a result of separate longitudinal σ_x and tangential σ_t stresses was determined from the $\sigma_t = f(\epsilon_t)$ curves, at points corresponding to $\epsilon_{0.2}$. The results of these tests are presented in Table 10. In these experiments, the principal stresses were in the x and y axes of symmetry of the material.

We compare the experimental data of [53] with the quadratic strength functions (see Section 5), for which we again determine coefficients A_{iklm} in Eq. (29) in the following manner.

After substituting $\tau_{xy} = 0$ in Eq. (29), we obtain

$$A_{1111}\sigma_x^2 + A_{2222}\sigma_y^2 + 2A_{1122}\sigma_x\sigma_y = 1,$$

and we then determine the values of coefficients A_{iklm} from three tests, the data of which are in Table 10:

$$\begin{aligned} 1) \quad & \sigma_x = 32,8 = \sigma_0; \quad \sigma_y = 0; \quad A_{1111} = \frac{1}{\sigma_0^2} = \frac{1}{32,8^2}, \\ 2) \quad & \sigma_y = 30,5 = \sigma_0; \quad \sigma_x = 0; \quad A_{2222} = \frac{1}{\sigma_0^2} = \frac{1}{30,5^2}, \\ 3) \quad & \sigma_x = \sigma_y = 29,0 = \sigma_0; \quad 2A_{1122} = \frac{1}{\sigma_0^2} - \frac{1}{\sigma_0^2} - \frac{1}{\sigma_0^2} = \\ & = \frac{1}{29^2} - \frac{1}{32,8^2} - \frac{1}{30,5^2}, \end{aligned}$$

TABLE 10. HAZARDOUS PRINCIPAL STRESSES IN
TWO DIMENSIONAL STRESS (kg/cm^2)

a Эксперимент [53]	Вычисле- ние по формуле (81)	
	$\sigma_t = \sigma_x$	$\sigma_t = \sigma_y$
3350	0	3350
3785	1835	3620
1695	3380	1890
2960	2960	2960
0	3110	0
3350	2580	3320
2510	3285	2330

Key: a. Experiment [53] b. Calculation by Eq. (81)

where σ_d is the strength under equal biaxial tension.

After this, Eq. (29) takes this form

$$\frac{\sigma_x^2}{\sigma_0^2} + \frac{\sigma_y^2}{\sigma_{30}^2} + \sigma_x \sigma_y \left(\frac{1}{\sigma_0^2} - \frac{1}{\sigma_{30}^2} - \frac{1}{\sigma_{30}^2} \right) = 1 \quad (80)$$

or

$$\frac{\sigma_x^2}{32,8^2} + \frac{\sigma_y^2}{30,5^2} + \sigma_x \sigma_y \left(\frac{1}{29,0^2} - \frac{1}{32,8^2} - \frac{1}{30,5^2} \right) = 1. \quad (81)$$

The results of calculation of $\sigma_x = \sigma_y$ by Eq. (81), obtained from the quadratic criterion (Eq. (29)), are presented in the third column of Table 10. In Fig. 23, they are marked by crosses and the experimental data, by dots. The curve was plotted from the fourth power criterion. For this, the following were assumed in Eq. (58): $\sigma_{12} = 0$ and

$$\left. \begin{array}{l} 1) \sigma_{22} = 0; \sigma_{11} = \sigma_0 = 32,8; a_{1111} = \frac{1}{\sigma_0}; \\ 2) \sigma_{11} = 0; \sigma_{22} = \sigma_{30} = 30,5; a_{2222} = \frac{1}{\sigma_{30}}; \\ 3) \sigma_{11} = \sigma_{22} = \sigma_0 = 29,0; 2a_{1122} = \frac{1}{\sigma_0} - \frac{1}{\sigma_0} - \frac{1}{\sigma_{30}}. \end{array} \right\} \quad (82)$$

With $\sigma_{12} = 0$, Eq. (58) will have this form:

$$(a_{1111}\sigma_x^2 + a_{2222}\sigma_y^2 + 2\sigma_x \sigma_y a_{1122})^2 = \sigma_x^2 + \sigma_y^2 + \sigma_x \sigma_y, \quad (83)$$

and, after substitution of the values of the coefficients from Eq. (82) in it, it takes the following form:

$$\frac{\sigma_x^2}{\sigma_0} + \frac{\sigma_y^2}{\sigma_{90}} + \sigma_x \sigma_y \left(\frac{\sqrt{3}}{\sigma_d} - \frac{1}{\sigma_0} - \frac{1}{\sigma_{90}} \right) = 1 - \sqrt{\sigma_x^2 + \sigma_y^2 + \sigma_x \sigma_y}. \quad (84)$$

To plot the curve from Eq. (84), we assigned a variable value of the ratio of the principal stresses $K = \sigma_y/\sigma_x$. By substituting $\sigma_y = K\sigma_x$ in Eq. (84), we obtain the following equation, for finding the hazardous value of σ_x as a function of K :

$$\sigma_x = \frac{\sqrt{1 - K + K^2}}{\left[\frac{1}{\sigma_0} + \frac{K^2}{\sigma_{90}} + K \left(\frac{\sqrt{3}}{\sigma_d} - \frac{1}{\sigma_0} - \frac{1}{\sigma_{90}} \right) \right]}. \quad (85)$$

TABLE 11. CALCULATION OF LIMIT CURVE COORDINATES (FIG. 23) BY EQ. (85)

K	σ_x	$\sigma_y = K\sigma_x$
0	3350	0
0.25	3690	923
0.50	3660	1830
0.75	3345	2510
1.00	2960	2960
1.50	2235	3350
2.00	1750	3455
3.00	1170	3465
4.00	867	3430

The results of calculation of $\sigma_x = \sigma_y$ by Eq. (85) are presented in Table 11, from which the curve of Fig. 23 was plotted. This curve is a good approximation of the test data. The results of calculation by the quadratic criterion (x's) are close to the curve plotted from the fourth power criterion, i.e., by Eq. (85).

Thus, with the principal stresses σ_x and σ_y along the axes of symmetry of an orthotropic material with slight anisotropy, the fourth power criterion gives a curve, the outline of which is close to a Mises ellipse, although Eq. (84) differs from Eq. (80). Both formulas fit the experimental data well. A characteristic feature of Eq. (80) and (84) is that not two, but three initial experimentally determined values of the characteristics of orthotropic materials, σ_0 , σ_{90} and σ_d , are included in them. This is due to the assumption that hydrostatic pressure affects the hazardous state of the material.

For an isotropic material, the following equation of limit curve

z (Fig. 22) is obtained from Eq. (80):

$$\sigma_x^2 + \sigma_y^2 + \sigma_x \sigma_y \left[\left(\frac{\sigma_0}{\sigma_0} \right)^2 - 2 \right] = \sigma_0^2, \quad (86)$$

where σ_0 is the hazardous stress in uniaxial and σ_d is the hazardous stress in equal biaxial tension (or compression).

For an isotropic material, Eq. (84) gives

$$\frac{\sigma_x^2 + \sigma_y^2 + \sigma_x \sigma_y \left(\sqrt{3} - \frac{\sigma_0}{\sigma_0} - 2 \right)}{\sigma_x^2 + \sigma_y^2 + \sigma_x \sigma_y} = \sigma_0. \quad (87)$$

In Eq. (86) and (87), the principal stresses σ_x and σ_y have the same sign, as applied to the data of [53] and Fig. 23, but for an isotropic material.

It is evident that formulas which contain two initial values can better approximate test results than conventional formulas, plotted on the assumption of invariability of the hazardous state functions upon addition of hydrostatic pressure, and which contain one such value.

The use of Eq. (86) and (87) evidently can prove to be advisable, in case accurate calculations are required. For metals, both equations give approximately the same results, but the second has an advantage if the material has low shearing strength.

CHAPTER 3. ANISOTROPY OF STRENGTH CHARACTERISTICS FROM EXPERIMENTAL DATA

8. Strength and Plasticity of Metals

The anisotropy of a pressure worked metal has been known for a very long time [21]. The explanation of the anisotropy of pure metals and solid solutions is that, during plastic deformation, the crystallites take on the shape of elongated disks, and their crystallographic axes become parallel to each other. This produces an oriented structure (texture). /62

The nature of the anisotropy can vary, depending on the structure of the metal. A minimum tensile strength at an angle to 45° to the rolling direction is characteristic of rolled copper and aluminum. The strength of brass decreases gradually away from the rolling direction, and it reaches a minimum in the transverse direction. The transverse strength of zinc is greater than in the rolling direction (Fig. 24).

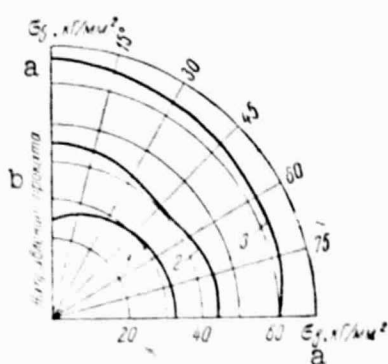


Fig. 24. Polar diagram of tensile strength σ_B of rolled nonferrous metal sheet, plotted from data of [21]: 1. zinc; 2. pure copper; 3. brass.

Key: a. kg/mm^2
b. Rolling direction

Tension is the most convenient method of testing the degree of anisotropy of a metal. Not only the strength, but the elastic limit and yield stress, as well as the plasticity characteristics display anisotropy under tension. In this case, the degree of anisotropy differs for different characteristics, and it can be different under tension and compression.

The tensile and compressive strength characteristics of an aluminum-magnesium alloy are presented in Table 12 [23]. Almost all the strength characteristics /63 of this alloy are lower under tension and higher under compression in the rolling direction than in the perpendicular direction.

Curves (Fig. 25) were plotted from the data of Table 12 and by Eq. (49), which show that the nature of anisotropy of this alloy is completely different under tension and under compression.

Fig. 26 shows curves of the change in strength of rolled aluminum sheet after annealing and recrystallization. The strength along and across the rolling direction is nearly the same but, as a result of the different texture, the strength of some sheets on the diagonal was higher and, for others, lower, than in the rolling direction.

Data on the anisotropy of the mechanical properties of cold rolled aluminum under tension are presented in Table 13 [54]. In this case, all the mechanical properties are most characteristic at an angle of

TABLE 12. TENSILE AND COMPRESSIVE STRENGTH CHARACTERISTICS OF ALUMINUM-MAGNESIUM ALLOY

a Характеристики прочности, кг/мм ²	Растяжение		Сжатие		
	b d ∠ гол с направлением проката, град		c		
	0	45	90	0	45
e _{0.02}	8.5	5.3	9.4	10.4	6.3
f _{0.2}	14.0	11.7	18.1	20.3	10.8
g _B	16.0	18.5	23.0	39.8	35.2

Key: a. Strength characteristic; b. Elastic limit $\sigma_{0.02}$, kg/mm²; c. Tension; d. Compression; e. Angle to rolling direction, degrees; f. Yield stress $\sigma_{0.2}$; g. Strength σ_B

45° to the rolling axis (see Fig. 24, curve 2, and Fig. 25, curve 6).

The Fig. 27 curves were plotted by Eq. (41) and (49), for Ergal aluminum alloy [55]. As is evident from this figure, both equations give practically coincident results. The anisotropies of the ultimate strength σ_B and the yield stress $\sigma_{0.2}$ of Avional aluminum alloy are compared in Fig. 28. The curves were plotted by Eq. (49), based on the data of [55].

Anisotropy of the ultimate strength and yield stress of domestic light alloys were investigated in the greatest detail in [12, 13, 88]. Samples were cut from hot extruded 42x250 mm cross section strips, at various angles to the axes of symmetry in the planes of extrusion and in the two vertical planes of symmetry of the stress. The ultimate strength σ_B anisotropy proved to be most significant in the plane of the sheet (Fig. 29 a). Through the strip, i.e., in the planes perpendicular to the sheet and parallel to the direction of extrusion, considerable anisotropy of yield stress $\sigma_{0.2}$ was found (Fig. 29 c).

Fig. 25. Anisotropy of tensile (solid curves) and compressive (dashed curves) strength characteristics of aluminum-magnesium alloy: 1 and 2. elastic limit $\sigma_{0.02}$; 3 and 4. yield stress $\sigma_{0.2}$; 5 and 6. strength σ_B .

Key: a. kg/mm²

Eq. (49) was tested by P.G. Miklyayev and Ya.B. Friedman, as applied to the strength characteristics of light alloys, and it demonstrated good convergence with the experimental data, including directions not in the planes of symmetry of the material.

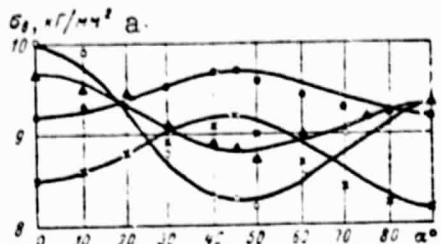


Fig. 26. Curves of change of tensile strength of rolled aluminum sheet after annealing and recrystallization, plotted by Eq. (49):
 ○ ● ▲ x experimental data of [23].

Key: a. kg/mm^2

TABLE 13. TENSILE ANISOTROPY OF MECHANICAL PROPERTIES OF ALUMINUM

Механические свойства a.	Угол с направлением проката, град b.		
	0	45	90
c. Предел текучести σ_T , kg/mm^2	3,2	2,0	2,8
d. Предел прочности σ_B , kg/mm^2	6,8	7,8	6,9
e. Относительное удлинение δ , %	20	43	27
f. Относительное сужение ψ , %	92	86	91

Key: a. Mechanical property
 b. Angle with rolling direction, degrees
 c. Yield stress σ_T , kg/mm^2
 d. Ultimate strength σ_B , kg/mm^2
 e. Relative elongation δ , %
 f. Relative waist ψ , %

Thus, the experimental data of many authors on the anisotropy of the strength and plasticity characteristics of metals confirm the applicability of Eq. (49), which originated from the fourth power criterion and permits study of the anisotropy of a material to be limited to experimental determination of the characteristic under study in three /65 directions: longitudinal, transverse and diagonal.

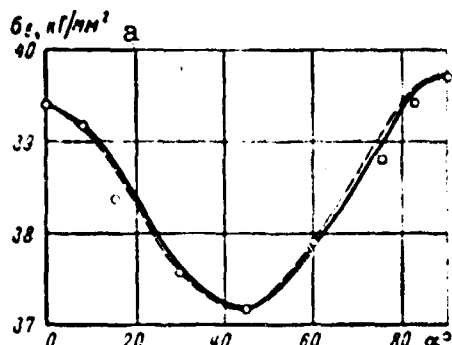


Fig. 27. Tensile anisotropy of Ergal aluminum alloy: dashed curves plotted by Eq. (41), solid curves by Eq. (49); o. average test results.

Key: a. kg/mm^2

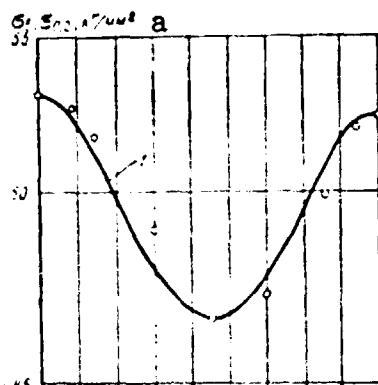


Fig. 28. Ultimate strength σ_B (1) and yield stress $\sigma_{0.2}$ (2) curves of Avional aluminum alloy: o. average test results.
Key: a. kg/mm^2

The results of study of the anisotropy of the impact strength of aluminum alloys were presented in [56]. A formula similar to Eq. (49) was proposed for this purpose in [41]. It approximates the curves of change in impact strength with less accuracy than the strength characteristic curves but, practically, this equation is suitable for approximate decision on the anisotropy of the impact strength of a metal.

The nonmetallic inclusions in the majority of rolled metals increase anisotropy and, in the opinion of some authors, they are its basic cause [57]. In pressure working, the nonmetallic inclusions are elongated and distributed in the rolled sheet in the form of thin films which form the so called line structure. The nature of the anisotropy of such a metal is nearly that of laminated materials with thin interlayers. Its failure frequently occurs along the planes parallel to the plane of the sheet, i.e., along the "line."

It is characteristic of the line structure that the ultimate strength always is greatest in the "fiber" direction of the metal and the least in the transverse directions.

The results of study of the anisotropy of cold rolled line structure steel with various degrees of cold working were presented in [58]. The purpose of this investigation was to study the causes of the development of "ears" (festoons), which result in defective products in the production of rolled steel cartridge cases by deep drawing.¹ The development of ears is associated with the fact that the metal is drawn easier in some directions and less easily in others, which characterizes anisotropy of the plastic properties. This phenomenon has been noted in copper, copper-nickel alloy, brass and steel sheet.

/66

¹The deformations resulting in ear formation were studied theoretically by Hill [59].

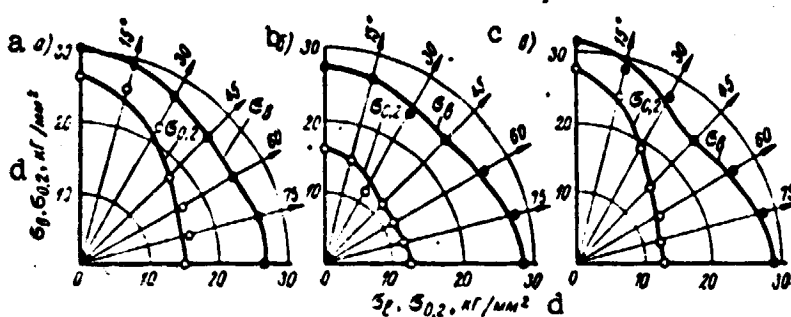


Fig. 29. Polar diagrams of ultimate strength σ_B and yield stress $\sigma_{0.2}$ of magnesium alloy vs. sample cut direction: a. in molding plane; b. in plane perpendicular to sheet; c. in plane perpendicular to sheet and parallel to molding direction; curves plotted by Eq. (49); o and ●. average test results.

Key: d. kg/mm^2

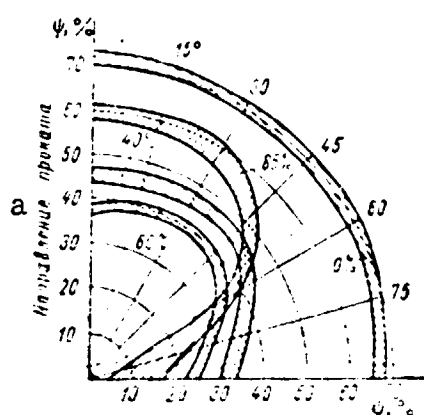


Fig. 30. Polar diagram of ultimate strength σ_B of cold rolled steel vs. degree of cold working (%), from data of Radvan; cross hatched strips, actual scatter of experimental data.

Key: a. Rolling direction

be, not the texture, but the fiber structure of the metal, in which cementite and nonmetallic inclusions are separated out on the grain faces, forming a kind of film separating the fibers. With more than 70% cold working, this fiber or line structure results in failure of samples, drawn at more than a 45° angle to the direction of rolling of the metal, along areas parallel to the fibers, which is characteristic mainly of such strongly anisotropic fibrous materials as wood.

The results of studies by M. Radvan [58] are presented in polar coordinates in Fig. 30-32. The angle between the direction of the ears and the rolling direction depends on the extent of preliminary cold working of the metal. This prompted Radvan to study experimentally the anisotropy of mechanical properties of cold rolled steel with various degrees of cold working. Samples were cut in the planes of the sheet, every 15° in seven directions from the rolling direction. The uniformity of the metal was carefully monitored, by cutting samples in one orientation from four different places in the sheet. In the initial state (before rolling), i.e., with 0% cold working, the sheet had low anisotropy, which was noticeable only on the diagram of relative elongation δ (Fig. 31).

Radvan considers the basic cause of anisotropy, especially with a high degree of cold working (over 70%) to be, not the texture, but the fiber structure of the metal, in which cementite and nonmetallic inclusions are separated out on the grain faces, forming a kind of film separating the fibers. With more than 70% cold working, this fiber or line structure results in failure of samples, drawn at more than a 45° angle to the direction of rolling of the metal, along areas parallel to the fibers, which is characteristic mainly of such strongly anisotropic fibrous materials as wood.

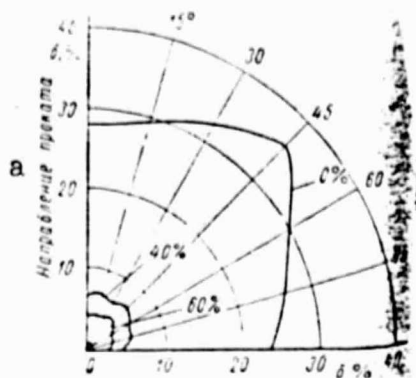


Fig. 31. Polar diagram of relative elongation δ of rolled steel vs. degree of cold working (%).

Key: a. Rolling direction

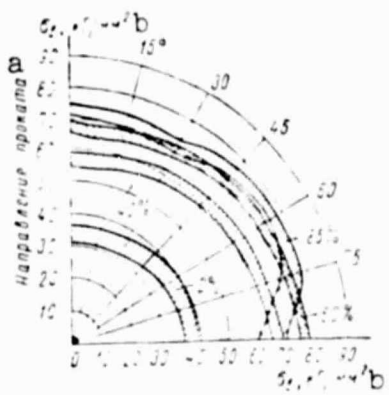


Fig. 32. Polar diagram of relative waist ψ of cross section vs. degree of cold working (%); cross hatched strips, actual scatter of experimental data.

Key: a. Rolling direction
b. kg/mm^2

length. The anisotropy of the impact strength of rolled steel, with a line structure due to nonmetallic inclusions, is still more substantial. According to the data of [61], the impact strength of transverse samples of structural steel is only 27.9% of the impact strength of longitudinal samples.

With a very high degree of cold working (85%), the ultimate strength perpendicular to the rolling direction ($\alpha=90^\circ$) decreases appreciably (Fig. 30). In this case, the relative waist also decreases. The material displays a tendency towards brittle failure, which is characteristic of all laminated materials stretched perpendicular to the layers.

The anisotropy of metals develops considerably more strongly at reduced test temperatures than under normal conditions. Deep cold near absolute zero has a particularly powerful effect. The curves of change in ultimate strength and yield stress of cold rolled stainless steel shown in Fig. 33 were plotted from the experimental data of [60] by Eq. (49), on the assumption of orthogonal strength anisotropy (a diagram of samples cut from the sheet is shown at the bottom of the figure). In plotting the curves, it was assumed that the strength can differ at $\alpha=45^\circ$ and $\alpha=135^\circ$, only because of non-uniformity of the metal. Therefore, the value of σ_{45} in Eq. (49) was calculated as the arithmetic average of the experimental data presented by the authors, for angles $\alpha=45^\circ$ and $\alpha=135^\circ$. As is evident from the figure, a low test temperature increases the anisotropy of the strength characteristics of rolled steel, without disturbing the orthogonal symmetry of the material or increasing the absolute values of the characteristics.

It was shown in [23, 56, 61, 62] that anisotropy of impact strength a_n can be very substantial. Thus, according to the data of [56], the value of a_n of samples of aluminum alloy extruded parallel to the width is twice that of samples parallel to the thickness and almost four times less than a_n of specimens parallel to the length.

/68

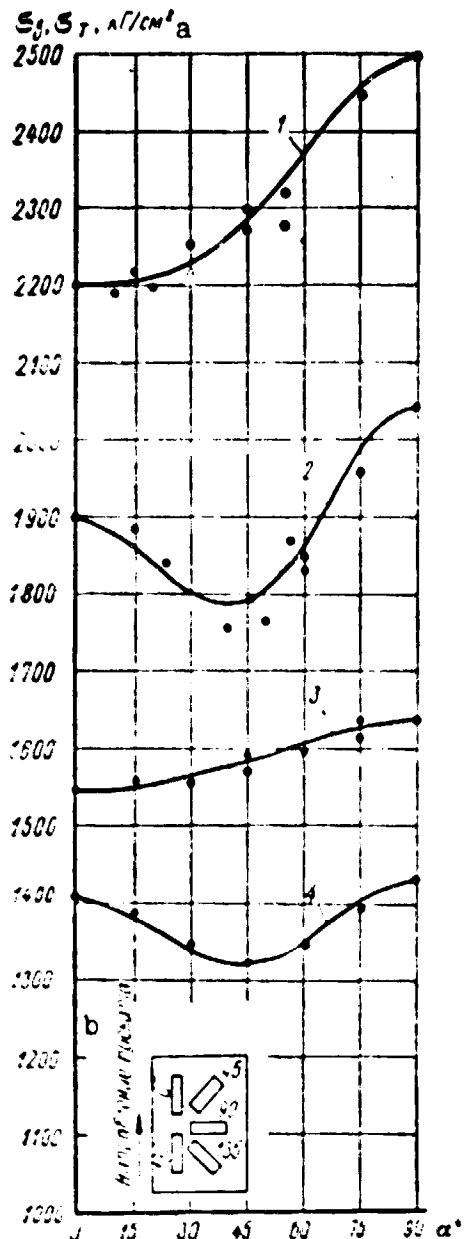


Fig. 33. Effect of low temperatures on anisotropy of mechanical properties of cold rolled stainless steel:
 1. ultimate strength σ_B at low temperature ($-235^\circ C$); 2. yield stress σ_T at low temperature ($-235^\circ C$); 3. ultimate strength σ_B at normal temperature ($+25^\circ C$); 4. yield stress σ_T at normal temperature ($+25^\circ C$);
 •. average test results.
 Key: a. kg/cm^2
 b. rolling direction

Curves plotted from the data of H. Hoover [62] are presented in Fig. 34. As is seen from this figure, the impact strength anisotropy (curve 3) is more significant than the tensile strength anisotropy (curves 1 and 2). Rolled steel was tested by H. Hoover in various directions from the rolling direction. Part of the steel strips (batch I) was rolled only longitudinally, in which the length of the rolled strips was 210 times the length of the ingot. The remaining steel strips (batch II) were obtained by first rolling longitudinally (the slab length was 13 times the length of the ingot) and, then, in the perpendicular direction (the length of the slab increased 19 times). No damage or defect was found on the surface of the strips here. The strength anisotropy of the batch II steel was low. The critical point of standard samples $\sigma_0/\sigma_{90} = 1.1$.

H. Hoover tested anisotropic steel strip on specimens in the form of bars with a deep notch drilled at the end of the notch. These samples were tested at various angles of inclination of the breaking force to the rolling direction of the strip, with the notch always remaining perpendicular to the breaking force. Two types of material were tested. Batch I steel underwent preliminary rolling in one direction before testing, and batch II steel differed from the batch I steel only in that it was rolled in two mutually perpendicular directions.

The ordinates of curves 1, 2 and 3 (Fig. 34) were calculated by Eq. (49). Quite close correspondence was obtained between the calculation and test data. Evidently, because of insignificant anisotropy of the elastic properties of rolled steel, the differences in stresses of differently oriented samples was negligible in these tests. The stress concentration

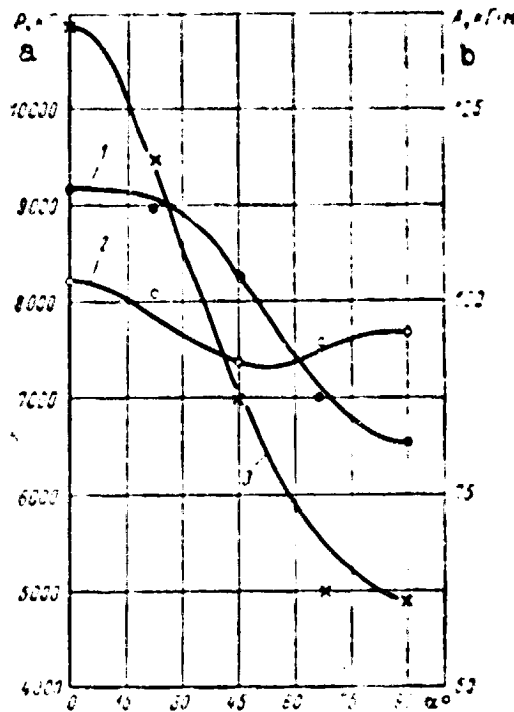


Fig. 34. Rolled steel strength vs. angle α of inclination of force to rolling direction (from data of H. Hoover): 1,2. failure force P for batch I and II steel; 3. failure work A for batch I steel.

Key: a. P , kg b. A , $\text{kg}\cdot\text{m}$

onal system have more clearly pronounced cold shortness, for which the anisotropy after cold rolling also is displayed most highly [21, 58]. The cold shortness phenomenon has not been found in pure metals with a cubic lattice [63]. As a rule, their anisotropy also is negligible [21, 58].

The hypothesis was expressed in [63] that cold shortness was absent in pure metals and that the brittle transition temperature decreased with decrease in nonmetallic impurities in rolled steel. Yet, the anisotropy of steel depends strongly on the presence of impurities, and it decreases with a decrease in impurities [64, 57]. More than that, it certainly would be incorrect to consider anisotropy the only cause of cold shortness. The question of the effect of anisotropy, especially with the line structure, on cold shortness of steel requires thorough experimental investigation.

Cast steel also displays reduced impact strength, an elevated cold shortness threshold temperature [63] and anisotropy of the mechanical properties. [65] dealt with study of the anisotropy of cast steel. The

factor, which changed the more as a function of the direction of the tensile force the greater the difference in the moduli of elasticity E along and across the rolled product, remained almost constant in this case. Therefore, it turned out that Eq. (49), derived for the stress characteristics in simple uniform stresses, is approximately valid in complex stresses, in which the test situation hardly changes with change in orientation of the sample.

The phenomenon of cold shortness of steel, which gives metallurgists many troubles, as far as we know, has not been investigated in connection with its anisotropy. Meanwhile, in comparing the sharp reduction in plastic properties (see Fig. 31) and the decrease in the transverse impact strength of rolled sheet (Fig. 34) with the fact that low temperatures promote an increase in anisotropy of the yield stress and ultimate strength of steel (Fig. 33), it can be proposed that anisotropy, especially with a line structure, can be a factor which contributes to the cold shortness of rolled steel.

It is known [63] that metals which crystallize in a simple hexagonal system have more clearly pronounced cold shortness, for which the anisotropy after cold rolling also is displayed most highly [21, 58]. The cold shortness phenomenon has not been found in pure metals with a cubic lattice [63]. As a rule, their anisotropy also is negligible [21, 58].

Cast steel also displays reduced impact strength, an elevated cold shortness threshold temperature [63] and anisotropy of the mechanical properties. [65] dealt with study of the anisotropy of cast steel. The

tendency towards anisotropy of mechanical properties of a cast metal is observed only with a columnar structure. Anisotropy develops especially strongly in the plasticity characteristics. Ingots of C27 chrome ferrite steel were studied. Transverse waist ψ of samples cut parallel to the direction of growth of the columnar crystals in a round cross section ingot turned out to be almost twice the waist of specimens perpendicular to this direction. In the direction of the cylinder generatrix, waist ψ was still smaller (by a few percent). The ultimate strength and yield stress displayed no appreciable anisotropy. The true ultimate strength S_k (of the fracture neck cross section) displayed just as significant anisotropy as the relative transverse waist ψ . Annealing had practically no effect on the anisotropy of C27 steel. For 35 carbon steel, anisotropy of the slab was found in determination of the yield stress, but annealing removed this anisotropy.

TABLE 14. TENSILE ANISOTROPY OF MECHANICAL PROPERTIES OF CAST STEEL

a Механическая свойства	b Грань №27			c Грань №33		
	x	y	z	x	y	z
d Образцы диаметром 1 мм. Скорость растяжения 1 мм/мин						
σ_0 , кг/мм ²	59	43	42	72	70	70
σ_y , кг/мм ²	26	26	27	40	37	33
Δ , %	15	12	11	17	16	11
ψ , %	68	38	33	46	37	38
S_k , кг/мм ²	105	59	57	122	106	110
e Образцы диаметром 5 мм. Скорость растяжения 5 мм/мин						
σ_0 , кг/мм ²	45	43	-	54	57	-
σ_y , кг/мм ²	36	36	-	28	29	-
ψ , %	11	6	-	39	32	-

Key: a. Mechanical property characteristic
 b. C27 steel
 c. 35 steel
 d. 1 mm diameter samples.
 e. 5 mm diameter samples.
 f. kg/mm²

Some data from [65] are presented in Table 14. The letters x, y and z designate the axes of assumed symmetry of mechanical properties of a cylindrical ingot. The z axis coincides with the generatrix of the cylinder, the x axis with the direction of the radius of a circular cross section, i.e., with the direction of growth of columnar crystals, and the y axis with the tangent to the circumference.

In the plane of a transverse cross section of the ingot, the y axis is perpendicular to the direction of crystal growth. To decide from the data of [65], in this case, cast steel can be classified approximately as a material with cylindrical anisotropy. The mechanical

properties (especially ψ and S_k) differ for the three directions of the x, y and z axes.

Impact strength a_k in testing samples, the axis of which (x) is parallel to the crystal growth direction, was approximately twice that in the case of coincidence of the axis of the samples with the longitudinal z axis. This difference is completely understandable, if the columnar structure is likened to a fibrous structure. The placement of the fibers along the x axis, i.e., along the radii of the ingot cross section, makes this direction, the length of which is parallel to the x axis, the strongest in the sample. In bending perpendicular to the x axis, the impact strength proves to be the highest. The location of the x axis perpendicular to the axis of bent impact specimens considerably decreases a_k .

9. Strength of Nonmetals

Laminated wood plastics (DSP). The results of compression tests of three types of plastic (DSP-B, DSP-V and DSP-G) in different directions with respect to the outside ply fibers were presented in [5]. DSP-B plastic is composed of layers of veneer with the fibers mutually perpendicular and 20 times more layers of veneer are stacked in the outside ply fiber direction than perpendicular to it. DSP-V plastic has the fibers of all adjacent layers of veneer perpendicular to each other, i.e., the number of longitudinally and cross stacked layers is the same. DSP-G plastic has a "star" structure, with the fibers in adjacent veneer layers at an angle of 30° with each other.

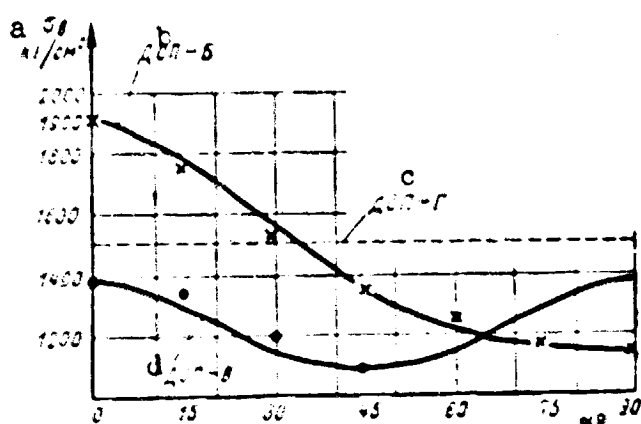


Fig. 35. Results of laminated wood plastic compression tests: o, x, experimental data of [5].

Key:
 a. kg/cm^2
 b. ISP-B
 c. ISP-G
 d. ISP-V

The results of compression tests of DSP are compared with curves plotted by tensorial Eq. (49) in Fig. 35. For DSP-B plastic, the coincidence of this curve with test data was even better than in plotting the corresponding curve by the correlation equation obtained in [5].

The results of shearing strength determination in variously oriented areas of several types of wood plastic were presented in the work of Kollmann [46]. The tests were done by Keylwerth in a device similar to that in which shearing tests of steel rods usually are done. The results of testing of 20 identical samples were averaged and plotted on a graph as one point. The graphs of Keylwerth, which he plotted from the results of testing beech laminated wood plastic

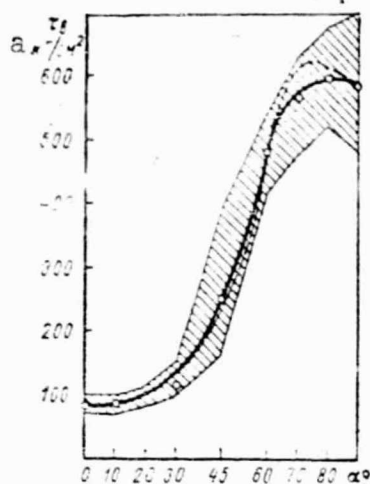


Fig. 36. Shearing test results of Sch-T-Bu-20 laminated beech wood plastic from Keylwerth: τ_B . shearing strength; solid curve plotted by Eq. (49); dashed curve, by empirical formula; cross hatched strip, actual scatter of test results.

Key: a. kg/cm^2

grades of DSP-G studied except DSP-G-90, the change in strength as a function of angle of inclination of the outside ply fibers is explained only by the scatter of the experimental data, and that averaging these data in accordance with the transverse isotropy hypothesis is statistically justified. /74

Thus, the theorem of V.L. German (see Section 1) is experimentally verified for the strength characteristics of wood materials if, in accordance with the assumptions substantiated in Chapter 2, it is considered that the strength characteristics correspond to a fourth order tensor.

Fiberglass plastics. The anisotropy of fiberglass plastics is determined by the method of reinforcing them and, as a rule, it corresponds to the orthogonal symmetry calculation scheme.

In oriented fiberglass plastics, the optimum is laying the glass reinforcement along the paths of action of the principal normal stresses in parts. Parallel winding or laying fibers in a single direction is used primarily in units which experience uniaxial stress. In fiberglass cloth reinforced sheet fiberglass plastics, the direction of the principal stresses is assumed to coincide with the direction of the warp of the cloth z, which corresponds to the greatest strength and rigidity of the material.

Sch-T-Bu-20, which approximately corresponds to the structure of DSP-B plastic, consisting of 20 parallel veneer layers, are presented in Fig. 36 and 37. The explanation of the maximum on the continuous curve of Fig. 36 evidently is that cutting the fibers of natural wood, parallel plywood [22] and Sch-T-Bu-20 beech plastic of similar structure to it requires the greatest forces when it is not done at right angles, but at an acute angle to the fiber direction. This is confirmed by the results of shearing tests of plywood [22], where the maximum resistance occurs at an angle of approximately $45-50^\circ$ to the outside ply fiber direction.

The practical use of laminated wood plastics in machine building, for gear production in particular, raises the problem of producing type DSP-G plastic of transversely isotropic (star) structure, with the optimum angle between the fiber directions in adjacent layers [82].

According to the data of P.E. Pyudik (Fig. 38), the highest tensile strength results with DSP-G-45 and DSP-G-60, i.e., with adjacent veneer layers laid at angles of 45 or 60° . There is practically no difference in the strengths of these two structures.

Calculations have shown [82] that, for all

/74

strength characteristics of wood materials if, in accordance with the assumptions substantiated in Chapter 2, it is considered that the strength characteristics correspond to a fourth order tensor.

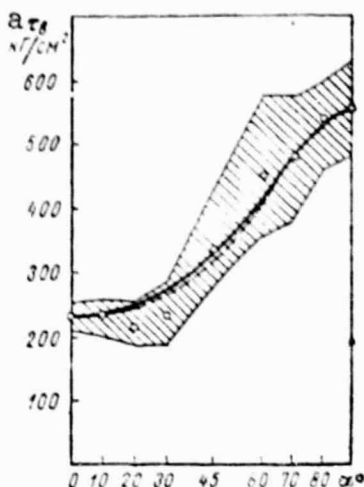


Fig. 37. Shearing test results of laminated beech wood plastic from Keylwerth: solid curve plotted by Eq. (49); dashed curve, by empirical formula; cross hatched strip, actual scatter of test results.

Key: a. kg/cm^2

Deviation of the axis of symmetry of the material from the direction assigned by the builder, sometimes called cross grain, can strongly affect the strength of a part made of an anisotropic material in some cases. This effect can be estimated by Eq. (49) and (50).

Three possible cases of deviation of the y and z axes of symmetry of sheet fiberglass plastic are shown in Fig. 39, which affect sheet strength differently under principal stress σ , in its plane. Even with a small angle α , the decrease in strength is appreciable, when there is an error in stacking the cloth (Fig. 39 a). The cross grain shown in Fig. 39 b has comparatively little effect on the static strength of fiberglass plastic. Another kind of cross grain (Fig. 39 c) quite strongly decreases the fatigue strength. In this case, it is recommended that both surfaces of the sheet be covered with a protective layer of cloth [35].

All three cases of cross grain can be either provided by the production technology or develop as a result of random errors.

In fiberglass reinforced fiberglass plastics (for example, SVAM²), the strength is very highly reduced, even at small angles α between the primary reinforcing direction and the direction of tension (Fig. 39 a). We will consider the primary reinforcing direction of SVAM to be along the z axis (Fig. 39 a). We consider the zy plane to be the glass veneer stacking plane. The reasons for which cross grain (Fig. 39 a) is hazardous for SVAM are clear from consideration of Fig. 40. Tensile strength anisotropy curves of SVAM, with different ratios of mutually perpendicular fibers in the plane of the sheet, are shown in this figure. With a 1:13 fiber ratio (curve 1), even a small deviation of the z axis (primary fiber placement, from which α is reckoned in the figure) from the direction of tension (for example, at $\alpha=5^\circ$) decreases the strength by more than 10%. This cannot be disregarded in building unidirectionally wound fiberglass plastic products.

With mutually perpendicular stacking of the same amount of fiber (SVAM, 1:1), the anisotropy is most pronounced under tension (Fig. 41). With shearing (curve 2), the anisotropy levels out, and the direction of greatest strength is nearly diagonal. For cold cured fiberglass plastic cloth (Fig. 42), the tensile anisotropy also has a greater effect than in shearing or compression.

²Anisotropic fiberglass material, produced by the Leningrad Laminated Plastics Plant, is abbreviated SVAM.

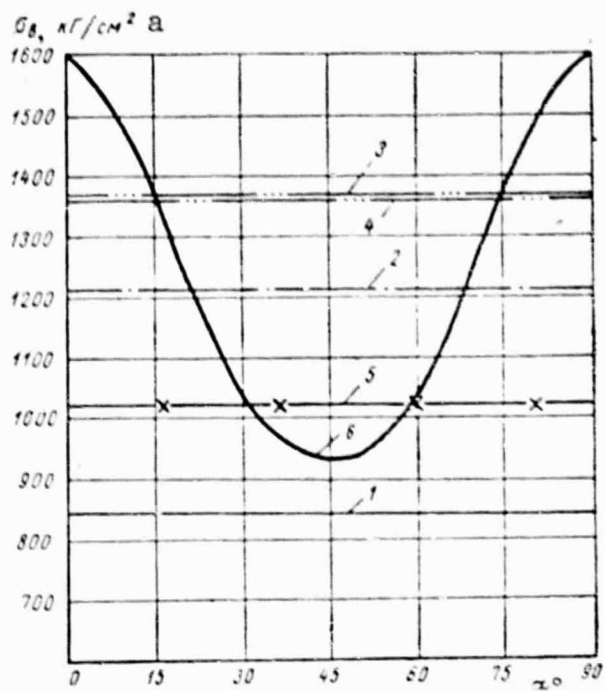


Fig. 38. Tensile test results of DSP-G of varied structure (from data of F.E. Pyudik): 1. DSP-G-15; 2. DSP-G-30; 3. DSP-G-45; 4. DSP-G-60; 5. DSP-G-75; DSP-G-90.

Key: a. kg/cm^2

Diagonal specimens, the strength of which depends on the properties of the binder and, therefore, on many purely technological factors, are especially convenient here.

Theoretical assumptions based on the "cut filament" concept lead to the statement that, in study of the dependence of fiberglass plastic strength on the angle the sample is cut cannot be employed with flat samples. Thus, V.L. Biderman [91] writes that points which correspond to failure of the glass filaments at angles other than $\alpha=0^\circ$ and $\alpha=90^\circ$ cannot be utilized with flat samples, since the ends of the filaments around which failure starts as a result of detachment of the filaments from the binder go out the sides of the sample.

The experimental data of [85] dispute the statement of V.L. Biderman: on the nature of the failure of samples, the axis of which does not coincide with the axes of symmetry of the fiberglass plastic. The failure of flat diagonal samples, recorded by means of frame by frame photography, begins with the development of cracks in the center of the sample, on which the greatest normal stresses act. In a detailed investigation, the edge areas of a stretched diagonal sample proved to be underloaded. The existence of the underloaded edge areas, the widths of which depend on the fiberglass plastic structure and is the greatest

The question of the method of determination of the strength characteristics of anisotropic materials has been raised repeatedly in the literature, in particular, those of fiberglass plastics under tension in directions which do not coincide with the axes of elastic symmetry of the material. Confirmation of the necessity of testing only tubular specimens instead of the traditional flat specimens, the axis of which is at some angle to the axis of symmetry of the material, has recently been appearing more and more often.

This question is important 178 for both fiberglass plastics and for all anisotropic materials, since all data available in the literature on the elastic properties and strength characteristics have been obtained primarily on flat samples. Flat samples are convenient in determination of the degree of anisotropy of mechanical properties of the material of large sized items and in testing the effect of the production technology on the properties of fiberglass plastics.

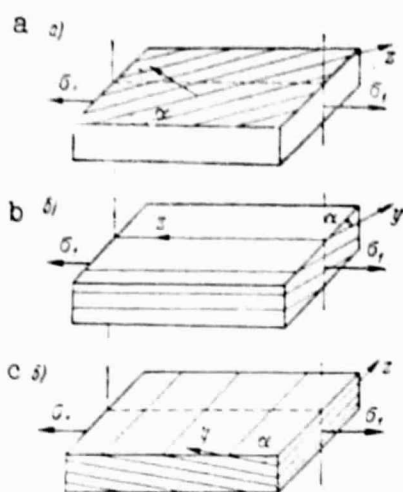


Fig. 39. Three possible cases of deviation of y and z axes of symmetry of fiberglass cloth plastic vs. direction of tension σ_1 :
 z . warp of cloth; y . weft of cloth.

for fiberglass laminate, was convincingly demonstrated in [85], by means of the polarization optical method of study of stresses. The edge effect, which was described in [91], evidently is associated with sample damage during mechanical treatment, and not with the effect of cut filaments.

A new explanation of the lower strength σ_{45} at an angle of 45° to the warp in flat samples than in testing tubing, based on the experimentally proved existence of underloaded areas in diagonal samples of textolite, was confirmed by study of the dependence of σ_{45} on sample width [85]. Increasing with increase in sample width (with a constant 3:1 length to width ratio), σ_{45} of fiberglass laminate reaches the highest values with a 70 mm sample width and, of type SVAM oriented fiberglass plastics, with a 15mm width [85]. Thus, the testing of flat samples at least 15 mm wide, with a length to width ratio of at least 3 [28], is completely justified for oriented fiberglass plastics.

V.D. Protasov and V.P. Georgiyevskiy [84] conducted extremely interesting tests of anisotropic fiberglass laminates at various angles to the reinforcing fiber direction. These tests were performed on tubes, in which the axes of symmetry of the material coincide with the axes of symmetry of the tube. The tubes were subjected to longitudinal forces, internal pressure and torque. It was considered here that the stress in the tube was linear and that the principal stress acted at a specific angle to the fibers. From the tube testing results, the authors obtain considerably higher elastic constants E and μ and strengths σ_B than in tensile testing of flat specimens in directions which do not coincide with the axes of symmetry of the material.

/79

Based on these tests, the authors of [84] state that study of the strength and elastic properties of flat samples of anisotropic reinforced materials in directions other than the reinforcing fiber direction results in obtaining distorted results.

It was shown in [85, 93] that study of the elastic properties of anisotropic reinforced fiberglass plastics in directions other than the reinforcing fiber direction, on flat samples of sufficient width and proper quality of production, gives satisfactory results. The question is important, since the use of flat samples permits control tests of the material of large structures, without introducing the unavoidable errors contributed by the difference in the technological processes of producing flat and tubular fiberglass plastic samples. The flat samples at a 45° angle to the fibers, specified by GOST [All-Union State Standards] 9620-61 and 9622-61 for laminated wood, plywood, board and

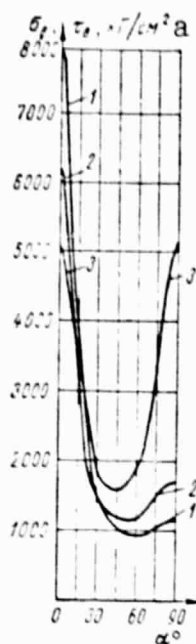


Fig. 40. Anisotropy of tensile strength σ_B of ED-6 epoxyphenol binder SVAM with fiber ratio: 1. 1:13; 2. 1:5; 3. 1:1; curves plotted by Eq. (49).

Key: a. kg/cm^2

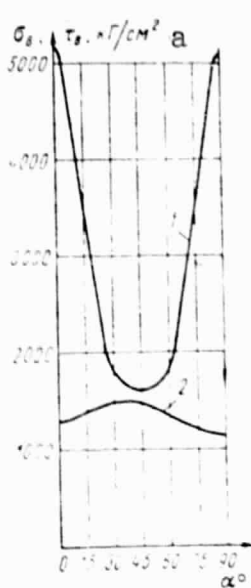


Fig. 41. Anisotropy of tensile strength σ_B (curve 1) and shearing strength τ_B (curve 2) of epoxyphenol binder SVAM with 1:1 fiber ratio; curves plotted by Eq. (49).

Key: a. kg/cm^2

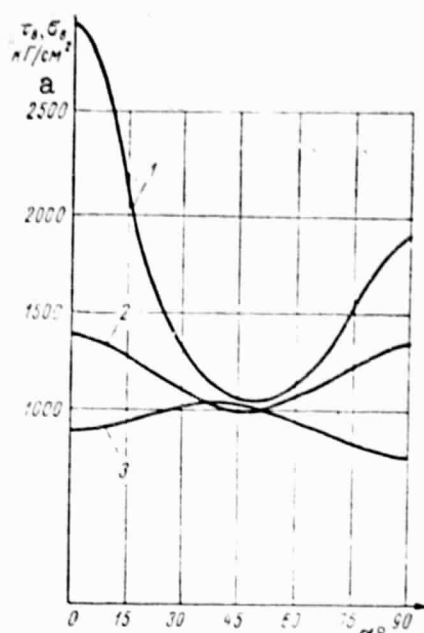


Fig. 42. Anisotropy of tensile strength σ_B (curve 1), compressive strength σ_B (curve 2) and shearing strength τ_B (curve 3) of PN-1 polyester binder cold cured fiberglass plastic; curves plotted by Eq. (49).

Key: a. kg/cm^2

DSP, requires further study of the effect of sample width and shape on the values of the mechanical strength characteristics determined. Of course, the tubular sample test method is unsuitable for both laminated and natural wood.

It is not always correct to decide the strength of fiberglass plastic from its mechanical characteristics in the plane of the sheet alone. Laminated fiberglass plastics, just like wood, have very poor resistance to shearing along the layers, i.e., to interlayer shearing. The interlayer shearing strength depends basically on the binder, and it is determined by the fiberglass production technology.

Unfortunately, the interlayer shearing strength of the material is not always indicated under industrial conditions. The high tensile strength of fiberglass plastics along the fibers, accepted by a builder without consideration of the property anisotropy and low shearing strength, can only result in discrediting this extremely promising material.

The results of study of the bending strength of various domestic fiberglass plastics (AG-4S, 27-63S, EF-32-301) were presented in [67, 68], and it was found that the ratio of the interlayer shearing strength to the tensile strength along the fibers changes from 0.03 to 0.12. Consequently, in bending fiberglass plastic samples, in which the neutral layer is parallel to the layers of the material (fiberglass cloth or veneer), failure can be of a fundamentally different nature. The cause of failure can turn out to be either maximum normal stresses σ_{\max} parallel to the glass fiber on the outsides of a hazardous cross section of the sample, or maximum tangential stresses τ_{\max} on the neutral layer of the sample, i.e., along the binder layer under interlayer shearing conditions.

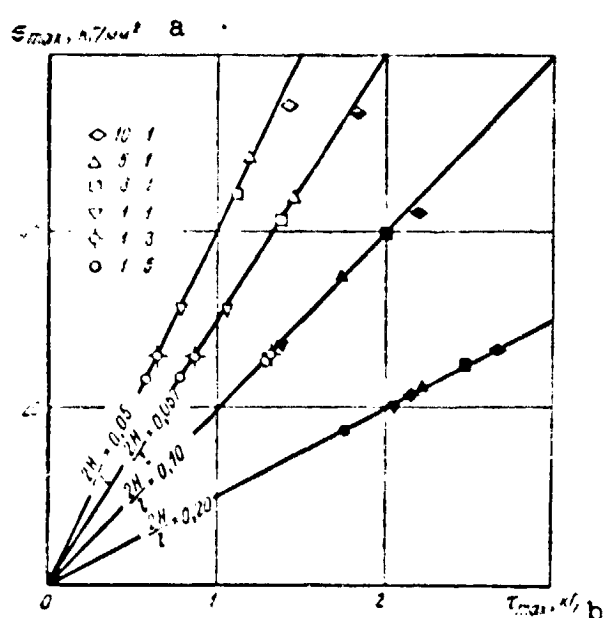


Fig. 43. Nature of failure of fiberglass plastics by bending (from data of Rose); fiber ratio shown by figures after conventional symbols of test results; results corresponding to sample splitting along layer noted by solid symbols.

Key: a. kg/mm^2 b. kg

determination of the interlayer shearing (shearing along the layer) strength, bending tests of samples with a larger height to span ratio ($2H/l > 0.2$) can be recommended, in which failure occurs only due to tangential stresses along the neutral layer of the beam (Fig. 43).

10. Scatter of Strength Characteristics

It is known that the results of mechanical testing of various anisotropic materials (wood, plywood, oriented fiberglass plastics) are dis-

Depending on the height to span ratio of the sample cross section, failure can occur either because the stresses σ_{\max} exceed the longitudinal tensile (compressive) strength σ_0 , or because stresses τ_{\max} under lower loads turn out to equal the interlayer shearing strength.

The results of the tests of Rose [67] of AG-4S fiberglass plastic, with different ratios of the fibers laid along and across the length of the sample, are shown in Fig. 43. In the conventional symbols, the number of fibers laid along the sample axis is indicated first. The rays connect test result points. The cross section $2H$ to span l ratio of the test sample is given on each ray. Ray $2H/l=0.1$ corresponds to a sample according to GOST 4648-56, in which failure of materials with considerable anisotropy occurred by shearing (shearing along the layer). At $2H/l=0.2$, all the materials failed by shearing upon bending. It follows from these data that the results of bending tests of anisotropic fiberglass plastics must be approached critically. For determina-

tinguished by substantial scatter. For fiberglass plastics, the scatter of the results is especially large in testing in the reinforcing direction. It decreases in testing samples, the axis of which is inclined at some angle to the reinforcing fiber direction.

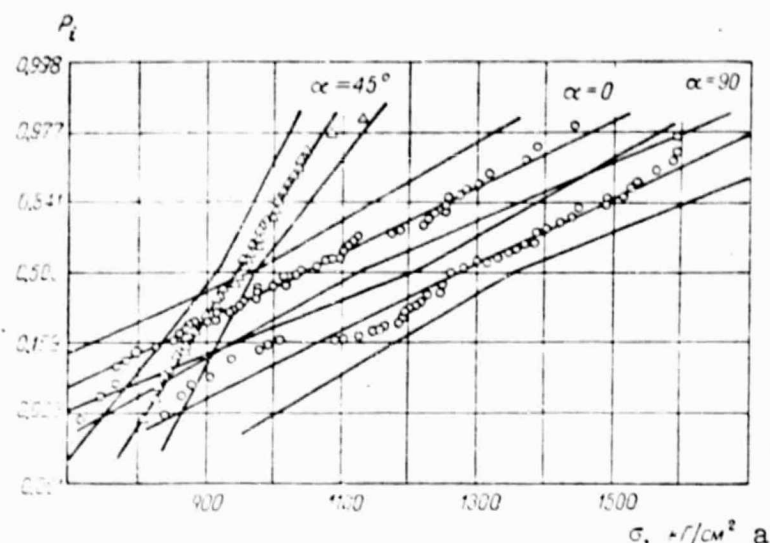


Fig. 44. Distribution of compressive strength characteristics of fiberglass cloth plastic.

Key: a. kg/cm^2

The distribution of the compressive strength characteristics (GOST 4651-49) of samples of cold cured PN-1 binder fiberglass plastic cloth are shown in Fig. 44 [38, 69]. The cumulative frequencies of strength σ_B of samples, the axes of which coincide with the warp ($\alpha=0^\circ$) and weft ($\alpha=90^\circ$) are plotted on normal probability paper, and angle $\alpha=45^\circ$ is compared with these directions. For all three cases, the points are located nearly on a straight line. This does not contradict the assumption of normal distribution of the experimental data. Five percent probability intervals are plotted here for average straight lines. The slope of the resulting straight lines to the abscissa, which approximately characterizes the scatter of the results, is approximately the same for angles α of 0 and 90° but, for angle $\alpha=45^\circ$, this slope is significantly greater. This indicates a considerably smaller scatter of the diagonal sample test results than those of the longitudinal and transverse samples.

/82

This has a very simple explanation, based on consideration of the anisotropy of the material. Curve 2 (Fig. 42) shows the change in compressive strength of this fiberglass plastic as a function of the angle of inclination of the fibers α . Near $\alpha=45^\circ$, the curve is nearly horizontal but, around angles α of 0 and 90° , it is steeper. If it is assumed that the scatter of the test results is determined primarily by error in orientation of the samples, the decrease of this scatter at $\alpha=45^\circ$ is explained by consideration of this curve. Even a $\pm 5^\circ$ error in orientation of the sample axis does not result in a change in the value of σ_B near angle $\alpha=45^\circ$. For the longitudinal and transverse

samples, such an error can change the strength. In tensile testing of SVAM with a 1:13 fiber ratio (Fig. 40), a 5° error in orientation of a longitudinal sample can reduce the strength by almost 10%.

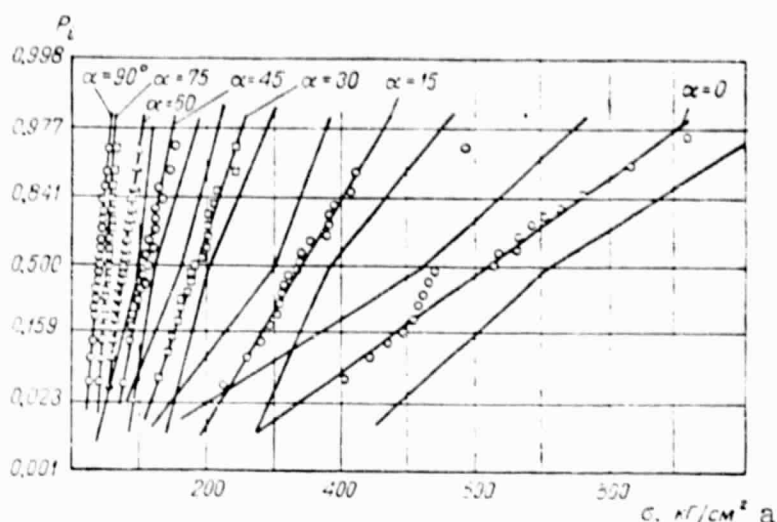


Fig. 45. Distribution of tensile strength characteristics of pine wood.

Key: a. kg/cm^2

This effect shows up still more clearly in the results of testing such a strongly anisotropic material as pine wood. The distribution of the tensile strength characteristics of pine wood at various angles α to the fibers is shown in Fig. 45. The test method and material were described in detail in [22]. It follows from the figure that the greatest scatter of the results happens with the direction of the force along the fibers ($\alpha=0^\circ$) and the least, perpendicular to this ($\alpha=90^\circ$). In this case, just as for fiberglass plastic, the results correspond quite closely to a linear change of the integral probability function, especially at $\alpha=90^\circ$ and angles close to it [69].

A curve of change of the tensile strength of pine wood as a function of α was presented in Fig. 10 of [22]. This curve is steep near $\alpha=0^\circ$, which results in significant scatter of the test results, with the direction of the force along the fibers and negligible error in sample orientation. The nearly horizontal section of the curve corresponds to angles $\alpha=75-90^\circ$ for the wood. Therefore, at these angles, even a substantial error in sample orientation does not result in scatter of the values of σ_B .

Thus, one cause of significant scatter of the results of testing anisotropic materials in the directions of greatest strength can be inexact matching of the sample axis with these directions.

In testing metals, the anisotropy of which is not as substantial, nonuniformity of the properties of the material plays the basic part in the scatter of the results. Different degrees of cold working at

various points of a rolled metal sheet can result in greater than normal nonuniformity of the mechanical properties of the metal.

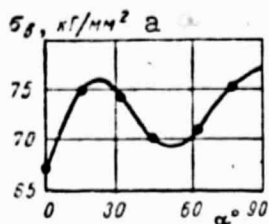


Fig. 46. Change of ultimate strength σ_B of rolled steel, from data of Braynin [71].

Key : a. kg/mm²

As a rule, testing of a large number of identical specimens is not required for a decision on the mechanical properties of a metal, because of the relative uniformity of the characteristic properties of a metal. However, this procedure can lead to errors associated with the nonuniformity of rolled metal in study of anisotropy. E.I. Braynin [71] committed such an error in study of the strength anisotropy of cold rolled 08KP steel. He tested one or two samples 130x18x0.5 mm in size, at 7 different orientations (at angles α of 0, 15, 30, 45, 60, 75 and 90°), for four different states of the steel and, in three cases, he obtained substantial disagreement of the experimental results with the results of calculation by Eq. (49). The greatest disagreement happened with steel, after cold rolling with 75% reduction (the curve of change of σ_B vs. angle α (Fig. 46) had a maximum at $\alpha=15^\circ$ and a minimum at $\alpha=50^\circ$).

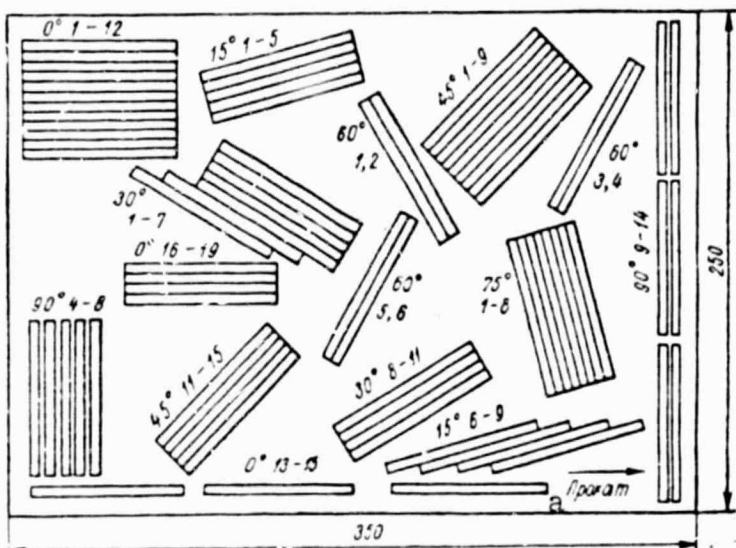


Fig. 47. Location of samples in steel sheet.

Key: a. Rolling

est strengths and those at the bottom, the lowest strength. In this case, the difference in strengths of the samples cut from different places in the sheet with the same orientation exceed the disagreements in strength which were obtained for variously oriented specimens cut from one part of the sheet.

A 250x260x0.5 mm sheet from the same batch of cold rolled steel was given to E.I. Bray-nin by the author of this work, to repeat his tests [72]. In order to test the degree of uniformity of the material in the sheet and obtain reliable average test data on a large number of specimens, smaller dimensions were selected.

Samples cut perpendicular to the rolling direction ($\alpha=90^\circ$) from the left and from the right parts of the sheet gave the same average strengths, but samples cut parallel to the rolling direction displayed different strengths depending on their location in the sheet. Specimens cut in the middle of the sheet gave the high-

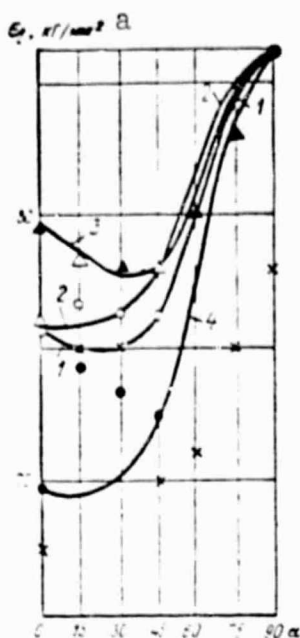


Fig. 48. Change of tensile strength σ_B of steel vs. angle α between sample axis and rolling direction. Curves plotted by Eq. (49): 1. sheet average; 2. upper part of sheet; 3. center; 4. lower; average strength values from data of author: o. in center of sheet; ●. in lower part of sheet; Δ. upper; ▲. middle; x. experimental data of E.I. Braynin.

Key: a. kg/mm²

To estimate fatigue strength anisotropy, testing with uniform stress and a symmetrical loading cycle, i.e., with transverse tension-compression in pulsers, should be recognized as the best. Yet, machines for continuously variable bending tests are favorable distinguished by greater simplicity of design and operation. Therefore, they are more widely used.

The bending fatigue limit of metals usually is determined by testing rotating cylindrical samples. The fatigue limit thus obtained extends to parts which work with variable bending, with a constant location of the plane of action of the load with respect to the part. In itself, this is not justified even for an isotropic metal.

Together with the data of the author, strength data obtained experimentally by E.I. Braynin are presented in Fig. 48 for comparison. The Braynin data are much lower than the data of the author along and across the rolling direction.

With $\alpha=0^\circ$, only two samples of 19 tested displayed as low a strength. These were samples No. 14 and 15, located in the lower part of the sheet. There is some increase in strength at angle $\alpha=15^\circ$ to the rolling direction, compared with the strength along the rolling direction (at $\alpha=0^\circ$) according to the test results of the author but, on the average over the sheet, the increase in strength is only 1.3%, while the difference in strength at $\alpha=0^\circ$, which depends only on the location of the sample, reaches 14%.

Thus, the existence of a strength maximum at $\alpha=15^\circ$ is doubtful, and the strength values obtained by Braynin at $\alpha=15^\circ$, which are higher than the strengths at $\alpha=0^\circ$, can be explained by nonuniformity of the material.

The curves presented in Fig. 48 were plotted by tensorial Eq. (49), separately for different parts of the sheet and averaged over the sheet. As far as can be decided from available data, tensorial Eq. (49) correctly describes the regularities of change in the strength of metals as a function of the angle between the direction of the tensile force and the rolling direction. /86

In other cases, the detection of regularities not contained in Eq. (49) or (41) should thoroughly verify the scatter of the characteristics of rolled metal determined, which are connected with various degrees of its cold working in different parts of a sheet.

11. Fatigue

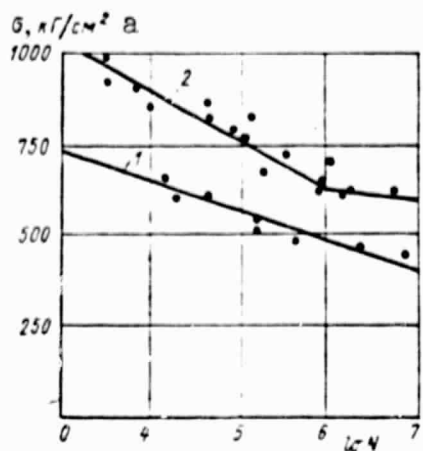


Fig. 49. Fatigue diagram of cold cured fiberglass cloth plastic made of linen weave cloth in PN-1 polyester resin, in pure bending along weft of cloth (symmetrical cycle): 1. by testing rotating cylindrical samples in NU machine; 2. by testing flat samples in machine of I.P. Boksberg; • experimental results.

Key: a. kg/cm^2

ple. In comparing the results of testing a rotating circular sample with a flat fixed sample, the ratio of the cross section dimensions is important.

Comparative tests of anisotropic fiberglass plastic cloth with a symmetrical cycle and pure bending were conducted on rotating cylindrical and fixed flat samples [38]. The fatigue curves for these two cases are shown in Fig. 49. The axes of all samples were along the weft of the fiberglass cloth. Tests of circular cross section rotating specimens 11 mm in diameter gave correlation line 1, which is lower than fatigue curve 2 for a fixed 10 mm wide sample. The explanation of this relationship is that the area of action of the maximum normal stresses in a rotating sample was approximately 1.5 times that of the fixed flat sample in this case and, therefore, the fatigue limit turned out lower.

In testing fixed flat samples of laminated materials at a low stress level, a tendency was noted for them to separate into layers, if the layers are parallel to the neutral layer. It was pointed out in [75] that, for laminated fiberglass plastic at low stress levels, failure of the fiberglass cloth in the zone of greatest normal stresses precedes failure of the binder in layers parallel to the planes of the cloth. This characteristic circumstance of static bending tests (see Section 9) requires a cautious approach to the practical use of bending fatigue test results.

An explanation of the differences in fatigue limit in pure bending, determined on circular rotating and fixed samples, is presented in [73]. In testing a fixed cylindrical specimen by an alternate upward and downward vertical bending load, the maximum stresses occur only at the farthest points from the neutral layer. If a specimen rotates under a constant vertical load, in a complete revolution all points of its perimeter will experience the greatest stresses in turn. The area of the material covered by the maximum stresses proves to be greater in a rotating sample than in a fixed sample and, correspondingly, the fatigue limit should be less.

For anisotropic sheet materials, it is more convenient to conduct fatigue testing on flat samples, with a continuously variable bending moment in the vertical plane [74, 75]. A fixed flat sample of rectangular cross section should give a lower bending fatigue limit than a fixed sample of circular cross section [73], since the area of exposure to the maximum stresses of a flat sample is greater than that of a circular sample.

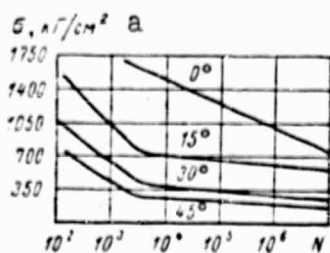


Fig. 50. Fatigue diagram of fiberglass cloth plastic.

Key: a. kg/cm^2

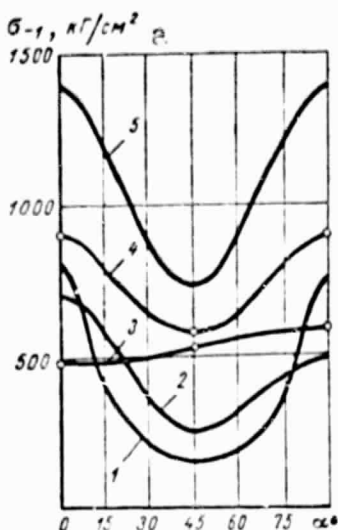


Fig. 51. Fatigue limit anisotropy of fiberglass plastics: 1. epoxy resin fiberglass plastic [44]; 2. PN-3 polyester resin fiberglass cloth plastic [81]; 3. cold cured PN-1 resin fiberglass laminate [38]; 4. epoxyphenol binder SVAM with 1:1 fiber ratio [38]; 5. epoxy resin fiberglass laminate [76].

Key: a. kg/cm^2

The two branches of the fatigue diagram, which are characteristic of bending tests of flat fiberglass plastic samples, can be considered schematically (in the first approximation) to correspond to two forms of disruption of the fatigue strength of a material: by failure of fiberglass cloth in the zone of the greatest normal stresses, and by the development of layer separation cracks in areas parallel to the neutral layer. The first form of failure frequently corresponds to high and the second, to low stress levels [75]. In testing flat samples, the axes of which are at 45° to the axes of symmetry of the material (the direction of placement of the fiberglass reinforcing in SVAM), failure at low stress levels also was accompanied by separation into layers along the binder layers [38]. /88

The fatigue curves of epoxy resin fiberglass plastic with mutually perpendicular fiber stacking, with axial tension-compression at various angles to the fiber direction, are shown in Fig. 50 [44]. The angle between the axis of the sample and the direction of the glass fiber is indicated on each curve. The strength of this fiberglass plastic is the same in two mutually perpendicular directions. Therefore, only four sample orientations in the planes of the fiberglass plastic sheet were tested.

The fatigue strength anisotropy of some fiberglass plastics is presented in Fig. 51. The bending fatigue strength anisotropy of fiberglass plastics is less pronounced (curves 2, 3 and 4) than in continuously variable tension-compression tests (curves 1 and 5).

A comparison of the anisotropy of fiberglass plastic in static and continuously variable loading along the sample axis is shown in Fig. 52, from the data of [44]. As is evident from the figure, the fatigue strength anisotropy of fiberglass plastics in the same kind of test is approximately half the static strength anisotropy.

In [64], A.L. Bukh points out that the fatigue strength anisotropy of rolled steel shows up more strongly in a symmetrical cycle than in a variable cycle. A.L. Bukh considers the effect of nonmetallic inclusions to be a basic cause of the anisotropy of rolled steel properties. In this case, the properties in the rolling direction scarcely depend on the presence of nonmetallic inclusions in the steel, but the mechanical properties in the transverse direction decrease with increase in impurities in the steel. The nonmetallic inclusion

/89

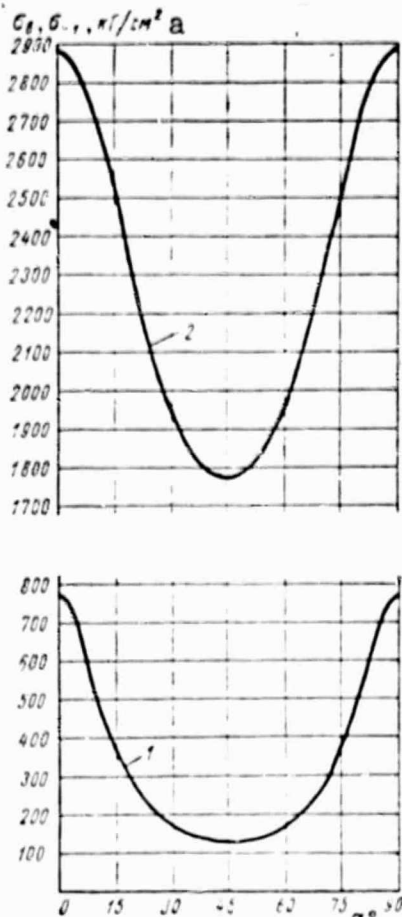


Fig. 52. Fatigue limit σ_{-1} (curve 1) and ultimate strength σ_B (curve 2) anisotropy of epoxy-phenol binder SVAM (1:1 fiber ratio) under axial loading (symmetrical cycle).

Key: a. kg/cm^2

The fatigue limit of transverse samples, determined by tension-compression in a symmetrical cycle, proved to be 20-30% lower than that of longitudinal samples for all materials studied [77]. Unfortunately, there are no data on the results of testing diagonal samples in [77]. In a number of cases when all the longitudinal and transverse mechanical properties, including the fatigue limit, were nearly the same, testing of samples, the axis of which is at a 45° angle to these directions, permits anisotropy to be discovered.

In continuously variable torsion tests of tubular nickel-chrome-molybdenum steel samples, Khodorovskiy found [78] that longitudinal and transverse samples give nearly the same fatigue limit, but that samples

content affects the mechanical property anisotropy of steel more strongly than the degree of cold working. The effect of large size brittle inclusions is especially significant [64]. As a result of the effect of nonmetallic inclusions, the fatigue limit anisotropy can prove to be still more substantial than the transverse waist anisotropy in static failure.

In all cases, the inclusions, which assume an elongated shape in the rolling direction during rolling, act as stress concentrators. As a result, their particularly great effect on the fatigue limit of the metal is clear. The higher the degree of cold working, the more elongated the shape of the inclusions becomes and the higher the stress concentration coefficient due to them under tension perpendicular to the rolling direction. With very small inclusions, their effect is within the limits of the natural scatter of the test results.

The scatter of the fatigue limit of a rolled metal can be extremely significant, if the samples are cut from different parts of the ingot [78]. Nonuniformity of the material affects its characteristics still more in fatigue tests than in static tests.

The anisotropy of rolled sheets of low alloy structural steel sometimes cannot be discovered from static test results which are conducted only on samples cut in the rolling direction and perpendicular to it. Thus, in [77], it was shown that the longitudinal and transverse yield stress, tensile strength and relative elongation of grade ten steel were practically the same, and that only relative waist ψ and true tensile strength S_k displayed anisotropy.

/90

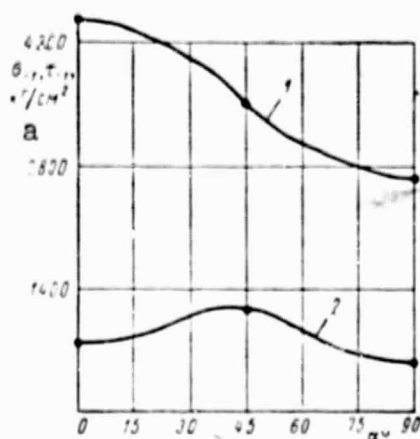


Fig. 53. Bending (curve 1) and torsion (curve 2) fatigue limit anisotropy of 76S-T61 aluminum alloy.

Key: a. kg/cm^2

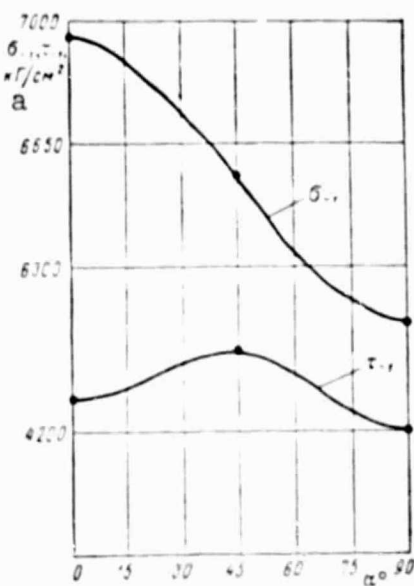


Fig. 54. Bending (σ_1) and torsion (τ_1) fatigue limit anisotropy of rolled steel.

Key: a. kg/cm^2

cut at an angle to the rolling direction give a higher fatigue limit under torsion. The authors of [79] reached similar conclusions. Besides, they determined that the fatigue limit anisotropy of aluminum alloys and rolled steel is less strongly expressed in torsion than in bending.

Fatigue limit curves of rolled aluminum alloy and rolled steel, plotted from the data of [79], are shown in Fig. 53 and 54. The results of determination of the fatigue limit for three different sample orientation in the planes of a sheet of rolled metal are presented in this work: parallel to the rolling direction (0°); perpendicular to it (90°); at a 45° angle to it. While fatigue limit anisotropy in bending is appreciable, even in comparing the first two orientations, only the third orientation permits anisotropy to be established in torsion.

With a 0.68 ratio of fatigue limits σ_{-1} across and along the roll, the ratio of cross section waist ψ in the same directions was 0.34 for the most anisotropic batch of samples [80]. For another, slightly anisotropic batch, where the transverse waist was almost the same across and along the roll (ψ ratio was 0.92), transverse fatigue limit σ_{-1} was 0.84 of the value of longitudinal σ_{-1} . Thus, /92 the σ_{-1} and ψ characteristics are connected with each other, but are by no means directly proportional to each other.

The ψ value of transverse samples is proposed in [80] as an indicator for approximate decision on the anisotropy of rolled metals. It should be noted that the anisotropy of steel cannot be decided from ψ , measured only on longitudinal and transverse samples. It is likely that information on anisotropy which can be obtained from true tensile strength³ S_k will be faulty, if it is determined only longitudinally and transversely as was proposed in [77].

The results of study of the anisotropy of the damping properties and fatigue limit

³It was pointed out in [66] that the fatigue limit anisotropy of metals can be decided approximately from true tensile strength S_k , if S_k is determined in three directions: longitudinal, transverse and diagonal.

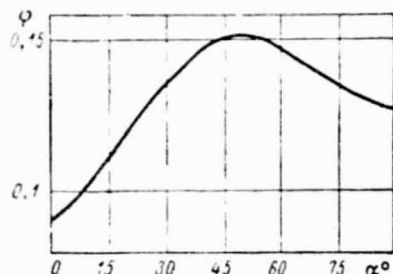


Fig. 55. Anisotropy of damping properties of fiberglass cloth plastic in bending: ϕ . coefficient of energy absorption during vibration; α . angle between warp of cloth and sample axis (see Fig. 56).

of a fiberglass plastic made of satin weave ASTT (b)-S fiberglass cloth in PN-3 polyester resin are presented in [81]. Energy absorption coefficient ϕ , which is approximately double the logarithmic decrement of vibration damping, was determined experimentally. The tests were conducted on freely suspended flat specimens with the natural bending vibrations.

A graph of energy absorption coefficient ϕ vs. angle between the sample axis and the fiberglass cloth warp fiber direction, plotted from the data of [81], is presented in Fig. 55. Data on the anisotropy of this fiberglass plastic, obtained by testing large flat samples, are presented in Table 15. Energy absorption factor α is compared to the ratio of energy dissipated in the vibration.

TABLE 15. ANISOTROPY OF PN-3 FIBERGLASS CLOTH PLASTIC

Угол α в градусах	Коэффициент изделия ϕ	Модуль уп- ругости $E \cdot 10^5$, kg/cm^2	Линейный коэффициент α_{-1}
0	0.086	1.44	700
45	0.150	0.77	275
90	0.120	0.96	500

Key: a. Angle with warp direction α , degrees
 b. Coefficient of energy absorption ϕ
 c. Modulus of elasticity $E \cdot 10^5$, kg/cm^2
 d. Fatigue limit σ_{-1} , kg/cm^2

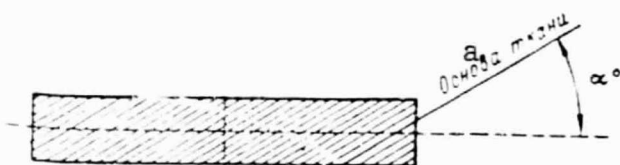


Fig. 56. Sample position in determination of damping property anisotropy of fiberglass plastic.

Key: a. Warp of cloth

characteristics. The damping property anisotropy is so high that the resonance vibration amplitude can be changed 1.5-1.7 fold, only by changing the angle between the sample axis and the fiberglass cloth warp direction.

period to the greatest potential energy of the cycle.

The orientation of the samples which correspond to the tests of [81] presented in Fig. 55 is shown in Fig. 56. As should be expected the damping properties of the fiberglass plastic are the greatest, in the case of forces acting in the direction of the lowest elastic and strength

CHAPTER 4. ANISOTROPY IN MACHINE PARTS AND STRUCTURES

12. Strain Measurement Characteristics

The experimental study of deformation of working machine parts and structures for the purpose of investigation of strain is called strain measurement. Strain measurement usually is resorted to in those cases when theoretical determination of stresses is impossible, or when the degree of correspondence of theoretical formulas to reality must be verified.

/93

The principal stresses at danger points are calculated from the results of strain measurements on isotropic materials. In the event the strength of parts made of an isotropic material is studied, calculation of the principal stresses is not necessary. Testing strengths under two dimensional stress requires determination of the stresses along the areas of symmetry of the material (see Chapter 2). If the direction of the axes of symmetry of the material is known beforehand, this task is significantly simplified.

The location of the axes of symmetry of an orthotropic material in a part can be determined by various methods. Sometimes, it is predetermined with great accuracy by the production technology as, for example, in rolled metal sheet: the rolling direction quite accurately defines the location of one axis of symmetry of all mechanical properties of the metal.

In parts made of fiberglass plastics, especially when they are hot molded, the direction of the glass fiber (and, consequently, the axes of elastic symmetry) can deviate quite strongly from the assumed direction. This is explained by errors in the technological process. Cutting, impregnation and laying the cloth in the mold can involve misalignment, and molding a part of complex configuration can involve disturbance of the arrangement of the layers. All these technological process errors have the result that the actual glass fiber arrangement is unknown in a finished part.

The actual direction of primary orientation of the glass fiber and, consequently, the location of the axes of elastic symmetry in the orthogonal stacking of fibers can be found by means of ultrasound [83]. For this, a circle of arbitrary radius is drawn on the finished part (Fig. 57). The ultrasonic wave is passed through two diametrically opposite points 1 and 2. The time in which the wave covers the distance between the mark points is recorded by the instrument and, from the known distance between the points (it is the diameter of the circle), the velocity of the ultrasound is determined. The wave traverses the x axis of greatest rigidity of the material, which coincides with the primary orientation of the fibers or with the direction of the warp in fiberglass plastic cloth, most rapidly. Therefore, by measuring the velocity of the wave in several directions, the axis of greatest rigidity, i.e., the axis of elastic symmetry of the material can easily be determined.

/94

Wire sensors (electric strain gauges), which are convenient in study of stress in parts made of anisotropic materials, are the most

widespread. Three sensor rosettes are used for stress determination. Two sensors of the rosette are cemented along the axes of symmetry of the material and the third, at a 45° angle to the first two.

Stresses acting on areas of elastic symmetry can be determined by solving Eq. (7) for stress, with $\sigma_z = \tau_{zx} = \tau_{yz} = 0$:

$$\left. \begin{aligned} \sigma_x &= \frac{E_x(\epsilon_x + \mu_{xy}\epsilon_y)}{1 - \mu_{xy}\mu_{yx}}; \\ \sigma_y &= \frac{E_y(\epsilon_y + \mu_{xy}\epsilon_x)}{1 - \mu_{xy}\mu_{yx}}; \\ \tau_{xy} &= G_{xy}\gamma_{xy}. \end{aligned} \right\} \quad (88)$$

In the general case, both normal stresses σ_x and σ_y and tangential stresses τ_{xy} act along areas perpendicular to the axes of symmetry of the material. Therefore, for strain measurement, a three sensor rosette is used. Two sensors, cemented strictly along the x and y axes of symmetry, are used to determine the relative longitudinal deformations ϵ_x and ϵ_y , and one sensor, cemented at a 45° angle to the first two on the same part, is used to calculate angle of displacement γ_{xy} . The following formula is used here, which was obtained from geometric considerations:

$$\gamma_{xy} = 2\epsilon_{45} - \epsilon_x - \epsilon_y, \quad (89)$$

where ϵ_x , ϵ_y and ϵ_{45} are the relative longitudinal deformations along the x and y axes of elastic symmetry and at a 45° angle to them (Fig. 57).

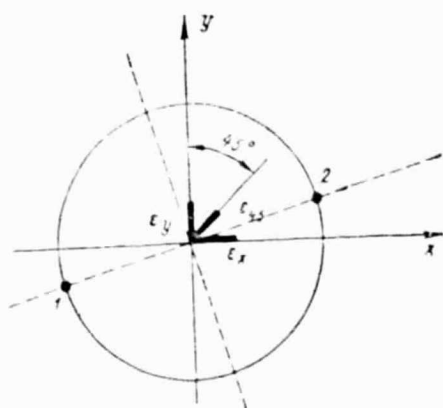


Fig. 57. Wire sensor rosette on surface of part of orthotropic material: x and y , axes of symmetry of material.

It should be noted that deviation of the sensor axes from the axes of elastic symmetry of the material can result in substantial errors. Eq. (88) then is unusable, and it should be replaced by the more complex formulas presented in [83]. The simplest and least erroneous strain measurement of anisotropic materials is carried out by means of a three sensor rosette, in the event of coincidence of the axes of the rosette with the axes of symmetry of the material.

Unlapped sensors should be preferred in strain measurement of parts made of anisotropic materials, since the effect of the loops can introduce significant errors to the results in small base measurements, especially in certain stresses. This is

because the coefficients of transverse deformation of anisotropic materials differ in different directions. Therefore, the effect of the loops will differ for the three sensors of one rosette.

The features of strain gauge determination of stresses in parts made of anisotropic materials can serve as an example of the practical application of the theoretical considerations of the first chapter in engineering practice. Strain gauge determination of stresses in an anisotropic material, performed without taking account of the characteristics discussed, can prove to be erroneous.

13. Effect of Anisotropy on Machine Part Strength

Since the time of publication of the classical works of D.K. Chernov, it has been known that macroscopic anisotropy of the mechanical properties of metals is observed. It is the result of oriented arrangement of heterogeneous components of the metal [10].

In senior practical physical metallurgy courses [21], recommendations have been formulated for the design of parts made of anisotropic metals. It is not recommended that load carrying parts made of such metals be made by cutting. The shape of the parts should be such that the fiber direction follows the load direction [21], i.e., the fibers of the fabric should not be cut during manufacture. These recommendations are widely utilized in pressure working of such standard machine parts as gears, /96 crankshafts and the like.

Cases also are known [10] when, for example, a stamping tool (knives for cutting out cylindrical intermediate products and dies) failed, because it was improperly made of an anisotropic metal.

In pressure working, the metal fibers should be set so that no tensile stresses act across the fibers and no tangential stresses act on areas parallel to the fibers. The areas parallel to the fibers are the weakest in a rolled metal. If possible, they must be positioned so that there are no stresses along these areas or, at least, there are only compressive stresses. A similar, but considerably more extreme phenomenon occurs in wood. Tensile and shearing stresses along areas parallel to the fibers are a great danger to wood and cause its brittle failure. This limits the use of wood as a structural material. Anisotropic rolled metal behaves the same way. With tensile and shearing stresses along areas parallel to the fibers, failure can be brittle, even for soft steel, since it occurs along weak interlayers of non-metallic inclusions and is aggravated by stress concentrations near these layers. An analysis of stamping tool failure was carried out in [10], which showed that, with improper fiber placement, failure of the metal occurs by breaking off, without macroscopic indications of plastic deformation. /97

Failure of a stamping tool with incorrect fiber placement is shown, and a diagram of correct placement of the fibers in dies and cutters is given in Fig. 58 and 59 [10]. The direction of the forces is shown by arrows. Placement of the fibers along the axis of the die (Fig. 58 a) is the most dangerous case, in which "splitting" of the die occurs along areas parallel to the fibers, similar to the splitting of

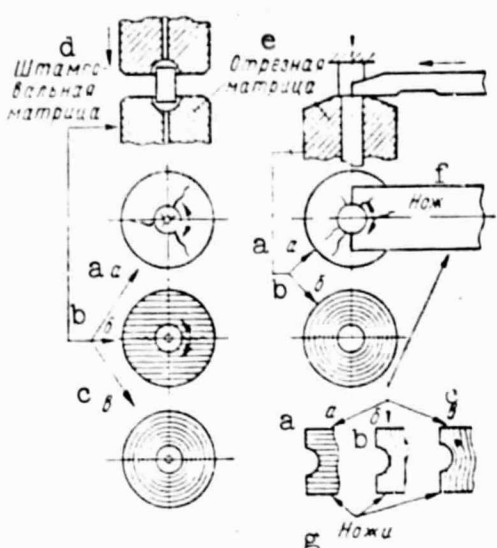


Fig. 58. Failure of shearing dies, cutters and stamping dies with incorrect fiber arrangement (a and b) and diagrams of correct fiber arrangement (c).

Key: d. Stamping die
e. Shearing die
f. Cutter
g. Cutters

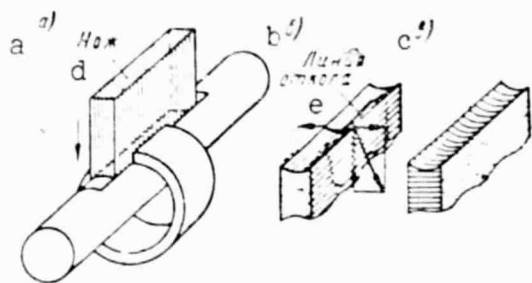


Fig. 59. Failure of slot cutters with incorrect fiber arrangement (a and b) and diagram of correct fiber arrangement (c).

Key: d. Cutter
e. Breakaway line

but the least tensile strength. While the strength characteristics along and across the fibers (or the roll) differ little from each other, as a rule, the diagonal corresponds to extreme strengths: the maximum shearing strength and the minimum tensile strength. This rule was confirmed in fatigue testing of metals.

wood with axes.

Thus, placement of the fibers according to the configuration of the part turns out to be insufficient. In working, metal fibers should be matched with the paths of the principal tensile stresses, just like the reinforcing in reinforced concrete. Some recommendations presented in [10] are reproduced in Fig. 60.

It should be noted that rolling a metal in two mutually perpendicular directions does not eliminate its anisotropy.

The production of a sheet isotropic metal by pressure working possibly could succeed, if it is rolled in at least three directions at 60° angles from each other (see Section 1), but this method requires additional experimental study.

In study of the anisotropy of a metal, experimental study of all orientations of the forces is not needed. The formulas presented in Section 6 are sufficiently simple for practical use [42], and they permit experimental determination of the mechanical property characteristics in only the longitudinal, transverse and diagonal directions in each plane of symmetry of the material (Section 1).

It should be noted, that with /98 the same kind of mathematical relationships, the form of the curves which define the resistance of materials to normal and tangential stresses is completely different. The diagonal frequently corresponds to the greatest shearing strength

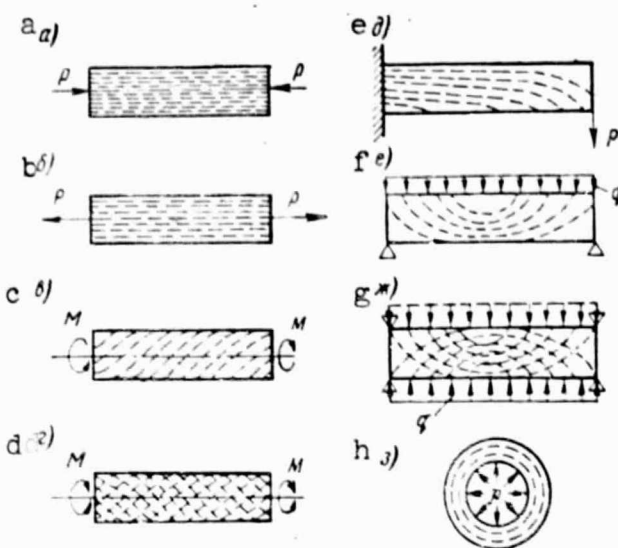


Fig. 60. Recommended fiber arrangement in metal parts: a and b. in simple compression and tension; c. in torsion; d. in reversed torsion; e and f. in bending; g. in reversed bending; h. in pipe under internal pressure.

Fig. 60. Recommended fiber arrangement in metal parts: a and b. in simple compression and tension; c. in torsion; d. in reversed torsion; e and f. in bending; g. in reversed bending; h. in pipe under internal pressure.

It follows from Eq. (49) that the extreme ultimate strength σ_B corresponds to the extreme value of the denominator on the right side of the equation. By making the first derivative of this denominator equal to zero, from angle α , we obtain the following condition of the extreme σ_B :

$$\cos^3 \alpha \sin \alpha = b \sin 2\alpha \cos 2\alpha + c \sin^3 \alpha \cos \alpha. \quad (90)$$

In particular, it follows from this that, to reach extreme values of σ_B on the diagonal ($\alpha=45^\circ$), where $\sin^3 \alpha \cos \alpha = \cos^3 \alpha \sin \alpha = 1/4$, and $\sin 2\alpha \cos 2\alpha = 0$, it is necessary that $c=1$, i.e., $\sigma_0=\sigma_{90}$. In other words, if any characteristic of an orthotropic sheet material has the same longitudinal and transverse values, this means that the greatest or least value of this characteristic will occur diagonally.

With $\alpha=60^\circ$, equality (90) can be satisfied with $\sigma_{45}=\sigma_{90}$. Similarly, with $\alpha=30^\circ$, the maximum or minimum can occur if $\sigma_0=\sigma_{45}$.

In producing wound fiberglass plastic products, nonorthogonal fiber placement frequently is used (see Fig. 2). In this case, if it is assumed that the maximum strength occurs in the primary fiber placement

With increase in the degree of anisotropy of a material, i.e., differences between the longitudinal and transverse strengths, the extreme values correspond with the diagonal but, as before, the resistance to normal stresses is at a minimum, and the resistance to tangential stresses is at a maximum. With a very high degree of anisotropy, the extreme corresponds with the longitudinal or transverse directions.

Mathematical relationships (see Sections 5 and 6) permit easy determination of the direction of least or greatest strength of an anisotropic material, in distinction from the purely empirical approach to the question, which does not make this possible. In this case, the same or nearly the same longitudinal and transverse strength characteristics still are not indicators of the isotropy of a material. Its strength in any other direction (for example, diagonal) can prove to be considerably reduced.

/99

direction, i.e., along the x'_1 axis, the approximate value of σ_{45} can be calculated and, in this case, it is sufficient to determine the strengths experimentally along the x_1 and x_2 axes of symmetry of the material, i.e., σ_0 and σ_{90} (see Fig. 2).

We assume that the strength of a nonorthogonal fiberglass plastic changes according to tensorial Eq. (49), depending on angle α between the x_1 axis and the direction of the tensile stress. Then, the maximum strength occurs with $\alpha=\gamma$ and, consequently, the zero value of the first derivative of the strength σ_B according to angle α . After simple calculations, we obtain

$$\sigma_{45} = \frac{4(1-\tan^2\gamma)}{\frac{3-\tan^2\gamma}{\sigma_0} + \frac{1-3\tan^2\gamma}{\sigma_{90}}}.$$

In this case, the strength criterion can be utilized without experimental determination of strength σ_{45} at an angle of 45° to the axes of symmetry of the material.

It must be noted that the value of σ_{45} calculated by this equation /100 proved to be quite close to the value of σ_{45} determined directly from testing flat samples. The tensile strength anisotropy from test results was somewhat more pronounced than from the calculated data.

Eq. (49) was used in [81] to describe the anisotropy of the vibrational characteristics of fiberglass plastics. Based on this formula, the optimum reinforcing angle, at which the damping properties of the fiberglass plastic are at a maximum, is determined. The question is of practical importance in selecting the reinforcing angle which ensures the least noise emission of fiberglass plastic ship hulls.

Primarily cold cured fiberglass plastic is used in ship hulls, in connection with its purely technological advantages for the production of large items. Hot molded fiberglass parts, which ensure higher mechanical property characteristics of the material, are used more often in machine building.

Analysis of the structure of material in parts of complex configurations produced by hot molding shows that the fiber arrangement determined by the designer actually cannot be ensured in the finished product. This can significantly reduce the strength of the part, although its external appearance and dimensions correspond to the drawing.

The causes of disruption of the structure of the material are associated primarily with creep of the layers of fiberglass cloth, tape or veneer during molding of the item. This phenomenon is characteristic of items of complex shape (ship propeller blades, compressor and turbine blades), which are subjected to pressure during molding, which does not act perpendicular to their curvilinear surfaces. The strength

of such items can frequently be increased without change in properties of the binder or reinforcing, only by a technology which ensures the proper structure of the material and the use of nondestructive methods of monitoring the structure of the item.

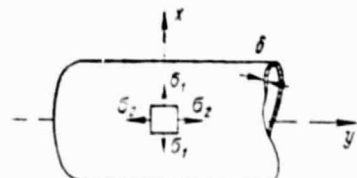
In fiberglass plastic hulls, the use of parallel deck and bottom reinforcing schemes and parallel-diagonal reinforcing of the sides, which reduce shearing deformations, is considered the optimum [81, 29].

Star stacking of the reinforcing fibers (or fiberglass cloth layers) is expedient, in the event of a need to decrease the stress concentration. This is particularly important in large fiberglass plastic structures.

The coefficient of tensile stress concentration along the axis of greatest rigidity is the larger, the more pronounced the elastic anisotropy. Star stacking of reinforcing elements can be done with an isotropic material near the place of stress concentration, with reduction in the concentration coefficient.

14. Use of Strength Criteria for Calculation of Pipe Wall Thickness

Fiberglass plastic pipe has been widely used recently in various branches of the national economy. Such pipe usually is produced by winding glass tape or glass roving on a mandrel. As a result of lengthwise-crosswise or cross bias winding, orthogonal or nonorthogonal laid fiberglass plastic is formed, with the axes of symmetry, as a rule coincident with the cylinder generatrix, pipe cross section radius and tangent to the cross section circumference.



We consider a pipe subjected to internal pressure. It can be considered that two dimensional stress develops in the walls of such a pipe, with the principal stresses σ_1 and σ_2 along the areas of symmetry of the material (Fig. 61).

These stresses are determined by the formulas

$$\sigma_1 = \frac{pr}{\delta}; \quad \sigma_2 = \frac{pr}{2\delta}; \quad \sigma_1 = 2\sigma_2$$

Fig. 61. Directions of principal stresses in wall of pipe under internal pressure.

where p is the internal pressure; r is the pipe radius; δ is the wall thickness.

As is known, stress σ_2 acts along areas perpendicular to the axis of the pipe, i.e., in the directions of the axis of symmetry of the material.

We designate the axis of the pipe, i.e., the axis of symmetry of the material, by the letter y . Then, for the problem under considera-

tion (Table 7), the stress tensor will have the following form:

σ_1	0	0
0	σ_2	0
0	0	0

At each point, the x axis passes along the tangent to the circumference of the pipe and the z axis along its radius.

We assume that we know the following strength characteristics of the pipe material:

σ_{90} is the tensile strength along the y axis, i.e., along the axis of the pipe;

σ_0 is the tensile strength on the tangent, i.e., along the x axis of symmetry of the material; /102

τ_0 is the tensile strength at an angle of 45° to the x and y axes;

τ_0 is the shearing strength, in which the tangential stresses act along areas perpendicular to the x and y axes.

We calculate the pipe wall thickness δ which corresponds to a hazardous state of the material. We use the strength criteria obtained in Sections 5 and 6 for this.

Initially, we substitute the stress values in the quadratic strength criterion, i.e., in Eq. (35)

$$\frac{\sigma_1^2}{\sigma_0^2} + \frac{\sigma_2^2}{\sigma_{90}^2} + \sigma_1 \sigma_2 \left(\frac{4}{\sigma_{45}^2} - \frac{1}{\sigma_0^2} - \frac{1}{\sigma_{90}^2} - \frac{1}{\tau_0^2} \right) = 1. \quad (91)$$

From this formula, it happens that failure occurs at

$$\sigma_2 = \sqrt{\frac{1}{\frac{2}{\sigma_0^2} - \frac{1}{\sigma_{90}^2} + \frac{8}{\sigma_{45}^2} - \frac{2}{\tau_0^2}}}. \quad (92)$$

By substituting the values of stress σ_2 , we obtain the value of δ , at which the pipe fails due to internal pressure p . It is evident that, after selecting valid strength safety factors k , pipe wall thickness δ at which pressure p is safe can be calculated:

$$\delta \geq \frac{prk}{2\sigma_0} \sqrt{8a^2 - 2d^2 - c^2 + 2}, \quad (93)$$

where $a = \sigma_0/\sigma_{45}$, $d = \sigma_0/\tau_0$, $c = \sigma_0/\sigma_{90}$ (see pp. 27-28 for notation).

For the same purpose, we now use the fourth power criterion (see Section 6) and, from Eq. (66), we obtain

$$\begin{aligned} \frac{\sigma_1^2}{\sigma_0} + \frac{\sigma_2^2}{\sigma_{90}} + \sigma_1\sigma_2 \left(\frac{4}{\sigma_{45}} - \frac{1}{\sigma_0} - \frac{1}{\sigma_{90}} - \frac{1}{\tau_0} \right) = \\ = 1 / \sqrt{\sigma_1^2 + \sigma_2^2 + \sigma_1\sigma_2}. \end{aligned} \quad (94)$$

The following condition of failure of the pipe is obtained from this formula:

$$\sigma_2 = \frac{\sqrt{\tau}}{\frac{2}{\sigma_0} - \frac{1}{\sigma_{90}} + \frac{8}{\sigma_{45}} - \frac{2}{\tau_0}}. \quad (95)$$

The corresponding safe pipe wall thickness is

/103

$$\delta \geq \frac{prk}{2\sqrt{\tau}\sigma_0} (8a - 2d - c + 2). \quad (96)$$

A similar calculation procedure can be used to determine the wall thickness of thin walled vessels and casings exposed to internal or external hydrostatic pressure. The active stresses can be determined with the anisotropic elastic properties of the material taken into account or, in the first approximation, as for isotropic materials. The use of the strength criteria proposed in Sections 5 and 6 is particularly convenient in these cases, since the stress is characterized by two principal stresses of the same sign. If principal tensile stresses are involved, determination can be limited to the tensile strength of the material without determination of the compressive strength.

F.P. Pekker experimentally tested the applicability of strength criteria in the form of fourth power polynomial (94), to estimate the destructive internal axisymmetric pressure of fiberglass plastic pipe. Two series of pipes, each 150 cm long, were tested. One series, with lengthwise-crosswise orthogonal laid glass roving, had an average diameter of 53 mm and a wall thickness of approximately 3 mm. The second series, with nonorthogonal cross laid fiberglass cloth tape, had an average diameter of 52 mm and a 2.8 mm wall thickness.

All the initial characteristics of the material and the destructive pressure were determined on samples cut from each pipe, and they were averaged for the pipe batch, with statistical evaluation of the test results and with the effect of the sample width on σ_0 and σ_{45} taken into account. To determine τ_0 , torsion and shearing tests and the indirect method proposed in [36] were used.

The torsion test gave understated results, especially for the second series of pipe, the outer layer of which consisted of lengthwise roving. The maximum tangential stresses under torsion, along areas parallel to the pipe axis, were taken up by the binder alone in this case, which explained the understated destructive torque. Shearing tests, with their great complexity, do not make it possible to achieve pure shearing stress [36], and they lead to overstated values of τ_0 . Therefore, the indirect method of determination of τ_0 , based on plotting limit curves from the known values of σ_0 , σ_{45} and σ_{90} , were used in the work.

Determination of strength τ_0 from the results of tensile tests of three kinds of samples, which were oriented differently toward the axes /104 of symmetry of the material, was described in Section 14 of [36]. The indirect method of determination of pure shearing strength τ_0 permits the number of experimentally determined strength characteristics of the material included in the strength criteria to be reduced to three, in the special case of pipe calculation of the effect of two dimensional stress in elements of the material. Estimation of the destructive pressure from the results of simple tests of three kinds of samples cut from the pipe is of great practical importance.

The results of the experiments of F.P. Pekker are presented in Tables 16 and 17. The maximum high and low values, at the 0.95 confidence level, were determined in these tables by the formula $\bar{X} \pm 2S$ (\bar{X} is the arithmetical average of the determined value and S is its root mean deviation).

Comparison of the destructive internal pressure obtained in these /105 tests with its value calculated by the fourth power polynomial strength criterion show completely satisfactory agreement.

It follows from the fourth power polynomial strength criterion that the strength of an anisotropic material can be completely characterized by a fourth order tensor. It follows from this that the notation formulated on p. 17, which permit establishment of a calculation scheme for the elastic property anisotropy of a material, is classified as strength characteristics. Only that material can be considered isotropic in strength under any kind of loading, for which, in this type of loading

$$\sigma_x^{(0)} = \sigma_y^{(0)} = \sigma_z^{(0)} = \sigma_{xy}^{(45)} = \sigma_{yz}^{(45)} = \sigma_{xz}^{(45)}.$$

TABLE 16. TUBE MATERIAL CHARACTERISTICS

a Показатели	б Пределы прочности в кг/см ²			
	σ_s	σ_{av}	σ_{min}	τ_s
с Трубы тканевые				
d Предельное наибольшее значение с вероятностью 0,95	5564	2248	1952	846
e Среднее арифметическое	3108	1855	1775	768
f Предельное наименьшее значение с вероятностью 0,95	2552	1462	1598	694
g Трубы жгутовые				
d Предельное наибольшее значение с вероятностью 0,95	5604	3813	2610	1149
e Среднее арифметическое	4667	3080	2322	994
f Предельное наименьшее значение с вероятностью 0,95	3729	2347	2034	876

Key: a. Characteristic
 b. Strength, kg/cm²
 c. Cloth tubing
 d. Maximum value with
 0.95 probability
 e. Arithmetical average
 value
 f. Minimum value with
 0.95 probability
 g. Roving tubing

TABLE 17. DESTRUCTIVE INTERNAL PRESSURE (ATM)

a Показатели	По формуле (94)	h По данным эксперимента	
		b	c
с Трубы тканевые			
Предельное наибольшее значение с вероятностью 0,95 d	311	320	
		265	
		285	
e Среднее арифметическое значение	284	300	
		305	
f Предельное наименьшее значение с вероятностью 0,95	256	270	
		260	
g Трубы жгутовые			
Предельное наибольшее значение с вероятностью 0,95 d	416	407	
		415	
e Среднее арифметическое значение	383	392	
		360	
Предельное наименьшее значение с вероятностью 0,95 f	335		

Key: a. Characteristic
 b. By Eq. (94)
 c. Cloth tubing
 d. Maximum value with
 0.95 probability
 e. Arithmetical average
 value
 f. Minimum value with
 0.95 probability
 g. Roving tubing
 h. Experimental data

The requirement $\tau_{xy}^{(0)} = \tau_{yz}^{(0)} = \tau_{zx}^{(0)}$ is less significant, and it is more difficult to test experimentally, because of the difficulties of testing a sample of anisotropic material to failure under uniform pure shearing stress conditions. Here, as before, $\sigma_x^{(0)}$, $\sigma_y^{(0)}$, $\sigma_z^{(0)}$ are the strengths under uniaxial stress, with the principal stress coincident with the axes of structural symmetry of the material, and $\sigma_{xy}^{(45)}$, $\sigma_{yz}^{(45)}$ and $\sigma_{zx}^{(45)}$ are the strengths under uniaxial stress, with the principal stress coincident with directions in the planes of structural symmetry of the material at 45° angles to the axes of symmetry, and $\tau_{xy}^{(0)}$, $\tau_{yx}^{(0)}$ and $\tau_{zx}^{(0)}$ are the shearing strengths along areas parallel to the planes of symmetry of the material.

Establishment of the calculation scheme of anisotropy of a material and experimental determination of the complete set of its strength characteristics is of great practical importance, since it permits an increase in carrying capacity of a structure, by means of the correct use of an anisotropic material. References to examples of this kind are presented in [88], where methods of monitoring and regulating anisotropy in metals also are described.

It must be noted in conclusion that, at present, scientific data still have not been obtained for constructing a physically valid theory of the strength of anisotropic materials, and methods of determination of the actual strength characteristics of a material also have not been found. Phenomenological strength criteria under complex stresses and determination of the material constants included in them, known to be inaccurate methods of mechanical testing of samples, are the first approximation in the solution of these problems, as applied to items made of anisotropic materials.

Strength criteria of anisotropic materials still are not sufficiently widely used in engineering practice, and data still have not been accumulated on the performance of structures calculated by these criteria. The question of substantiated selection of strength safety factors has not been worked out to the proper extent, and the very method of experimental determination of strength characteristics of anisotropic materials is still the subject of controversy. In addition to that, the development of modern technology makes urgent the consideration of the broadest aspects of the questions raised here.

REFERENCES

1. Mekhanicheskiye svoystva novykh materialov [Mechanical Properties of New Materials], Mir Press, Moscow, 1966 (Mekhanika collection Library).
2. Karoll-Porzhinskiy, Ts., Materialy budushchego [Materials of the Future], Khimiya Press, Moscow, 1966.
3. Mitinskiy, A.N., "Elastic constants of wood as an orthotropic material," Trudy LTA (Leningrad) 63, (1948).
4. Kupch, L.Ya., "Plywood made of veneer sheets glued at an angle," Izv. AN LatSSR (Riga) 5, (1959).
5. Belyankin, F.P. et al, Mekhanicheskiye kharakteristiki plastika DSP [Mechanical Characteristics of DSP Plastic], AN UkrSSR Press, Kiev, 1961.
6. Keylwerth, R., "Achieved and achievable reduction in anisotropy of fiberboard," Holz als Roh und Werkstoff 17/6, (1959).
7. Slonimskiy, G.L. and T.A. Dikareva, "Investigation of anisotropy of mechanical properties of uniaxially oriented polymer films," Vysokomolekulyarnyye soyedineniya 1, (1964).
8. Kargin, V.A., Sovremennyye problemy nauki o polimerakh [Current Problems of Polymer Science], Moscow State Univ. Press, 1962.
9. Bolotin, V.V., "Two dimensional problem of elasticity theory for parts made of reinforced materials," Raschety na prochnost' [Strength Calculations], issue 12, Mashinostroyeniye Press, Moscow, 1966.
10. Grigorovich, V.K. et al, "The most favorable fiber direction in products made of anisotropic materials," DAN SSSR 86/4, (1952).
11. Rabotnov, Yu.N., Polzuchest' elementov konstruktsiy [Creep of Structural Elements], Nauka Pres, Moscow, 1966.
12. Fridman, Ya.B. and P.G. Miklyayev, "Calculation of elastic and strength characteristics of anisotropic metals," DAN SSSR 167/1, (1966).
13. Miklyayev, P.G. and Ya.B. Fridman, "Method of estimation of anisotropy of mechanical properties of metals," Zavodskaya laboratoriya 4, (1965).
14. Lyav, A., Matematicheskaya teoriya uprugosti [Mathematical Theory of Elasticity], ONTI, Moscow, 1935.
15. Ashkenazi, Ye.K., "Experimental determination of elastic constants of wood as an anisotropic material," Trudy LTA (Leningrad) 70, (1950).
16. Ashkenazi, Ye.K., "Determination of the elastic constants of wood," Zavodskaya laboratoriya 3, (1955).
17. Iekhnitskiy, S.G., Teoriya uprugosti anizotropnogo tela [Theory of Elasticity of an Anisotropic Material], GTTI, Moscow, 1950.

18. Rabinovich, A.L., "Elastic constants and strengths of anisotropic materials," Trudy TsAGI (Moscow) 582, (1946).
19. Rabinovich, A.L. and Ya.D. Avrasin, "Mechanical characteristics of some laminated plastics in connection with the strength of bolting and riveting compounds," Steklotekstolity i drugiye konstruktsionnyye plastiki /Fiberglas Laminates and Other Structural Plastics/, Oborongiz Press, Moscow, 1960.
20. Smotrin, N.T. and V.M. Chebanov, "Mechanical properties of anisotropic laminated plastics in brief tests," Issledovaniya po uprugosti i plastichnosti. Sbornik No. 2 /Studies in Elasticity and Plasticity, Collection No. 2/, Leningrad State Univ. Press, 1963.
21. Zaks, G., Prakticheskoye metallovedeniye /Practical Physical Metallurgy/, Part 2, ONTI NKTP SSSR, Moscow-Leningrad, 1938.
22. Ashkenazi, Ye.K et al, Anizotropiya mekhanicheskikh svoystv drevesiny i fanery /Anisotropy of Mechanical Properties of Wood and Plywood/, Goslesbumizdat Press, Moscow, 1958.
23. Wassermann, G. and G. Grewen, Texturen metallischen Werkstoffe /Textures of Metallic Structural Materials/, Springer, Berlin, 1962.
24. Semenov, P.I., "Determination of modulus of shear of orthotropic materials from torsional tests," Mekhanika polimerov /Mechanics of Polymers/, AN LatSSR Press, Riga, No. 1, 1966.
25. Snitko, N.K., "Theory of the strength of metals with structure taken into account," ZhTF 6, (1948).
26. Boas, W. and J.K. Mackenzie, "Anisotropy in metals," Progress in Metal Physics, 2, New York-London, 1950, pp. 90-120.
27. Auerbach, F. and W. Hort, Handbuch der physikalischen und technischen Mechanik /Handbook of Physical and Technical Mechanics/, vol. 3, Leipzig, 1927, pp. 239-278.
28. Ashkenazi, Ye.K. and A.A. Pozdnyakov, "Shape of samples for tensile testing of anisotropic fiberglas plastics," Zavodskaya laboratoriya 10, (1955).
29. Smirnova, M.K. et al, Prochnost' korpusa sudna iz stekloplastika /Strength of a Fiberglas Plastic Ship Hull/, Sudostroyeniye Press, Leningrad, 1965.
30. Aynbinder, S.B. et al, "Effect of hydrostatic pressure on mechanical properties of polymers," Mekhanika polimerov /Mechanics of Polymers/, AN LatSSR Press, Riga, No. 1, 1965.
31. Bridgman, P.W., Journal Applied Physics 12, (1941).
32. Regel', V.G., "Mechanism of brittle fracture of plastics," ZhTF 21/3, (1951).
33. Mises, R., "Mechanics of plastic alteration of crystals," ZAMM 8/3, (1928).
34. Ivanov, Yu.M., "Compressive strength of wood at various angles to the fibers," Trudy Instituta lesa AN SSSR /Proceedings of

Forest Institute, USSR Academy of Sciences⁷, vol. 9, AN SSSR Press, Moscow, 1953.

35. Ganov, E.I., "Study of the possibility of production of large single piece ships of fiberglass," author's abstract of candidate's dissertation, Leningrad Design Institute, 1967.
36. Ashkenazi, Ye.K., Prochnost' anizotropnykh drevesnykh i sinteticheskikh materialov /Strength of Anisotropic Wood and Synthetic Materials/, Lesnaya promyshlennost' Press, Moscow, 1966.
37. Ashkenazi, Ye.K., "Questions of Strength anisotropy," Mekhanika polimerov /Mechanics of Polymers/, AN LatSSR Press, Riga, No. 2, 1965.
38. Ashkenazi, Ye.K., Anizotropiya mekhanicheskikh svoystv nekotorykh stekloplastikov /Anisotropy of Mechanical Properties of Some Fiberglass Plastics/, LDNTP, 1961.
39. Ashkenazi, Ye.K., "Symmetry of the strength of wood as an anisotropic material," Trudy LTA (Leningrad) 78, 1957.
40. Ashkenazi, Ye.K. et al, "Study of the impact compressive strength of pine wood," Doklady mezhvyzovskoy konferentsii po ispytaniyam sooruzheniy /Reports of Conference of Schools of Higher Education on Testing Structures/, LISI, Leningrad, 1958.
41. Ashkenazi, Ye.K., "Strength anisotropy of structural materials," ZhTF 29/3, (1959).
42. Ganov, E.V., "The use of graphic methods in study of mechanical property anisotropy of orthotropic materials," Zavodskaya laboratoriya 11, (1966).
43. Pozdnyakov, A.A., "Fatigue of wood at various angles to the fiber direction," Lesnoy zhurnal 3, (1960).
44. Heywood, R.B., Designing Against Fatigue, London, 1962.
45. Rachkovskiy, Ya., "Anisotropy of swelling pressure of wood," Folia Forestalia Polonica 2, Suppl. B, (1960).
46. Kollmann, F., Technologie des Holzes und der Holzwerkstoffe /Technology of Wood and Wood Materials/, vol. 1, 1951, Sec. 452, p. 4.
47. Sidorin, Ya.S., "Experimental study of fiberglass plastic anisotropy," Izv. AN SSSR 3, (1964).
48. Malmeister, A.K., "Geometry of strength theory," Mekhanika polimerov /Mechanics of Polymers/, AN LatSSR Press, Riga, No. 4, 1966.
49. Institute of Mining, USSR Academy of Sciences, Mekhanicheskiye svoystva gornykh porod /Mechanical Properties of Rocks/, AN USSR Press, Moscow, 1963.
50. Aynbinder, S.B., Issledovaniya treniya i stsepleniya tverdykh tel /Research on Friction and Cohesion of Solids/, survey paper on published works as doctor of technical sciences thesis, AN LatSSR Press, Riga, 1966.

51. Protasov, V.D. and V.A. Kopnov, "Study of the strength of fiber-glas plastics under two dimensional stress," Mekhanika polimerov [Mechanics of Polymers], AN LatSSR Press, Riga, No. 5, 1965.
52. Gol'denblat, I.I. and V.A. Kopnov, "Strength of fiber-glas plastics under complex stresses," Mekhanika polimerov [Mechanics of Polymers], AN LatSSR Press, Riga, No. 2, 1965.
53. Bastun, V.N. and N.I. Chernyak, "Applicability of certain plasticity conditions for anisotropic steel," Prikladnaya mekhanika (Kiev) 11/1, (1966).
54. Bessonov, K.A. et al, "Mechanical property anisotropy in cold rolled aluminum," Trudy Khimiko-metallurgicheskogo instituta Sib. otd. AN SSSR [Proceedings of Chemical-Metallurgical Institute, Siberian Section, USSR Academy of Sciences], issue 14, Novosibirsk, 1960.
55. Gatto and Mori, "Experimental study of anisotropy of rolled high strength light metal alloys," Alluminio (Milan) 24/3, 1955.
56. Miklyayev, P.G. and Ya.B. Fridman, "Estimation of anisotropy of sensitivity of metals to notching and initial cracking in one time impact bending," Zavodskaya laboratoriya 4, (1967).
57. Chodorowski, J. and A. Buch, Fatigue Resistance of Materials and Metal Structural Parts, Pergamon Press, London, 1964.
58. Radwan, M., "Study of anisotropy of cold rolled steel strip made from deep drawing steel," Bulletyn Wojskowej Akademii technicznej. Prace kandydaski (Warsaw) 4/14, (1955).
59. Hill, R., Matematicheskaya teoriya plastichnosti [Mathematical Theory of Plasticity], State Publishing House of Technical and Theoretical Literature, Moscow, 1956.
60. Christian, J.L., "Effects of chemistry and processing on the mechanical properties of engineering alloys of cryogenic temperatures," Materials, Science and Technology for Advanced Applications (American Society for Metals) 11, series A-1, 32 (1964).
61. Drozdovskiy, B.A. and Ya.B. Fridman, Vliyaniye treshchin na mekhanicheskiye svoystva konstruktsionnykh stalej [Effect of Cracks on Mechanical Properties of Structural Steels], Metallurgizdat Press, Moscow, 1960.
62. Hoover, H., ASTM Proceedings 53, (1953).
63. Pogodin-Alekseyev, G.I., Dinamicheskaya prochnost' i khrupkost' metallov [Dynamic Strength and Brittleness of Metals], Mashinostroyeniye Press, Moscow, 1966.
64. Buch, A., "Relation between steel purity and anisotropy of tensile and fatigue properties," Conference on Fracture, Sendai, Japan, B. III-9-53, 1965.
65. Gurevich, Ya.B., "Anisotropy of mechanical properties of cast metal," Prokatnoye i trubnoye proizvodstvo [Rolled and Pipe Production], supplement to the journal Stal', Metallurgizdat Press, Moscow, 1959.

66. Miklyayev, P.G. and Ya.B. Fridman, "Anisotropy of resistance of metals to fatigue failure," Zavodskaya laboratoriya 7, (1967).
67. Roze, A.V., "Characteristics of calculation of parts made of materials with low shearing hardness and strength." author's abstract of candidate's dissertation, Institute of the Mechanics of Polymers, LatSSR Academy of Sciences, Riga, 1966.
68. Tarnopol'skiy, Yu.M. and A.V. Roze, "Bending strength of oriented fiberglass plastics," Mekhanika polimerov [Mechanics of Polymers], AN LatSSR Press, Riga, No. 4, 1966.
69. Ashkenazi, Ye.K. and V.N. Yelokhov, "A cause of scatter of results of mechanical tests of anisotropic materials," Zavodskaya laboratoriya 5, (1966).
70. Davidenkov, N.N. and E.I. Braynin, "Effect of heat treatment on orientation of slip lines in cold rolled steel," Izv. vyzov. Chernaya metallurgiya 10, (1959).
71. Braynin, E.I., "Anisotropy of construction material strength," ZhTF 30/8, (1960).
72. Ashkenazi, Ye.K., "Anisotropy of construction material strength," ZhTF 31/5, (1961).
73. Kushelev, N.Yu., "Effect of geometric factors on fatigue failure," Prochnost' materialov i konstruktsiy [Strength of Materials and Structures], Gosstroyizdat Press, Moscow-Leningrad, (1959) [Trudy LPI, No. 197].
74. Boksberg, I.P., "Machine for fatigue testing of fiberglass plastics," Zavodskaya laboratoriya 2, (1961).
75. Sharapova, N.P., "Method of fatigue testing of fiberglass plastics and fatigue strength of fiberglass cloth plastic," Polimery v mashinakh [Polymers in Machines], Mashinostroyeniye Press, Moscow, 1966 (Scientific Research Institute of Machines, Collection 9).
76. Tompson, A., "Fatigue strength of reinforced plastics," Khimiya i tekhnologiya polimerov, sb. perevodov No. 10 [Chemistry and Technology of Plastics, Collection of Translations No. 10], Foreign Literature Publishing House, Moscow, 1962.
77. Shevandin, Ye.M. et al, "Effect of anisotropy of properties of rolled steel on its fatigue strength," Zavodskaya laboratoriya 10, (1951).
78. Veybull, V., Ustalostnyye ispytaniya i analiz ikh rezul'tatov [Fatigue Tests and Analysis of Their Results], Mashinostroyeniye Press, Moscow, 1964.
79. Findley, W.N. and P.N. Mathur, "Anisotropy of fatigue strength of a steel and two Al alloys in bending and in torsion," ASTM Proceedings 55, 924-937 (1955).
80. Ransom, J.T. and R.F. Mehl, "The anisotropy of the fatigue properties of SAE 4340 steel forging," ASTM Proceedings 52, 779-787 (1952).

81. Sborovskiy, A.K. et al, Vibratsiya sudov s korpusami iz steklo-plastika [Vibration of Ships with Fiberglas Plastic Hulls], Sudostroyeniye Press, Leningrad, 1967.
82. Pyudik, P.E., "Study of the physical and mechanical properties and selection of the optimum grade of laminated wood plastics for production of gears," author's abstract of candidate's dissertation, LTA, Leningrad, 1967.
83. Gol'fman, I.B. and Ye.K. Ashkenazi, "Method of experimental study of stress in anisotropic parts," Materialy nauchno-tehnicheskoy konferentsii LTA [Materials of Scientific-Technical Conference of LTA], Issue 5, LTA, Leningrad, 1966.
84. Protasov, V.D. and V.P. Georgiyevskiy, "Anisotropy of elastic and strength properties of reinforced plastics," Mekhanika polimerov [Mechanics of Polymers], AN LatSSR Press, Riga, No. 4, 1967.
85. Gol'dman, A.Ya. and N.F. Savel'yeva, "Stress and certain features of failure of fiberglas plastic samples under tension at an angle to the fibers," Mekhanika polimerov [Mechanics of Polymers], AN LatSSR Press, Riga, No. 6, 1967.
86. Ashkenazi, Ye.K., "Strength of wood under complex stresses: Technical information on results of scientific research of LTA," Prochnost' materialov [Strength of Materials], LTA, Leningrad, 1967.
87. Ashkenazi, Ye.K., "Geometry of strength theory," Mekhanika polimerov [Mechanics of Polymers], AN LatSSR Press, Riga, No. 4, 1967.
88. Miklyayev, P.G. and Ya.B. Fridman, Anizotropiya mekhanicheskikh svoystv metallov [Anisotropy of Mechanical Properties of Metals], Metallurgiya Press, Moscow, 1969.
89. Ashkenazi, Ye.K. and F.P. Pekker, "Strength of fiberglas plastics under complex stresses: Technical information on results of scientific research of LTA," Prochnost' materialov [Strength of Materials], LTA, Leningrad, 1967.
90. Verkhovskiy, I.A. and A.L. Rabinovich, "Constants of elastic and highly elastic deformations of oriented fiberglas plastics," Fizikokhimiya i mekhanika orientirovannykh stekloplastikov [Physical Chemistry and Mechanics of Oriented Fiberglas Plastics], Nauka Press, Moscow, 1967.
91. Biderman, V.L., "Elasticity and strength of anisotropic fiberglas plastics," Raschety na prochnost' [Strength Calculations], collection No. 11, Mashinostroyeniye Press, Moscow, 1965.
92. Gastev, V.A., Kratkiy kurs soprotivleniya materialov [Short Course on Strength of Materials], Fizmatgiz Press, Moscow, 1959.
93. Gol'dman, A.Ya. and V.N. Rivkind, "The 'cut fiber' effect in fiberglas plastics," Mekhanika polimerov [Mechanics of Polymers], AN LatSSR Press, Riga, No. 2, 1968.